

Contents

- 5.1 Introduction
- 5.2 Lumped-Element versus Distributed Characteristics
- 5.3 Effects of Parasitic (Stray) Characteristics
 - 5.3.1 Parasitic Inductance
 - 5.3.2 Parasitic Capacitance
 - 5.3.3 Self-Resonance
 - 5.3.4 Inductors and RF Chokes at Radio Frequencies
 - 5.3.5 Skin Effect
 - 5.3.6 RF Heating
 - 5.3.7 Effect on Q
 - 5.3.8 Dielectric Breakdown and Arcing
 - 5.3.9 Radiative Losses
 - 5.3.10 Bypassing and Decoupling
 - 5.3.11 Effects on Filter Performance
- 5.4 Semiconductor Circuits at RF
 - 5.4.1 The Diode at High Frequencies
 - 5.4.2 The Transistor at High Frequencies
 - 5.4.3 Amplifier Classes
 - 5.4.4 RF Amplifiers with Feedback
- 5.5 Ferrite Materials
 - 5.5.1 Ferrite Permeability and Frequency
 - 5.5.2 Resonances of Ferrite Cores
 - 5.5.3 Ferrite Series and Parallel Equivalent Circuits
 - 5.5.4 Type 31 Material
 - 5.5.5 Determining Ferrite Type
- 5.6 Impedance Matching Networks
 - 5.6.1 L Networks
 - 5.6.2 Pi Networks
 - 5.6.3 T Networks
 - 5.6.4 Impedance Inversion
- 5.7 RF Transformers
 - 5.7.1 Air-Core Nonresonant RF Transformers
 - 5.7.2 Air-Core Resonant RF Transformers
 - 5.7.3 Broadband Ferrite RF Transformers
- 5.8 Noise
 - 5.8.1 Noise Power
 - 5.8.2 Signal to Noise Ratio
 - 5.8.3 Noise Temperature
 - 5.8.4 Noise Factor and Noise Figure
 - 5.8.5 Losses
 - 5.8.6 Cascaded Amplifiers
 - 5.8.7 Antenna Temperature
 - 5.8.8 Image Response
 - 5.8.9 Background Noise
- 5.9 Two-Port Networks
 - 5.9.1 Two-port Parameters
 - 5.9.2 Return Loss
- 5.10 References and Bibliography

Chapter 5

RF Techniques

This chapter is a compendium of material from ARRL publications and other sources. It assumes the reader is familiar with the concepts introduced in the **Electrical Fundamentals**, **Radio Fundamentals**, and **Circuits and Components** chapters. The topics and techniques discussed here are associated with the special demands of circuit design in the HF and VHF ranges. The material is collected from previous editions of this book written by Leonard Kay, K1NU; *Introduction to Radio Frequency Design* by Wes Hayward, W7ZOI; and *Experimental Methods in RF Design* by Wes Hayward, W7ZOI, Rick Campbell, KK7B, and Bob Larkin, W7PUA. Material on ferrites is drawn from publications by Jim Brown, K9YC. The section on Noise was written by Paul Wade, W1GHZ, with contributions from Joe Taylor, K1JT.

Chapter 5 — Online Content

Articles

- Designing Wide-band Transformers for HF and VHF Power Amplifiers by Chris Trask, N7ZWY
- Reflections on the Smith Chart by Wes Hayward, W7ZOI
- Simplified Design of Impedance-Matching Networks, Parts I through III by George Grammer, W1DF
- The Galactic Background in the Upper HF Band by Dave Typinski, AJ4CO

Tools and Data

- *LTSpice* simulation files for Effects of Parasitic Characteristics (Section 5.3)
- *MATCH.EXE* software (for use with Tuned (Resonant) Networks discussion)

5.1 Introduction

When is an inductor not an inductor? When it's a capacitor! This statement may seem odd, but it suggests the main message of this chapter. In the earlier chapter, **Electrical Fundamentals**, the basic components of electronic circuits were introduced. As you may know from experience, those simple component pictures are ideal. That is, an ideal component (or element) by definition behaves exactly like the mathematical equations that describe it, and only in that fashion. For example, the current through an ideal capacitor is equal to the capacitance times the rate of change of the voltage across it without consideration of the materials or techniques by which a real capacitor is manufactured.

It is often said that, "Parasitics are anything you don't want," meaning that the component is exhibiting some behavior that detracts from or compromises its intended use. Real components only approximate ideal components, although sometimes quite closely. Any deviation from ideal behavior a component exhibits is called *non-ideal*, *parasitic*, or *stray*. One way of thinking about parasitic and stray effects — although this is by no means universal — is that parasitic effects are intrinsic to the component and stray effects include both parasitics and environmental effects such as coupling to nearby materials. Since most of what we'll discuss in the following sections deals with the characteristics of actual components, we'll use the term parasitic. Remember that stray and parasitic are often treated as interchangeable terms.

The important thing to realize is that *every* component has parasitic aspects that become significant when it is used in certain ways. This chapter deals with parasitic effects that are commonly encountered at radio frequencies. Knowing to what extent and under what conditions real components cease to behave like their ideal counterparts, and what can be done to account for these behaviors, allows the circuit designer or technician to work with circuits at radio frequencies. We will explore how and why the real components behave differently from ideal components, how we can account for those differences when analyzing circuits and how to select components to minimize, or exploit, non-ideal behaviors.

5.2 Lumped-Element versus Distributed Characteristics

Most electronic circuits that we use every day are inherently and mathematically considered to be composed of *lumped elements*. That is, we assume each component acts at a single point in space, and the wires that connect these lumped elements are assumed to be perfect conductors (with zero resistance and insignificant length). This concept is illustrated in **Figure 5.1**. These assumptions are perfectly reasonable for many applications, but they have limits. Lumped element models break down when:

- Circuit impedance is so low that the small, but non-zero, resistance in the wires is important. (A significant portion of the circuit power may be lost to heat in the conductors.)
- Lead and interconnection inductance is high enough (or the frequency is high enough) that the additional reactance affects circuit behavior.
- Operating frequency is high enough that the length of the connecting wires is a significant fraction (>0.1) of the wavelength causing the propagation delay along the conductor

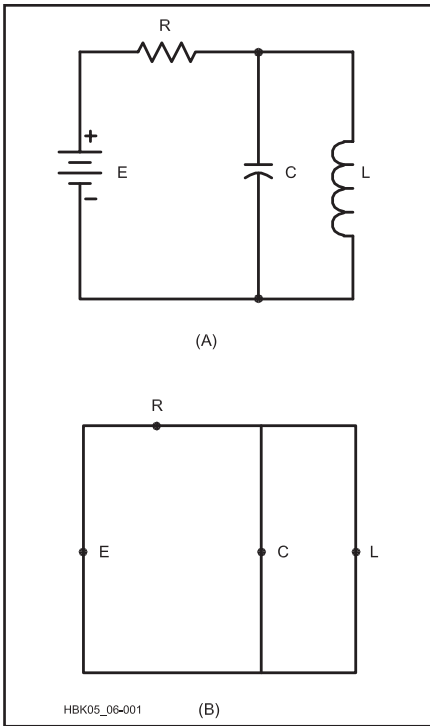


Figure 5.1 — The lumped element concept. Ideally, the circuit at A is assumed to be as shown at B, where the components are isolated points connected by perfect conductors. Many components exhibit nonideal behavior when these assumptions no longer hold.

or radiation from it to affect the circuit in which it is used.

- Transmission lines are used as conductors. (Their characteristic impedance is usually significant, and impedances connected to them are transformed as a function of the line length. See the **Transmission Lines** chapter for more information.)

Effects such as these are called *distributed*, and we talk of *distributed elements* or effects to contrast them to lumped elements.

To illustrate the differences between lumped and distributed elements, consider the two resistors in **Figure 5.2**, which are both 12 inches long. The resistor at A is a uniform rod of carbon. The second “resistor” B is made of two 6-inch pieces of silver rod (or other highly conductive material), with a small resistor soldered between them. Now imagine connecting the two probes of an ohmmeter to each of the two resistors, as in the figure. Starting with the probes at the far ends, as we slide the probes toward the center, the carbon rod will display a constantly decreasing resistance on the ohmmeter. This represents a distributed resistance. On the other hand, the ohmmeter connected to the other 12-inch “resistor” will

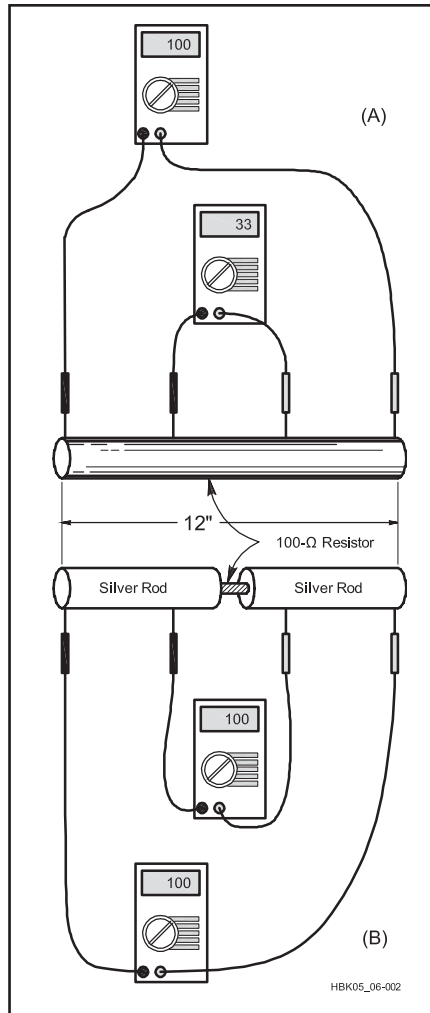


Figure 5.2 — Distributed (A) and lumped (B) resistances. See text for discussion.

display a constant resistance as long as one probe remains on each side of the small resistance and as long as we neglect the resistance of the silver rods! This represents a lumped resistance connected by perfect conductors.

Lumped elements also have the very desirable property that they introduce no phase shift resulting from propagation delay through the element. (Although combinations of lumped elements can produce phase shifts by virtue of their R, L and C properties.) Consider a lumped element that is carrying a sinusoidal current, as in **Figure 5.3A**. Since the element has negligible length, there is no phase difference in the current between the two sides of the element — *no matter how high the frequency* — precisely *because* the element length is negligible. If the physical length of the element were long, say 0.25 wavelength

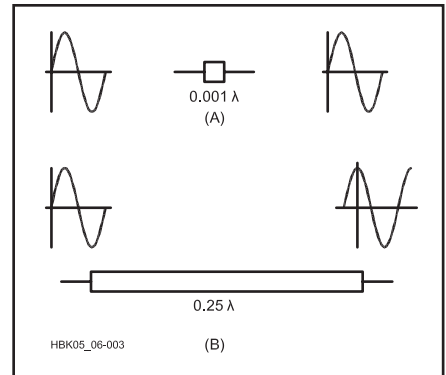


Figure 5.3 — The effects of distributed resistance on the phase of a sinusoidal current. There is no phase delay between ends of a lumped element.

(0.25 λ) as shown in **Figure 5.3B**, the current phase would *not* be the same from end to end. In this instance, the current is delayed by 90 electrical degrees as it moves along the element. The amount of phase difference depends on the circuit’s electrical length.

Because the relationship between the physical size of a circuit and the wavelength of an ac current present in the circuit will vary as the frequency of the ac signal varies, the ideas of lumped and distributed effects actually occupy two ends of a spectrum. At HF (30 MHz and below), where $\lambda \geq 10$ m, the lumped element concept is almost always valid. In the UHF and microwave region (300 MHz and above), where $\lambda \leq 1$ m and physical component size can represent a significant fraction of a wavelength, nearly all components and wiring exhibits distributed effects to one degree or another. From roughly 30 to 300 MHz, whether the distributed effects are significant must be considered on a case-by-case basis.

Of course, if we could make resistors, capacitors, inductors and so on, very small, we could treat them as lumped elements at much higher frequencies. For example, surface-mount components, which are manufactured in very small, leadless packages, can be used at much higher frequencies than leaded components and with fewer non-ideal effects.

It is for these reasons that circuits and equipment are often specified to work within specific frequency ranges. Outside of these ranges the designer’s assumptions about the physical characteristics of the components and the methods and materials of the circuit’s assembly become increasingly invalid. At frequencies sufficiently removed from the design range, circuit behavior often changes in unpredictable ways.

5.3 Effects of Parasitic (Stray) Characteristics

Parasitic effects can be important at almost any frequency where performance is held to tight specifications. Stray reactances can have a big effect even at audio frequencies, for example. Lightning protection is very sensitive to grounding conductor inductance. Power connections to high-current solid-state amplifiers must have very low resistance, and so on. At HF and above (where we do much of our circuit design) these considerations become very important, in some cases dominant, in the models we use to describe our components. To understand what happens to circuits at RF we turn to a brief discussion of some electromagnetic and microwave theory concepts.

Parasitic effects due to component leads, packaging, leakage and so on are relatively common to all components. When working at frequencies where many or all of the parasitics become important, a complex but completely general model such as that in **Figure 5.4** can be used for just about any component, with the actual component placed in the box marked *. Parasitic capacitance, C_p , and leakage conductance, G_L , appear in parallel across the device, while series resistance, R_s , and parasitic inductance, L_s , appear in series with it. Package capacitance, C_{pkg} , appears as an additional capacitance in parallel across the whole device.

These small parasitics can significantly affect frequency responses of RF circuits. Either take steps to minimize or eliminate them, or use simple circuit theory to predict and anticipate changes. This maze of effects may seem overwhelming, but remember that it is very seldom necessary to consider all parasitics at all frequencies and for all applications. The **Computer-Aided Circuit Design** chapter shows how to incorporate the effect of multiple parasitics into circuit design and performance modeling. Files for the *LTSpice* simulation package that include parasitic characteristics for a resistor, capacitor and inductor are provided in the online content for this *Handbook*.

5.3.1 Parasitic Inductance

Maxwell's equations — the basic laws of electromagnetism that govern the propagation of electromagnetic waves and the operation of all electronic components — tell us that any wire carrying a current that changes with time (one example is a sine wave) develops a changing magnetic field around it. This changing magnetic field in turn induces an opposing voltage, or *back EMF*, on the wire. The back EMF is proportional to how fast the current changes (see **Figure 5.5**).

We exploit this phenomenon when we make an inductor. The reason we typically form inductors in the shape of a coil is to concentrate the magnetic field and thereby maxi-

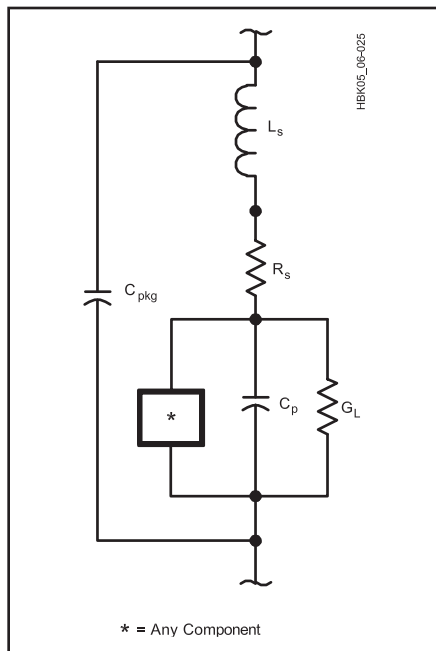


Figure 5.4 — A general model for electrical components at VHF frequencies and above. The box marked * represents the component. See text for discussion.

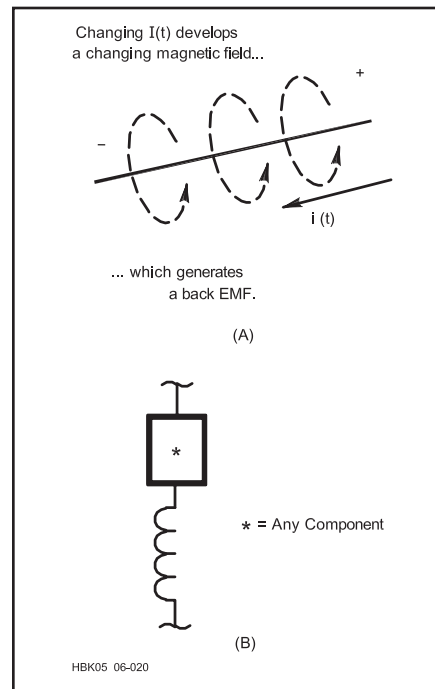


Figure 5.5 — Inductive consequences of Maxwell's equations. At A, any wire carrying a changing current develops a voltage difference along it. This can be mathematically described as an effective inductance. B adds parasitic inductance to a generic component model.

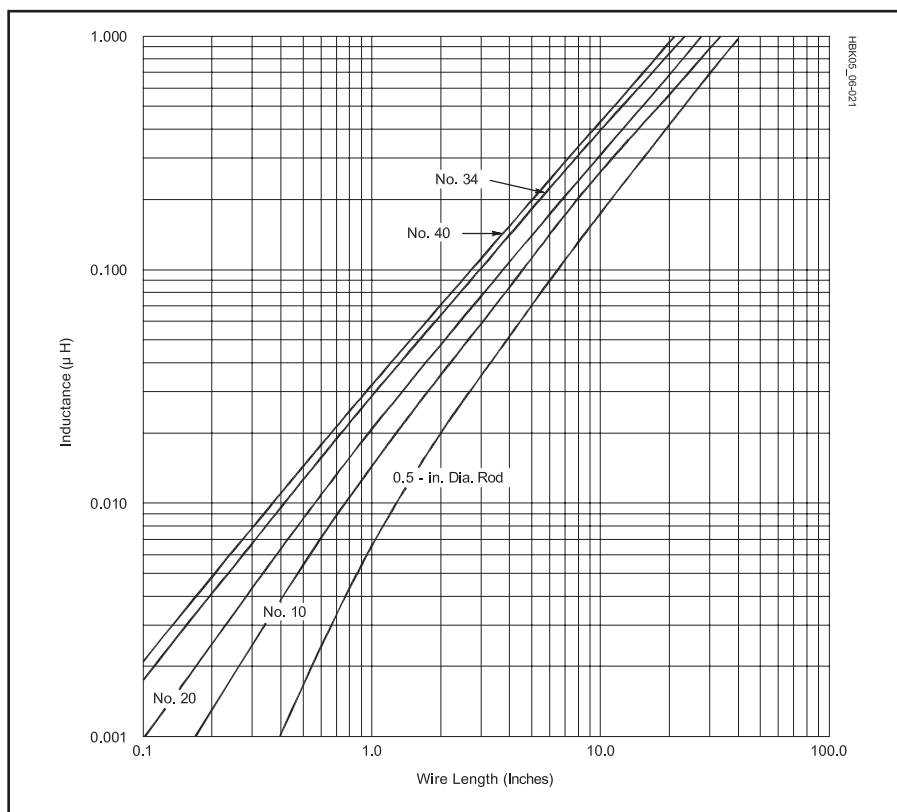


Figure 5.6 — A plot of inductance vs length for straight conductors in several wire sizes.

mize the inductance for a given physical size. However, *all* wires carrying varying currents have these inductive properties. This includes the wires we use to connect our circuits, and even the *leads* of capacitors, resistors and so on. The inductance of a straight, round, nonmagnetic wire in free space is given by:

$$L = 0.00508 b \left[\ln \left(\frac{2b}{a} \right) - 0.75 \right] \quad (1)$$

where

- L = inductance, in μH ,
- a = wire radius, in inches,
- b = wire length, in inches, and
- ln = natural logarithm ($2.303 \times \log_{10}$).

Skin effect (discussed below) changes this formula slightly at VHF and above. As the frequency approaches infinity, the value 0.75 in the above equation increases to approach 1. This effect usually causes a change of no more than a few percent.

As an example, let's find the inductance of a typical #18 wire (diameter = 0.0403 inch and a = 0.0201) that is 4 inches long (b = 4):

$$L = 0.00508 (4) \left[\ln \left(\frac{8}{0.0201} \right) - 0.75 \right]$$

$$= 0.0203 [5.98 - 0.75] = 0.106 \mu\text{H}$$

Wire of this diameter has an inductance of about 25 nH per inch of length. In circuits operating at VHF and higher frequencies, including high-speed digital circuits, the inductance of component leads can become sig-

nificant. (The #24 AWG wire typically used for component leads has an inductance on the order of 20 nH per inch.) At these frequencies, lead inductance can affect circuit behavior, making the circuit hard to reproduce or repair. Good design and construction practice is to minimize the effects of lead inductance by using surface-mount components or trimming the leads to be as short as possible.

The impact of reactance due to parasitic inductance is usually very small; at AF or LF, parasitic inductive reactance of most components is practically zero. To use this example, the reactance of a 0.106 μH inductor even at 10 MHz is only 6.6 Ω . **Figure 5.6** shows a graph of the inductance for wires of various gauges (radii) as a function of length. Whether the reactance is significant or not depends on the application and the frequency of use.

We can represent parasitic inductance in component models by adding an inductor of appropriate value in series with the component since the wire leads are in series with the element. This (among other reasons) is why minimizing lead lengths and interconnecting wires becomes very important when designing circuits for VHF and above.

PARASITIC INDUCTANCE IN RESISTORS

The basic construction of common resistor types is shown in **Figure 5.7**. The primary parasitic effect associated with resistors is parasitic inductance. (Some parasitic capacitance exists between the leads or electrodes due to packaging.) **Figure 5.8** shows some more

accurate circuit models for resistors at low to medium frequencies. The type of resistor with the most parasitic inductance are wire-wound resistors, essentially inductors used as resistors. Their use is therefore limited to dc or low-frequency ac applications where their reactance is negligible. Remember that this inductance will also affect switching transient waveforms, because the component will act as an RL circuit. The inductive effects of wire-wound resistors begin to become significant in the audio range above a few kHz.

As an example, consider a 1- Ω wire-wound resistor formed from 300 turns of #24 wire closely-wound in a single layer 6.3 inches long on a 0.5-inch diameter form. What is its approximate inductance? From the inductance formula for air-wound coils in the **Electrical Fundamentals** chapter:

$$L = \frac{d^2 n^2}{18d + 40l} = \frac{0.5^2 \times 300^2}{(18 \times 0.5) + (40 \times 6.3)} = 86 \mu\text{H}$$

If we want the inductive reactance to be less than 10% of the resistor value, then this resistor cannot be used above $f = 0.1 / (2\pi \times 86 \mu\text{H}) = 185 \text{ Hz}$! Real wire-wound resistors have multiple windings layered over each other to minimize both size and parasitic inductance (by winding each layer in opposite directions, much of the inductance is canceled). If we assume a five-layer winding, the length is reduced to 1.8 inches and the inductance to approximately 17 μH , so the resistor can then be used below 937 Hz. (This has the effect of increasing the resistor's parasitic capacitance, however.)

The resistance of certain types of tubular film resistors is controlled by inscribing a spiral path through the film on the inside of the tube. This creates a small inductance that may be significant at and above the higher audio frequencies.

NON-INDUCTIVE RESISTORS

The resistors with the least amount of parasitic inductance are the bulk resistors, such

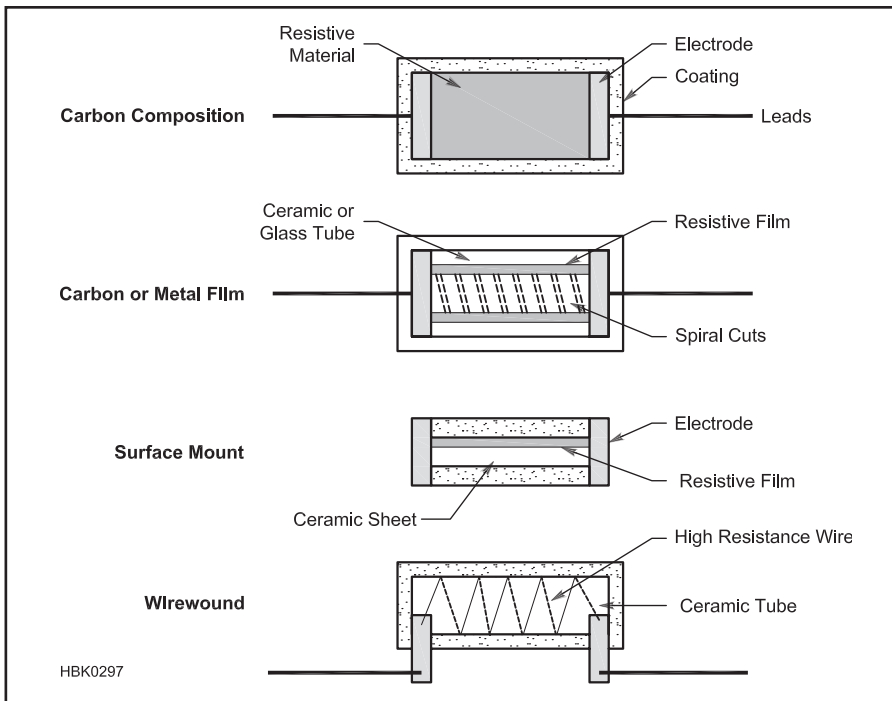


Figure 5.7 — The electrical characteristics of different resistor types are strongly affected by their construction. Reactance from parasitic inductance and capacitance strongly impacts the resistor's behavior at RF.

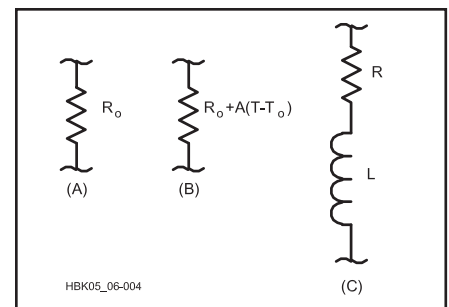


Figure 5.8 — Circuit models for resistors. The wire-wound model with associated inductance is shown at C. B includes the effect of temperature (T). For designs at VHF and higher frequencies, the model at C could be used with L representing lead inductance.

as carbon-composition, metal-oxide, and ceramic resistors. These resistors are made from a single linear cylinder, tube or block of resistive material so that inductance is minimized. Each type of resistor has a maximum usable frequency, above which parasitic capacitance and inductance begin to become significant. Review the manufacturer's data sheet for the component to learn about its performance at high frequencies.

Some resistors advertised as "noninductive" are actually wire-wound resistors with a special winding technique that minimizes inductance. These resistors are intended for use at audio frequencies and are not suitable for use at RF. If you are not sure, ask the vendor if the resistors are suitable for use in RF circuits.

Because resistors are manufactured with an insulating coating, it can be difficult to determine their internal structure and thus estimate their parasitic inductance. In cases where a surplus or used component is to be included, it is recommended that you test the component with an impedance meter or make some other type of reactance measurement if you are unable to access the manufacturer's specifications for the resistor.

PARASITIC INDUCTANCE IN CAPACITORS

The size and shape of a capacitor's plates and the leads used to connect them to circuits create parasitic inductance, often referred to as *equivalent series inductance* (ESL) by capacitor manufacturers. **Figures 5.9** and **5.10** show reasonable models for capacitors that are good up to VHF.

Figure 5.11 shows a roll-type capacitor made of two strips of very thin metal foil and separated by a dielectric. After leads are attached to the foil strips, the sandwich is rolled up and either placed in a metal can or coated with plastic. *Radial leads* both stick out of one end of the roll and *axial leads* from both ends along the roll's axis. Because of the rolled strips, the ESL is high. Electrolytic and many types of film capacitors are made with roll construction. As a result, they are generally not useful in RF circuits.

In the stack capacitor, thin sheets of dielectric are coated on one side with a thin metal layer. A stack of the sheets is placed under pressure and heated to make a single solid unit. Metal side caps with leads attached contact the metal layers. The ESL of stack capacitors is very low and so they are useful at high frequencies. Ceramic and mica capacitors are the most common stack-style capacitor.

Parallel-plate air and vacuum capacitors used at RF have relatively low parasitic inductance, but transmitting capacitors made to withstand high voltages and current are large enough that parasitic inductance becomes significant, limiting their use to low-VHF and lower frequencies. Adjustable capacitors (air

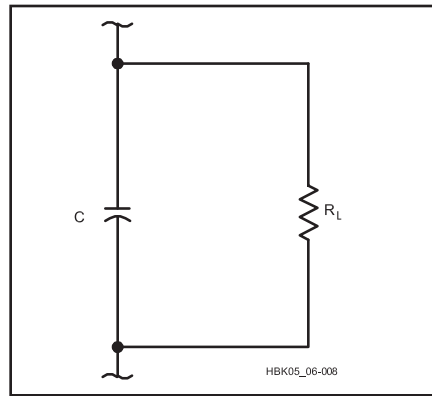


Figure 5.9 — A simple capacitor model for frequencies well below self-resonance.

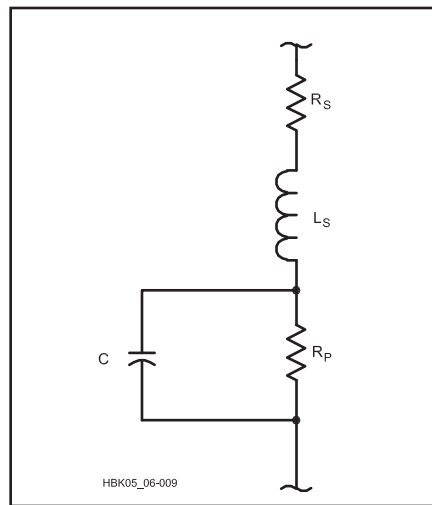


Figure 5.10 — A capacitor model for VHF and above including series resistance and distributed inductance.

variables and compression or piston trimmer capacitors) for tuning low-power circuits are much smaller and so have correspondingly lower parasitic inductance.

It is difficult for a single capacitor to work well over a very wide frequency range, so capacitors are often placed in parallel as discussed in the section below on Bypassing and Decoupling. It is often suggested that different types of capacitors be connected in parallel to avoid the effects of parasitic inductance at different frequencies, but without testing and careful modeling the results are often unpredictable or even counterproductive as the referenced discussion shows.

5.3.2 Parasitic Capacitance

Maxwell's equations also tell us that if the voltage between any two points changes with time, a displacement current is generated between these points as illustrated in **Figure 5.12**. This *displacement current* results from the propagation of the electromagnetic field between the two points and is not to be confused with *conduction current*, which is the movement of electrons. Displacement current is directly proportional to the rate at which the voltage is changing.

When a capacitor is connected to an ac voltage source, a steady ac current can flow because taken together, conduction current and displacement current "complete the loop" from the positive source terminal, across the plates of the capacitor, and back to the negative terminal.

In general, parasitic capacitance shows up *wherever* the voltage between two points is changing with time, because the laws of electromagnetics require a displacement

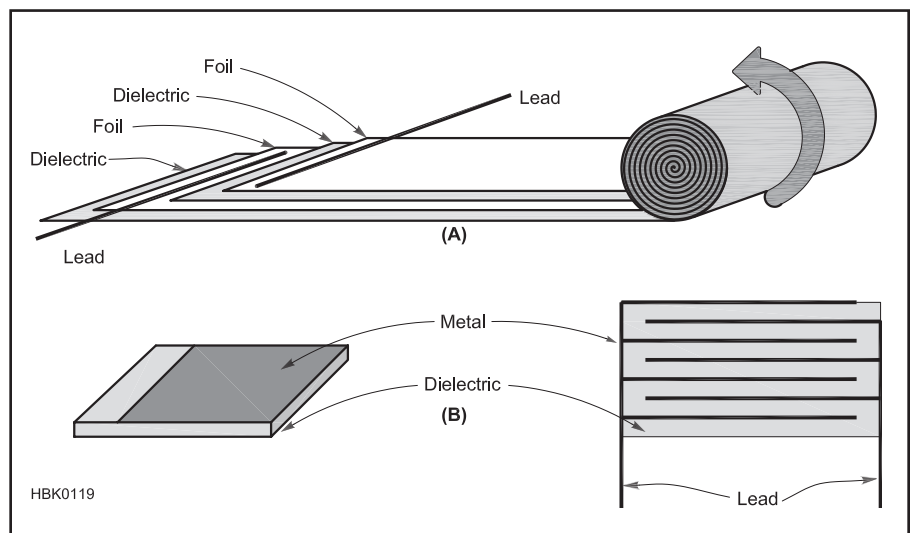


Figure 5.11 — Two common types of capacitor construction. (A) Roll construction uses two strips of foil separated by a strip of dielectric. (B) Stack construction layers dielectric material (such as ceramic or film), one side coated with metal. Leads are attached and the assembly coated with epoxy resin.

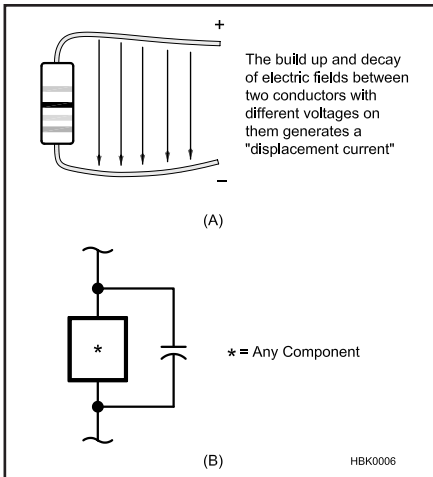


Figure 5.12 — Capacitive consequences of Maxwell's equations. A: Any changing voltage between two points, for example along a bent wire, generates a displacement current running between them. This can be treated mathematically as a capacitance. B adds parasitic capacitance to a generic component model.

current to flow. Since this phenomenon represents an *additional* current path from one point in space to another, we can add this parasitic capacitance to our component models by adding a capacitor of appropriate value in *parallel* with the component. These parasitic capacitances are typically less than 1 pF, so that below VHF they can be treated as open circuits (infinite reactances) and thus neglected.

PACKAGE CAPACITANCE

Another source of capacitance, also in the 1-pF range and therefore important only at

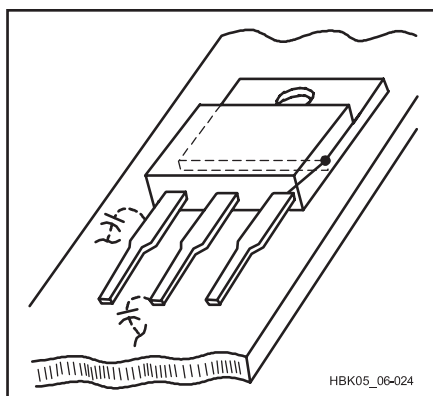


Figure 5.13 — Unexpected stray capacitance. The mounting tab of TO-220 transistors is often connected to one of the device leads. Because one lead is connected to the chassis, small capacitances from the other lead to the chassis appear as additional package capacitance at the device. Similar capacitance can appear at any device with a conductive package.

VHF and above, is the packaging of the component itself. For example, a power transistor packaged in a TO-220 case (see **Figure 5.13**), often has either the emitter or collector connected to the metal tab itself. This introduces an extra *inter-electrode capacitance* across the junctions.

The copper traces on a PC board also create capacitance with the circuit components, to other traces, and to power and ground planes. Double-sided PC boards have a certain capacitance per square inch between the layers of copper on each side of the board. (Multi-layer PC boards have higher values of capacitance due to the smaller separation between layers.) It is possible to create capacitors by leaving unetched areas of copper on both sides of the board. The dielectric constant of inexpensive PC board materials intended for use at low-frequencies is not well-controlled, however, leading to significant variations in capacitance. For this reason, the copper on one side of a double-sided board should be completely removed under frequency-determining circuits such as VFOs.

Stray capacitance (a general term used for any "extra" capacitance that exists due to physical construction) appears in any circuit where two metal surfaces exist at different voltages. Such effects can be modeled as an extra capacitor in parallel with the given points in the circuit. A rough value can be obtained with the parallel-plate formula given in the chapter on **Electrical Fundamentals**. Similar to parasitic inductance, *any* circuit component that has wires attached to it, or is fabricated from wire, or is near or attached to metal, will have a parasitic capacitance associated with it, which again, becomes important only at RF.

Stray capacitance can be difficult to account for in circuit design because it exists *between* components and other circuit structures, depending on the physical orientation of the component. Its presence may allow signals to flow in ways that disrupt the normal operation of a circuit and may have a greater affect in a high-impedance circuit because the capacitive reactance may be a greater percentage of the circuit impedance. Also, because stray capacitance often appears in parallel with the circuit, the stray capacitor may bypass more of the desired signal at higher frequencies. Careful physical design of an RF circuit and selection of components can minimize the effects of stray capacitance.

5.3.3 Self-Resonance

Because of parasitic effects, a capacitor or inductor — all by itself — exhibits the properties of a resonant RLC circuit at frequencies for which the parasitic effects are significant. Figures 5.10 and 5.14 illustrate RF models for the capacitor and inductor, which are based on the general model in Figure 5.4, leaving

out the packaging capacitance. Note the slight difference in configuration; the pairs C_p - R_p and L_s - R_s are in series in the capacitor but in parallel in the inductor. This is because of the different physical structure of the components.

At some sufficiently high frequency, both inductors and capacitors become *self-resonant* when the parasitic reactance cancels or equals the intended reactance, creating a series-resonant circuit. Similar to a series-resonant circuit made of discrete components, above the self-resonant frequency a capacitor will appear inductive, and an inductor will appear capacitive.

For an example, let's calculate the approximate self-resonant frequency of a 470-pF capacitor whose leads are made from #20 AWG wire (0.032-inch diameter), with a total length of 1 inch. Using equation 1, we calculate the approximate parasitic inductance

$$L (\mu\text{H}) = 0.00508 (l) \left[\ln \left(\frac{2(l)}{(0.032/2)} \right) - 0.75 \right]$$

$$= 0.021 \mu\text{H}$$

and the self-resonant frequency is roughly

$$f = \frac{1}{2\pi\sqrt{LC}} = 50.6 \text{ MHz}$$

Similarly, an inductor can also have a parallel self-resonance.

The purpose of making these calculations is to provide a feel for actual component values. They could be used as a rough design guideline, but should not be used quantitatively. Other factors such as lead orientation, shielding and so on, can alter the parasitic effects to a large extent. Large-value capacitors tend to have higher parasitic inductances (and therefore a lower self-resonant frequency) than small-value capacitors.

Self-resonance becomes critically important at VHF and UHF because the self-resonant frequency of many common components is at or below the frequency where the component will be used. In this case, either special techniques can be used to construct components to operate at these frequencies, by reducing the parasitic effects, or else the idea of lumped elements must be abandoned altogether in favor of microwave techniques such as striplines and waveguides.

5.3.4 Inductors and RF Chokes at Radio Frequencies

Inductors are perhaps the component with the most significant parasitic effects. Where there are many different varieties of form for capacitors and resistors, most inductors are fundamentally similar: a coil of wire on a tubular or toroidal form. As such, they are affected by both parasitic resistance and capacitance as shown in the simple inductor model of **Figure 5.14**.

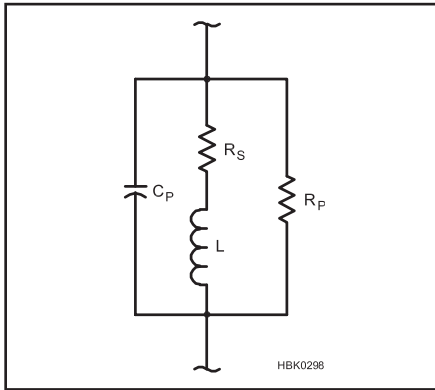


Figure 5.14 — General model for inductor with parasitic capacitance and resistance. The parasitic capacitance represents the cumulative effect of the capacitance between the different turns of wire. Parasitic resistance, R_S , depends on frequency due to the skin effect. R_P represents leakage resistance. At low frequencies, parasitic capacitance, C_P , can be neglected.

While the leakage conductance of a capacitor is usually negligible, the series resistance of an inductor often is not. This is caused by the long lengths of thin wire needed to create typical inductance values used in RF circuits and the skin effect (discussed below). Consider a typical air-core inductor, with $L = 33 \mu\text{H}$ and a minimum Q of 30 measured at 2.5 MHz. This would indicate a series resistance of $R_S = 2 \pi f L / Q = 17 \Omega$ that could significantly alter the bandwidth of a circuit. The skin effect also results in parasitic resistance in the upper HF ranges and above. To minimize losses due to the skin effect, inductors at these frequencies, particularly those intended for use in transmitters and amplifiers and that are expected to carry significant currents, are often made from large-diameter wire or tubing or even flat strap to maximize the surface area for current flow.

For coils with many turns for which large conductors are impractical, *Litz wire* is sometimes used. Litz wire is made of many fine insulated strands woven together, each with a diameter smaller than the skin depth at the expected frequency of use, thus presenting a larger surface area than a solid wire or normal stranded wire. This creates multiple resistive inductors in parallel, which reduces the total impedance. The reduction is not proportional to the number of parallel paths, however, because they are inductively coupled.

If an inductor is wound on a magnetic core, the core itself can have losses that are treated as parasitic resistance. Each type of core — iron, powdered iron or ferrite — has a frequency range over which it is designed for maximum efficiency. Outside of that range, the core may have significant losses, raising the parasitic resistance of the inductor.

Parasitic capacitance is a particular concern for inductors because of their construc-

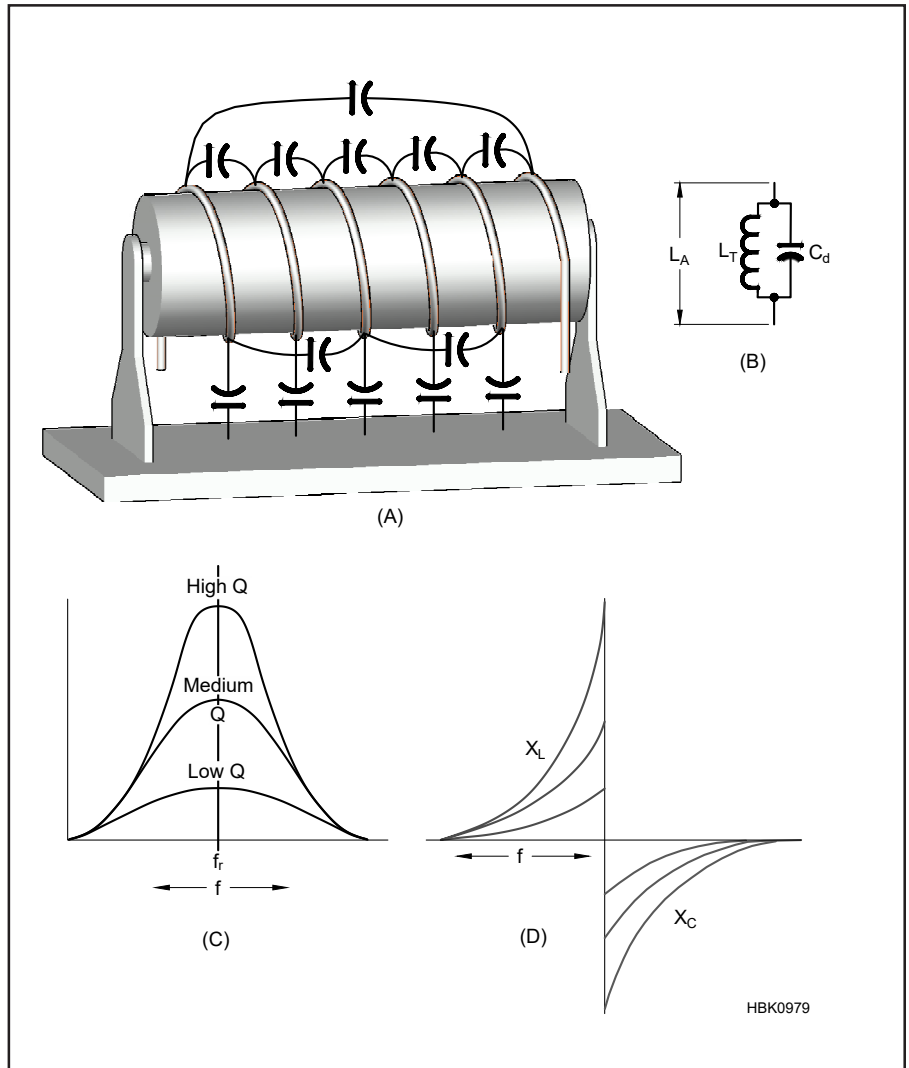


Figure 5.15 — Coils have distributed capacitance (A) between windings and from the coil to adjacent structures. This forms a parallel tuned circuit as shown in B with a resonant frequency, f_r . The coil's impedance and reactance vary with frequency as at C and D. Below resonance, the reactance is inductive and above resonance, the reactance is capacitive.

tion. Consider the inductor in **Figure 5.15**. If this coil has n turns, then the ac voltage between identical points of two neighboring turns is $1/n$ times the ac voltage across the entire coil. When this voltage changes due to an ac current passing through the coil, the effect is that of many small capacitors acting in parallel with the inductance of the coil. Thus, in addition to the capacitance resulting from the leads, inductors have higher parasitic capacitance due to their physical shape.

These various effects illustrate why inductor construction has such a large effect on performance. As an example, assume you're working on a project that requires you to wind a $5 \mu\text{H}$ inductor. Looking at the coil inductance formula in the **Electrical Fundamentals** chapter, it comes to mind that many combinations of length and diameter could yield the desired inductance. If you happen to have both 0.5 and 1-inch coil forms, why should

you select one over the other? To eliminate some other variables, let's make both coils 1 inch long, close-wound, and give them 1-inch leads on each end.

Let's calculate the number of turns required for each. On a 0.5-inch-diameter form:

$$n = \frac{\sqrt{L(18d + 40l)}}{d} = \frac{\sqrt{5[(18 \times 0.5) + (40 \times 1)]}}{0.5} = 31.3 \text{ turns}$$

This means coil 1 will be made from #20 AWG wire (29.9 turns per inch). Coil 2, on the 1-inch form, yields

$$n = \frac{\sqrt{5[(18 \times 1) + (40 \times 1)]}}{1} = 17 \text{ turns}$$

which requires #15 AWG wire in order to be close-wound.

What are the series resistances associated

with each? For coil 1, the total wire length is 2 inches + $(31.3 \times \pi \times 0.5) = 51$ inches, which at $10.1 \Omega / 1000$ ft gives $R_s = 0.043 \Omega$ at dc. Coil 2 has a total wire length of 2 inches + $(17.0 \times \pi \times 1) = 55$ inches, which at $3.18 \Omega / 1000$ ft gives a dc resistance of $R_s = 0.015 \Omega$, or about $\frac{1}{3}$ that of coil 1. Furthermore, at RF, coil 1 will begin to suffer from skin effect at a frequency about 3 times lower than coil 2 because of its smaller conductor diameter. Therefore, if Q were the sole consideration, it would be better to use the larger diameter coil.

Q is not the only concern, however. Such coils are often placed in shielded enclosures. A common rule of thumb says that to prevent the enclosure from affecting the inductor, the enclosure should be at least one coil diameter from the coil on all sides. That is, $3 \times 3 \times 2$ inches for the large coil and $1.5 \times 1.5 \times 1.5$ for the small coil, a volume difference of over 500%.

RF CHOKES

An RF choke is an inductor intended to pass low-frequency ac and dc power while presenting a high impedance to RF. They are not intended for use in tuned circuits, filters, or other high-Q applications. (A detailed online article “How to Select R.F. Chokes” is available on the RF Café website, www.rfcafe.com/references/electronics-world/select-rf-chokes-may-1966-electronics-world.htm.)

Miniature and subminiature chokes are similar in size to resistors, both through-hole and SMT. They use a small ferrite core and very fine wire. Chokes with a metal shield around them to reduce coupling (see next section) are available. DC current ratings for these chokes are fairly low — typically tens of mA at most. Inductance values range from nanohenries to millihenries for use in low-power audio and RF circuits or for managing EMI.

Power supplies often use high-current chokes wound on ferrite rods to block common-mode RF from getting into or out of equipment. Inductance of $10 \mu\text{H}$ to several hundred μH and current ratings up to 10 A are typical, with wire windings using heavy solid enameled wires.

Medium-duty chokes of several hundred μH to several mH are often wound on ceramic forms in several sections to minimize distributed capacitance. Each section is made of multiple turns formed into a small disk. The disks look a bit like a pie so these chokes are called “pie-wound” (also “pi-wound”). These are common in older tube equipment and high-power RF circuits. A photo of this type of RF choke is shown in the **Electrical Fundamentals** chapter’s section on inductors.

Heavy-duty transmitting chokes used in tube equipment are usually employed in the plate circuit to block RF from getting back into the high-voltage supply. Values of $100 \mu\text{H}$ to several hundred μH are typical with rat-

ings of several amps for plate chokes used at HF. Filament chokes have to handle many amps of low-voltage ac with the same range of inductance values.

An RF choke performs best well below its self-resonant frequency (SRF) but it can be used throughout the range for which it has an acceptably high impedance. The choke’s impedance will be inductive below the SRF and capacitive above the SRF (see Figure 5.15). If the choke is going to be used in a high-power transmitting circuit, resonances may produce very high voltages at one or more points along the coil. This can cause arcing and damage to the choke. These chokes are often specially wound to minimize the effect of resonances but this must be done to suit the exact application since distributed capacitance to the enclosure and other components affects the SRF.

Tom Rauch, W8JI, has written an informative paper about SRF and plate chokes which can be viewed at www.w8ji.com/rf_plate_choke.htm. His companion web page on inductors used in high-power RF circuits (www.w8ji.com/loading_inductors.htm) is also very informative.

Selecting the right type of choke is important to the success of the circuit. Like capacitors, there are many types of chokes with different characteristics. A reliable guide is to inspect well-engineered commercial equipment of the same type and frequency range to see what type of inductors are used. Handbooks and articles on equipment and choke design are also helpful, particularly for high-power applications. Manufacturer application notes and selection guides, such

as the Coilcraft “RF Inductor Design Center” (www.coilcraft.com/rfdc.cfm) are also helpful for lower-power circuits.

When selecting the choke, your choke will need to be rated adequately for the dc current load with a low dc voltage drop. The SRF should be higher than the frequency of use or at least have a high impedance. Be sure the Q is high enough to avoid excessive RF power dissipation. Finally, any magnetic core (powdered iron or ferrite) should be intended for the frequency of use.

INDUCTOR COUPLING

Mutual inductance (see the **Electrical Fundamentals** chapter) will also have an effect on the resonant frequency and Q of RF circuits. For this reason, inductors in frequency-critical circuits should always be oriented and with sufficient spacing to minimize coupling. For example, mount coils near each other with their axes perpendicular as in **Figure 5.16**. The use of ferrous cores also tends to keep magnetic fields within the

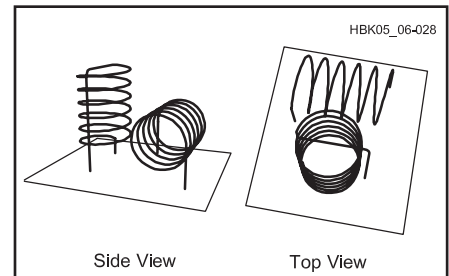


Figure 5.16 — Unshielded coils in close proximity should be mounted perpendicular to each other to minimize coupling.

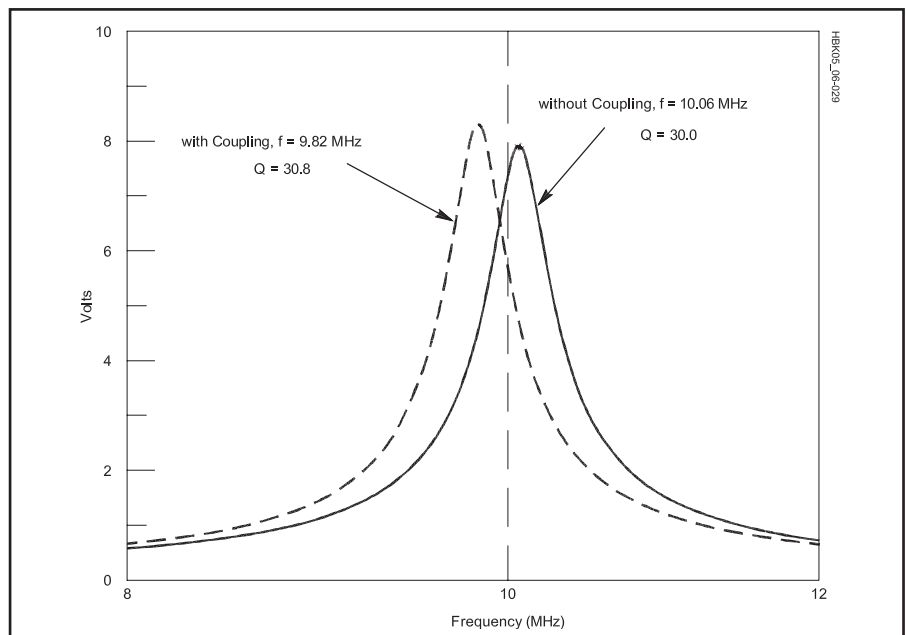


Figure 5.17 — Result of light coupling ($k = 0.05$) between two identical circuits of Figure 5.19A on their frequency responses.

core, reducing unwanted coupling.

As an example, assume we build an oscillator circuit that has both input and output resonant circuits. If we are careful to keep the two coils in these circuits uncoupled, the frequency response of either of the two circuits is shown by the solid line in **Figure 5.17**.

If the two coils are coupled either through careless placement or improper shielding, the resonant frequency and Q will be affected. The dashed line in Figure 5.17 shows the frequency response that results from a coupling coefficient of $k = 0.05$, a reasonable value for air-wound inductors mounted perpendicularly in close proximity on a circuit chassis. Note the resonant frequency shifted from 10.06 to 9.82 MHz, or 2.4%. The Q has gone up slightly from 30.0 to 30.8 as a result of the slightly higher inductive reactance at the resonant frequency.

Capacitance between coils can also affect a circuit's frequency response. Using shielded inductors or can-mounted coils reduces the effects of stray capacitance between components.

5.3.5 Skin Effect

The resistance of a conductor to ac is different than its value for dc because of the way ac fields interact with the conductor. As a result, thick, near-perfect conductors (such as metals) conduct ac only to a certain *skin depth*, δ , inversely proportional to the square root of the frequency of the current. Called the *skin effect*, this decreases the effective cross-section of the conductor at high frequencies and thus increases its resistance.

$$\delta = \frac{1}{\sqrt{\pi f \mu \sigma}} \quad (2)$$

where

μ is the conductor's permeability, and
 σ is the conducting material's conductance.

The increase in resistance caused by the skin effect is insignificant at and below audio frequencies, but beginning around 1 MHz (depending on the size of the conductor) it is so pronounced that practically all the current flows in a very thin layer near the conductor's surface. For example, at 10 MHz, the skin depth of a copper conductor is about 0.02 mm (0.00079 inch). For this reason, at RF a hollow tube and a solid rod of the same diameter and made of the same metal will have the same resistance and the RF resistance of a conductor is often much higher than its dc resistance. A rough estimate of the frequency above which a nonmagnetic wire (one made of nonferrous metal) will begin to show appreciable skin effect can be calculated from

$$f = \frac{124}{d^2} \quad (3)$$

where

f = frequency, in MHz, and
 d = diameter in mils (a mil is 0.001 inch).

Above this frequency, increase the resistance of the wire by 10× for every 2 decades of frequency (roughly 3.2× for every decade). For example, say we wish to find the RF resistance of a 2-inch length of #18 AWG copper wire at 100 MHz. From the wire tables in the **Component Data and References** chapter, we see that this wire has a dc resistance of 2 inches \times 6.386 Ω /1000 ft = 1.06 m Ω . From the above formula, the frequency is found to be $124 / 40.3^2 = 76$ kHz. Since 100 MHz is roughly three decades above this (100 kHz to 100 MHz), the RF resistance will be approximately $1.06 \text{ m}\Omega \times 3.2^3 = 1.06 \text{ m}\Omega \times 32.8 = 34.8 \text{ m}\Omega$. Again, values calculated in this manner are approximate and should be used qualitatively — like when you want an answer to a question such as, "Can I neglect the RF resistance of this length of connecting wire at 100 MHz?" Several useful charts regarding skin effect are available in *Reference Data for Engineers*, listed in the References section of this chapter.

Losses associated with skin effect can be reduced by increasing the surface area of the conductor carrying the RF current. Flat, solid strap and tubing are often used for that reason. In addition, because the current-carrying layer is so thin at UHF and microwave frequencies, a thin highly conductive layer at the surface of the conductor, such as silver plating, can lower resistance. Silver plating is too thin to improve HF conductivity significantly, however.

5.3.6 RF Heating

RF current often causes component heating problems where the same level of dc or low frequency ac current may not. These losses result from both the skin effect and from dielectric losses in insulating material, such as a capacitor dielectric.

An example is the tank circuit of an RF oscillator. If several small capacitors are connected in parallel to achieve a desired capacitance, skin effect will be reduced and the total surface area available for heat dissipation will be increased, thus significantly reducing the RF heating effects as compared to a single large capacitor. This technique can be applied to any similar situation; the general idea is to divide the heating among as many components as possible.

An example is shown in the circuit block in **Figure 5.18**, which is representative of the input tank circuit used in many HF VFOs. Along with L, C_{main} , C_{trim} , C1 and C3 set the oscillator frequency. Therefore, temperature effects are critical in these components. By using several capacitors in parallel, the

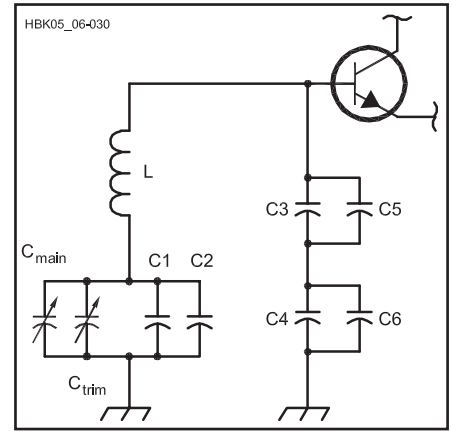


Figure 5.18 — A tank circuit of the type commonly used in VFOs. Several capacitors are used in parallel to distribute the RF current, which reduces temperature effects.

RF current (and resultant heating, which is proportional to the square of the current) is reduced in each component. Parallel combinations are used for the feedback capacitors for the same reason.

At high power levels, losses due to RF heating — either from resistive or dielectric losses — can be significant. Insulating materials may exhibit dielectric losses even though they are excellent insulators. For example, nylon plastic insulators may work very well at low frequencies, but being quite lossy at and above VHF, they are unsuitable for use in RF circuits at those frequencies. To determine whether material is suitable for use as an insulator at RF, a quick test can be made by heating the material in a microwave oven for a few seconds and measuring its temperature rise. (Take care to avoid placing parts or materials containing any metal in the microwave!) Insulating materials that heat up are lossy and thus unsuitable for use in RF circuits.

5.3.7 Effect on Q

Recall from the **Electrical Fundamentals** chapter that circuit Q, a useful figure of merit for tuned RLC circuits, can be defined in several ways:

$$Q = \frac{X_L \text{ or } X_C}{R} = \frac{\text{energy stored per cycle}}{\text{energy dissipated per cycle}} \quad (4)$$

Q is also related to the bandwidth of a tuned circuit's response by

$$Q = \frac{f_0}{\text{BW}_{3 \text{ dB}}} \quad (5)$$

Parasitic inductance, capacitance and resistance can significantly alter the performance

and characteristics of a tuned circuit if the design frequency is close to the self-resonant frequencies of the components.

As an example, consider the resonant circuit of **Figure 5.19A**, which could represent the frequency-determining resonant circuit of an oscillator. Neglecting any parasitics,

$$f_0 = \frac{1}{2\pi\sqrt{LC}} = 10.06 \text{ MHz}$$

As in many practical cases, assume the resistance arises entirely from the inductor series resistance. The data sheet for the inductor specified a minimum Q of 30, so assuming $Q = 30$ yields an R value of

$$\frac{X_L}{Q} = \frac{2\pi(10.06 \text{ MHz})(5 \mu\text{H})}{30} = 10.5 \Omega$$

Next, let's include the parasitic inductance of the capacitor (Figure 5.19B). A reason-

able assumption is that this capacitor has the same physical size as the example from the section on Parasitic Inductance for which we calculated $L_s = 0.106 \mu\text{H}$. This would give the capacitor a self-resonant frequency of 434 MHz — well above our frequency of interest. However, the added parasitic inductance does account for an extra $0.106/5.0 = 2\%$ inductance. Since this circuit is no longer strictly series or parallel, we must convert it to an equivalent form before calculating the new f_0 .

An easier and faster way is to *simulate* the altered circuit by computer. This analysis was performed on a desktop computer using *SPICE*, a standard circuit simulation program described in the **Electronic Design Automation (EDA)** chapter. The voltage response of the circuit (given an input current of 1 mA) was calculated as a function of frequency

for both cases, with and without parasitics. The results are shown in the plot in Figure 5.19C, where we can see that the parasitic circuit has an f_0 of 9.96 MHz (a shift of 1%) and a Q (measured from the -3 dB points) of 31.5. For comparison, the simulation of the unaltered circuit does in fact show $f_0 = 10.06 \text{ MHz}$ and $Q = 30$.

5.3.8 Dielectric Breakdown and Arcing

Anyone who has ever seen an arc form across a transmitting capacitor's plates, seen static discharges jump across an antenna insulator or touched a metal doorknob on a dry day has experienced the effects of dielectric breakdown.

In the ideal world, we could take any two conductors and put as large a voltage as we want across them, no matter how close together they are. In the real world, there is a voltage limit (*dielectric strength*, measured in kV/cm and determined by the insulating material between the two conductors) above which the insulator will break down.

Because they are charged particles, the electrons in the atoms of a dielectric material feel an attractive force when placed in an electric field. If the field is sufficiently strong, the force will strip the electron from the atom. This electron is available to conduct current, and furthermore, it is traveling at an extremely high velocity. It is very likely that this electron will hit another atom, and free another electron. Before long, there are many stripped electrons producing a large current, forming an *arc*. When this happens, we say the dielectric has suffered *breakdown*. Arcing in RF circuits is most common in transmitters and transmission line components where high voltages are common, but it is possible anywhere two components at significantly different voltage levels are closely spaced.

If the dielectric is liquid or gas, it will repair itself when the applied voltage is removed and the molecules in the dielectric return to their normal state. A solid dielectric, however, cannot repair itself because its molecules are fixed in place and the low-resistance path created by the arc is permanent. A good example of this is a CMOS integrated circuit. When exposed to the very high voltages associated with static electricity, the electric field across the very thin gate oxide layer exceeds the dielectric strength of silicon dioxide, and the device is permanently damaged by the resulting hole created in the oxide layer.

The breakdown voltage of a dielectric layer depends on its composition and thickness (see **Table 5.1**). The variation with thickness is not linear; doubling the thickness does not quite double the breakdown voltage. Breakdown voltage is also a function of geometry: Because of electromagnetic considerations,

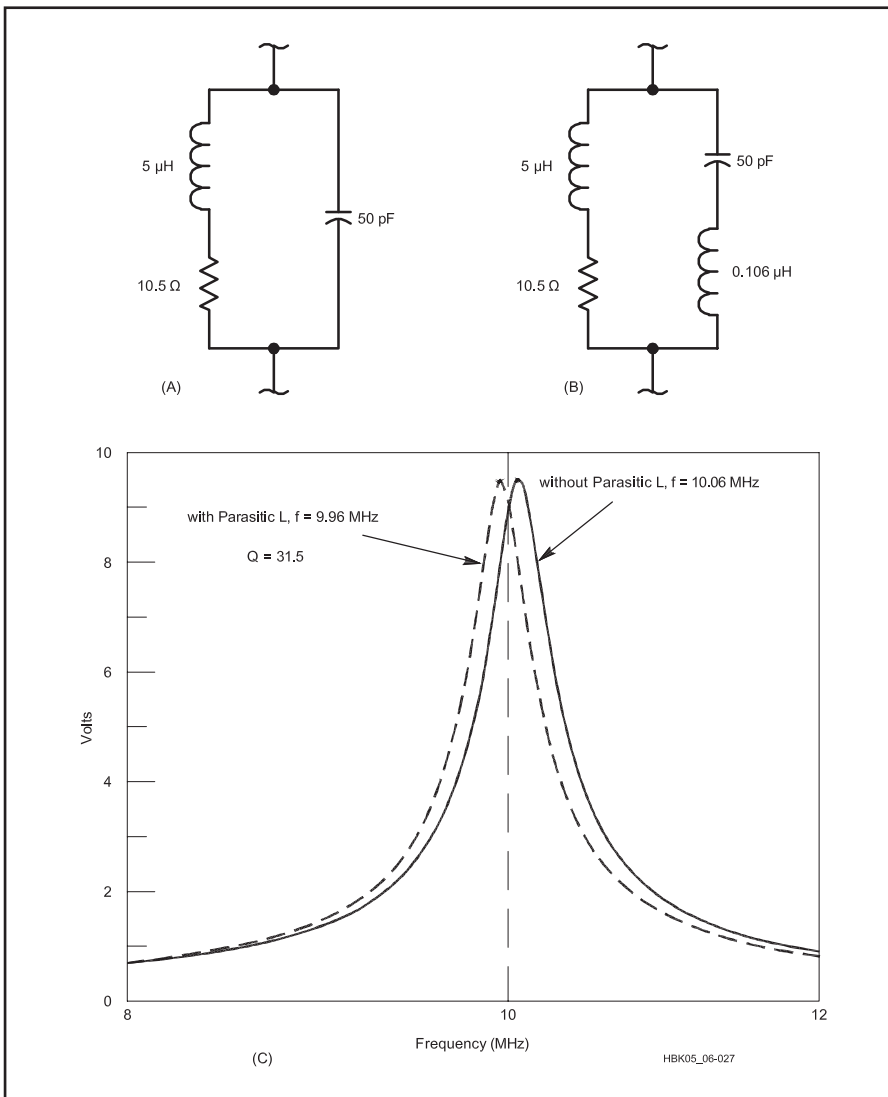


Figure 5.19 — A is a tank circuit, neglecting parasitics. B is the same circuit including L_p on capacitor. C is the frequency response curves for A and B. The solid line represents the unaltered circuit (also see Figure 5.17) while the dashed line shows the effects of adding parasitic inductance.

Table 5.1

Dielectric Constants and Breakdown Voltages

Material	Dielectric Constant*	Puncture Voltage**
Aisimag 196	5.7	240
Bakelite	4.4-5.4	240
Bakelite, mica filled	4.7	325-375
Cellulose acetate	3.3-3.9	250-600
Fiber	5-7.5	150-180
Formica	4.6-4.9	450
Glass, window	7.6-8	200-250
Glass, Pyrex	4.8	335
Mica, ruby	5.4	3800-5600
Mycalex	7.4	250
Paper, Royalgrey	3.0	200
Plexiglas	2.8	990
Polyethylene	2.3	1200
Polystyrene	2.6	500-700
Porcelain	5.1-5.9	40-100
Quartz, fused	3.8	1000
Steatite, low loss	5.8	150-315
Teflon	2.1	1000-2000

*At 1 MHz

**In volts per mil (0.001 in.)

the breakdown voltage between two conductors separated by a fixed distance is less if the surfaces are pointed or sharp-edged than if they are smooth or rounded. Therefore, a simple way to help prevent breakdown in many projects is to file and smooth the edges of conductors. (See the **Power Sources** and **RF Power Amplifier** chapters for additional information on high voltage applications.)

Capacitors are, by nature, the component most often associated with dielectric failure. To prevent damage, the working voltage of a capacitor — and there are separate dc and ac ratings — should ideally be two or three times the expected maximum voltage in the circuit. Capacitors that are not air-insulated or have a *self-healing dielectric* should be replaced if a dielectric breakdown occurs.

Resistors and inductors also have voltage ratings associated with breakdown of their insulating coating. High-value resistors, in particular, can be bypassed by leakage current flowing along the surface of the resistor. High-voltage resistors often have elongated bodies to create a long *leakage path* to present a high resistance to leakage current. Cleaning the bodies of resistors and inductors in high-voltage circuits helps prevent arcs from forming and minimizes leakage current.

5.3.9 Radiative Losses

Any conductor placed in an electromagnetic field will have a current induced in it. We put this principle to good use when we make an antenna. The unwelcome side of this law of nature is the phrase “any conductor;” even conductors we don’t intend to act as antennas will respond this way.

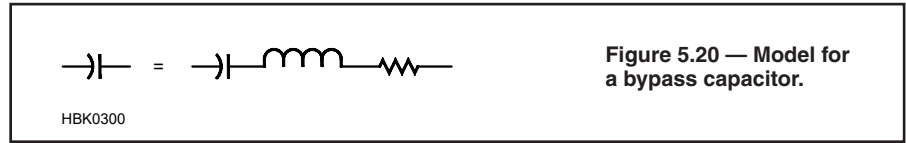


Figure 5.20 — Model for a bypass capacitor.

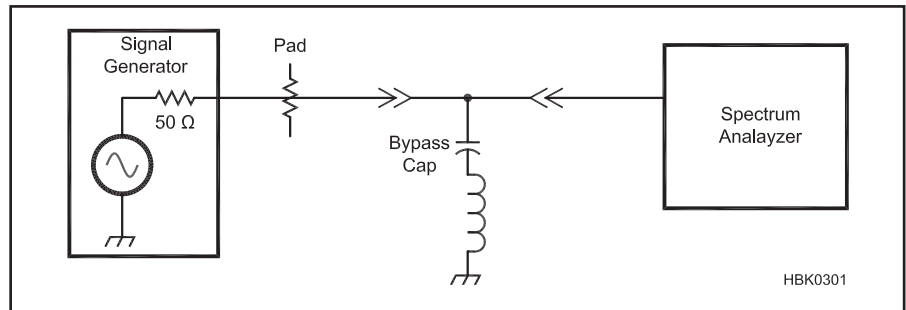


Figure 5.21 — Test set for home lab measurement of a bypass capacitor.

Fortunately, the efficiency of such “antennas” varies with conductor length. They will be of importance only if their length is a significant fraction of a wavelength. When we make an antenna, we usually choose a length on the order of $\lambda/2$. Therefore, when we *don’t* want an antenna, we should be sure that the conductor length is *much less* than $\lambda/2$, no more than 0.1λ . This will ensure a very low-efficiency antenna. This is why even unpaired 60-Hz power lines do not lose a significant fraction of the power they carry — at 60 Hz, 0.1λ is about 300 miles!

In addition, we can use shielded cables. Such cables do allow some penetration of EM fields if the shield is not solid, but even 95% coverage is usually sufficient, especially if some sort of RF choke is used to reduce shield current.

Radiative losses and coupling can also be reduced by using twisted or parallel pairs of conductors — the fields tend to cancel. In some applications, such as audio cables, this may work better than shielding. Critical stages such as tuned circuits should be placed in shielded compartments where possible.

This argument also applies to large components — remember that a component or long wire can both radiate and receive RF energy. Measures that reduce radiative losses will also reduce unwanted RF pickup. See the **RFI and EMC** chapter for more information.

5.3.10 Bypassing and Decoupling

BYPASSING

Circuit models showing ac behavior often show ground connections that are not at dc ground. Bias voltages and currents are neglected in order to show how the circuit responds to ac signals. Rather, those points are “signal grounded” through bypass capacitors.

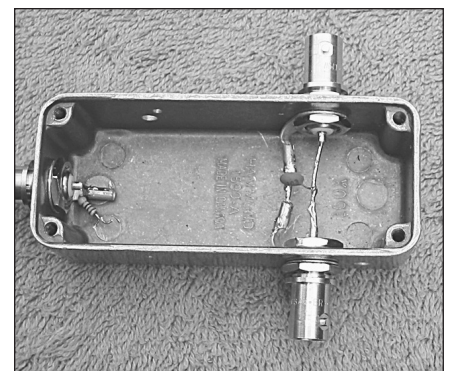


Figure 5.22 — Test fixture for measuring self-resonant frequency of capacitors.

Obtaining an effective bypass can be difficult and is often the route to design difficulty. The problem is parasitic inductance. Although we label and model parts as “capacitors,” a more complete model is needed. The better model is a series RLC circuit, shown in **Figure 5.20**. Capacitance is close to the marked value while inductance is a small value that grows with component lead length. Resistance is a loss term, usually controlled by the Q of the parasitic inductor. Even a leadless SMT (surface-mount technology) component will display inductance commensurate with its dimensions. As shown in the Parasitic Inductance section, wire component leads have an inductance of about 1 nH per mm of length (20-25 nH per inch).

Bypass capacitor characteristics can be measured in the home lab with the test setup of **Figure 5.21**. **Figure 5.22** shows a test fixture with an installed 470-pF leaded capacitor. The fixture is used with a signal generator and spectrum analyzer to evaluate capacitors. Relatively long capacitor leads were required to interface to the BNC connectors, even though the capacitor itself was small. The signal generator was tuned over its

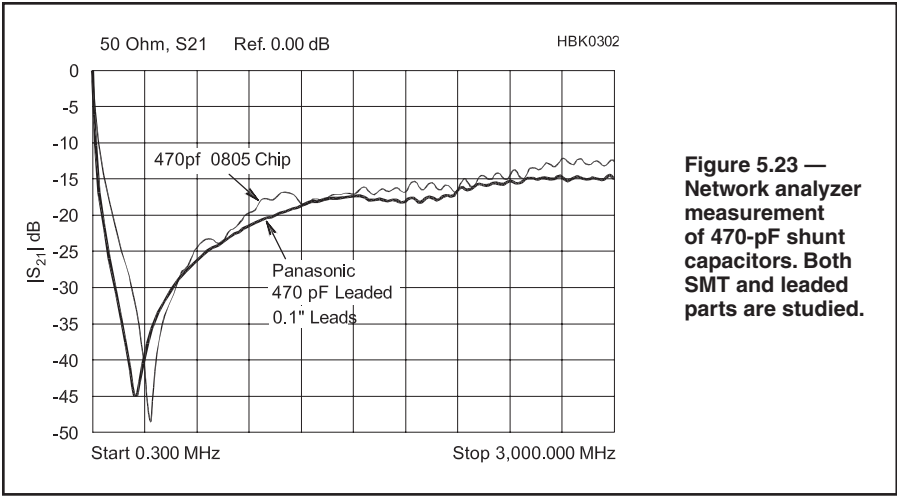


Figure 5.23 — Network analyzer measurement of 470-pF shunt capacitors. Both SMT and leaded parts are studied.

range while examining the spectrum analyzer response, showing a minimum at the series resonant frequency. Parasitic inductance is calculated from this frequency. The C value was measured with a low-frequency LC meter. Additional test instruments and techniques are discussed in the **Test Equipment and Measurement** chapter.

The measured 470-pF capacitor is modeled as 485 pF in series with an inductance of 7.7 nH. The L is larger than we would see with shorter leads. A 0.25-inch 470-pF ceramic disk capacitor with zero lead length will show a typical inductance closer to 3 nH. The measured capacitor Q was 28 at its self-resonance of 82 MHz but is higher at lower frequency. Data from a similar measurement, but with a network analyzer is shown in **Figure 5.23**. Two 470-pF capacitors are measured, one surface mounted and the other a leaded part with 0.1-inch leads.

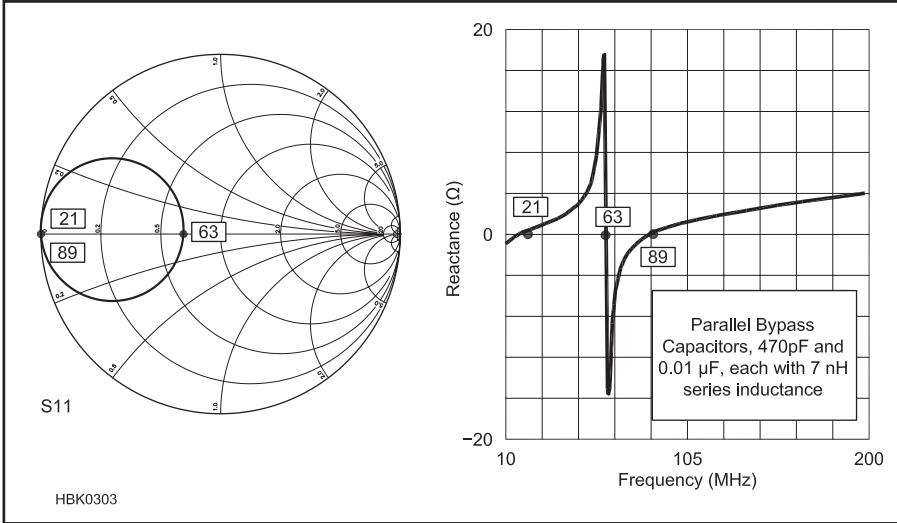


Figure 5.24 — The classic technique of paralleling bypass capacitors of two values, here 470 pF and 0.01 μF. This is a terrible bypass! See text.

It is often suggested that the bandwidth for bypassing can be extended by paralleling a capacitor that works well at one frequency with another to accommodate a different part of the spectrum. Hence, paralleling the 470 pF with a 0.01-μF capacitor should extend the bypassing to lower frequencies. The calculations are shown in the plots of **Figure 5.24**. The results are terrible! While the low frequency bypassing is indeed improved, a high impedance response is created at 63 MHz. This complicated behavior is again the result of inductance. Each capacitor was assumed to have a series inductance of 7 nH. A parallel resonance is approximately formed between the L of the larger capacitor and the C of the smaller. The Smith Chart plot shows us that the impedance is nearly 50 Ω at 63 MHz. Impedance would be even higher with greater capacitor Q.

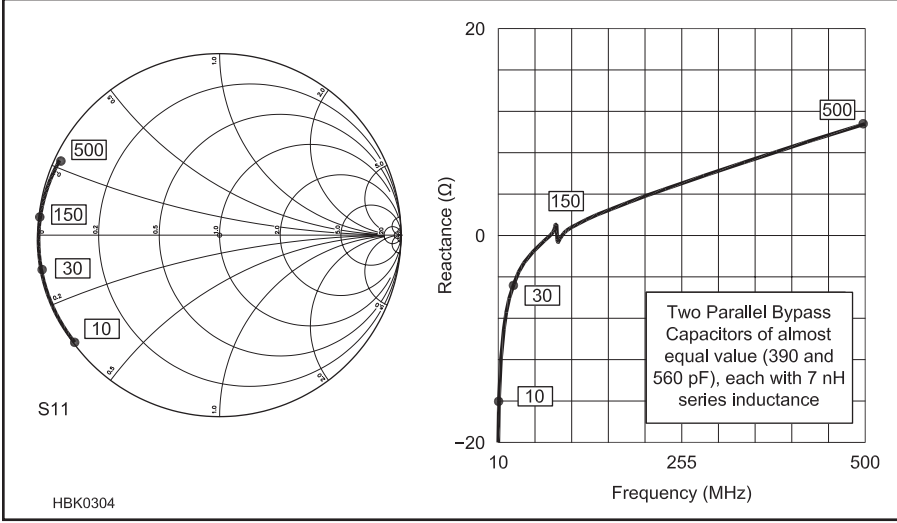


Figure 5.25 — Paralleling bypass capacitors of nearly the same value. This results in improved bypassing without complicating resonances.

Bypassing can be improved by paralleling capacitors. However, the capacitors should be approximately identical. **Figure 5.25** shows the result of paralleling two capacitors of about the same value. They differ slightly at 390 and 560 pF, creating a hint of resonance. This appears as a small perturbation in the reactance plot and a tiny loop on the Smith Chart. These anomalies disappear as the C values become equal. Generally, paralleling is the scheme that produces the best bypassing. The ideal solution is to place an SMT capacitor on each side of a printed circuit trace or wire at a point that is to be bypassed.

Matched capacitor pairs form an effective bypass over a reasonable frequency range. Two 0.01-μF disk capacitors have a reactance magnitude less than 5 Ω from 2 to 265 MHz. A pair of the 0.1-μF capacitors was even better, producing the same bypassing impedance from 0.2 to 318 MHz. The 0.1-μF capacitors are chip-style components with attached wire leads. Even better results can be obtained with multi-layer ceramic chip capacitors. Construction with multiple layers

creates an integrated paralleling.

Some applications (for example, IF amplifiers) require effective bypassing at even lower frequencies. Modern tantalum electrolytic capacitors are surprisingly effective through the RF spectrum while offering high enough C to be useful at audio. In critical applications, however, the parts should be tested to be sure of their effectiveness.

DECOUPLING

The bypass capacitor usually serves a dual role, first creating the low impedance needed to generate a “signal” ground. It also becomes part of a decoupling low-pass filter that passes dc while attenuating signals. The attenuation must function in both directions, suppressing noise in the power supply that might reach an amplifier while keeping amplifier signals from reaching the power supply. A low-pass filter is formed with alternating series and parallel component connections. A parallel bypass is followed by a series impedance, ideally a resistor.

Additional shunt elements can then be added, although this must be done with care. An inductor between shunt capacitors should have high inductance. It will resonate with the shunt capacitors to create high impedances just like those that came from parasitic inductance in the bypasses. This makes it desirable to have an inductance that is high enough that any resonance is below the band of interest. But series inductors have their own problems; they have parasitic capacitance, creating their own self-resonance. As an example, a pair of typical RF chokes (RFCs) were measured (now as series elements) as described earlier. A 2.7- μH molded choke was parallel resonant at 200 MHz, indicating a parallel capacitance of 0.24 pF. The Q at 20 MHz was 52. A 15- μH molded choke was parallel resonant at 47 MHz, yielding a parallel C of 0.79 pF. This part had a Q of 44 at 8 MHz.

Large inductors can be fabricated from series connections of smaller ones. The best wideband performance will result only when all inductors in a chain have about the same value. The reasons for this (and the mathematics that describe the behavior) are identical with those for paralleling identical capacitors.

Low inductor Q is often useful in decoupling applications, encouraging us to use inductors with ferrite cores. Inductors using the Fair-Rite Type #43 material have low Q in the 4 to 10 range over the HF spectrum. One can also create low-Q circuits by paralleling a series inductor of modest Q with a resistor.

Figure 5.26 shows a decoupling network and the resulting impedance when viewed from the “bypass” end. The 15- μH RFC resonates with a 0.1- μF capacitor to destroy the bypass effect just above 0.1 MHz. A low-value parallel resistor fixes the problem.

A major reason for careful wideband bypassing and decoupling is the potential for am-

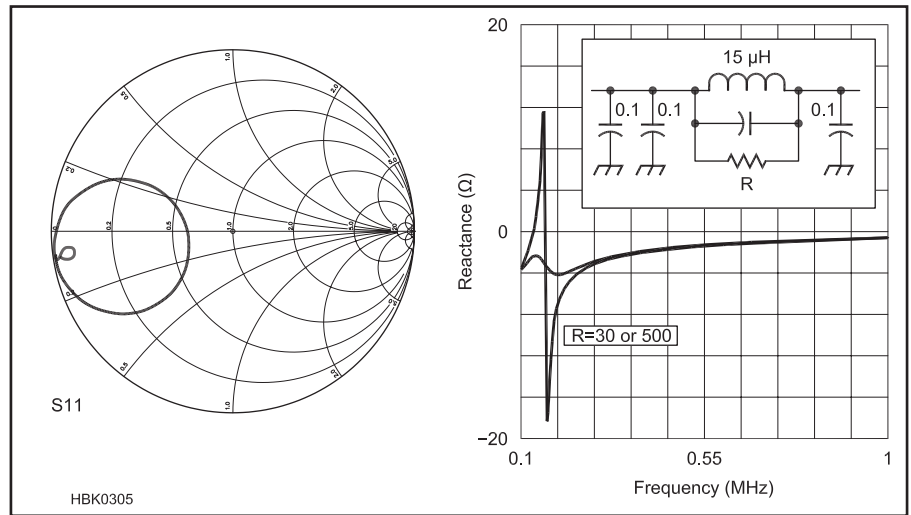


Figure 5.26 — Two different resistor values parallel a decoupling choke. The lower, 30- Ω value is more effective. See text.

plifier oscillation. Instability that allows oscillations is usually suppressed by low impedance terminations. The base and collector (or gate and drain) should both “see” low impedances to ensure stability. But that must be true at all frequencies where the device can produce gain. It is never enough to merely consider the operating frequency for the amplifier. A parallel resonance in the base or collector circuits can be a disaster. When wideband bypassing is not possible, negative feedback that enhances wideband stability is often used.

Emitter bypassing is often a critical application. As demonstrated in the **Circuits and Components** chapter, a few extra ohms of impedance in the emitter circuit can drastically alter amplifier performance. A parallel-resonant emitter bypass could be a profound difficulty while a series-resonant one can be especially effective.

Capacitors also appear in circuits as blocking elements. A blocking capacitor, for example, appears between stages, creating a near short circuit for ac signals while accommodating different dc voltages on the two sides. A blocking capacitor is not as critical as a bypass, for the impedances on either side will usually be higher than that of the block.

With parasitic effects having the potential to strongly affect circuit performance, the circuit designer must account for them wherever they are significant. The additional complexity of including parasitic elements can result in a design too complex to be analyzed manually. Clearly, detailed modeling is the answer to component selection and the control of parasitic effects.

5.3.11 Effects on Filter Performance

LC bandpass filters perform a critical function in determining the performance of a typical RF system such as a receiver. An

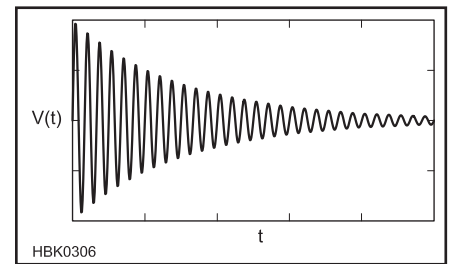


Figure 5.27 — The amplitude of a chime’s ring after being struck by a hammer. Units are arbitrary.

input filter, usually a bandpass, restricts the frequency range that the receiver must process. Transmitters use LC filters to reduce harmonic output. Audio and LF filters may also use LC elements. The LC filters we refer to in this section are narrow with a bandwidth from 1 to 20% of the center frequency. Even narrower filters are built with resonators having higher Q; the quartz crystal filter discussed in the **Analog and Digital Filtering** chapter is used where bandwidths of less than a part per thousand are possible. The basic concepts that we examine with LC circuits will transfer to the crystal filter.

LOSSES IN FILTERS AND Q

The key elements in narrow filters are tuned circuits made from inductor-capacitor pairs, quartz crystals, or transmission line sections. These resonators share the property that they store energy, but they have losses. A chime is an example. Striking the chime with a hammer produces the waveform of **Figure 5.27**. The rate at which the amplitude decreases with time after the hammer strike is determined by the filter’s Q, which is discussed in the chapter on **Circuits and Components**. The higher the Q, the longer it takes for the sound to disappear. The oscillator amplitude would

not decrease if it were not for the losses that expend energy stored in the resonator. The mere act of observing the oscillation will cause some energy to be dissipated.

A chime is an acoustic resonator, but the same behavior occurs in electric resonators. A pulse input to an LC circuit causes it to ring; losses cause the amplitude to diminish. The most obvious loss in an LC circuit is conductor resistance, including that in the inductor wire. This resistance is higher than the dc value owing to the skin effect, which forces high frequency current toward the conductor surface. Other losses might result from hysteresis losses in an inductor core or dielectric losses in a capacitor.

An inductor is modeled as an ideal part with a series or a parallel resistance. The resistance will depend on the Q if the inductor was part of a resonator with that quality. The two resistances are shown in **Figure 5.28**.

$$R_{\text{Series}} = \frac{2\pi f L}{Q} \quad \text{and}$$

$$R_{\text{Parallel}} = Q \times 2\pi f L \quad (6)$$

The higher the inductor Q, the smaller the series resistance, or the larger the parallel resistance is needed to model that Q. It does not matter which configuration is used. The Q of a resonator is related to the bandwidth of the tuned circuit by

$$BW = \frac{f_c}{Q} \quad (7)$$

where f_c is the tuned circuit's center frequency. This is also the Q of an inductor in a tuned circuit if the capacitor is lossless.

The single-tuned circuit is presented in two different forms in **Figure 5.29**. In the top, a parallel tuned circuit consisting of L and C has loss modeled by three resistors. The resistor R_p is the parallel loss resistance representing the non-ideal nature of the inductor. (Another might be included to represent capacitor losses.) But the LC is here paralleled by three resistors: the source, the load and the loss element. R_p would disappear if the tuned circuit was built from perfect components. The source and load remain; they represent the source resistance that must be present if

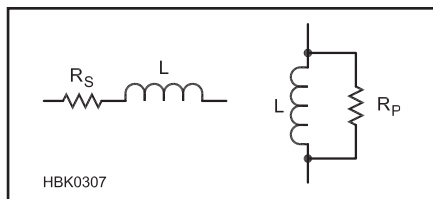


Figure 5.28 — Inductor Q may be modeled with either a series or a parallel resistance.

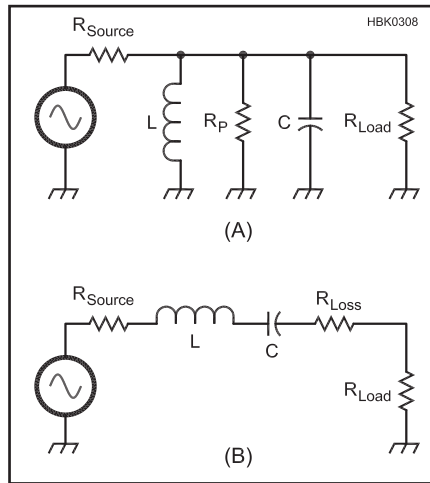


Figure 5.29 — Two simple forms of the single-tuned circuit.

power is available and a load resistance that must be included if power is to be extracted.

Equation 6 and 7 can be applied in several ways. If the resonator is evaluated with only its intrinsic loss resistance (in either series or parallel form) the resulting Q is called the *unloaded Q*, or Q_U . If, however, the net resistance is used, which is the parallel combination of the load, the source, and the loss in the parallel tuned circuit, the resulting Q is called the *loaded Q*, Q_L . If we were working with the series tuned circuit form, the loaded Q would be related to the total series R.

Consider an example, a parallel tuned circuit (Figure 5.29A) with a 2- μH inductor tuned to 5 MHz with a 507-pF capacitor. Assume the parallel loss resistor was 12.57 k Ω . The unloaded Q calculated from equation 6 is 200. The unloaded bandwidth would be 5 MHz/200 = 25 kHz. Assume that the source and load resistors were equal, each 2 k Ω . The net resistance paralleling the LC would then be the combination of the three resistors, 926 Ω . The loaded Q becomes 14.7 with a loaded bandwidth of 339 kHz. The loaded Q is also the filter Q, for it describes the bandwidth of the single-tuned circuit, the simplest of band-pass filters.

This filter also has *insertion loss* (IL). This is illustrated in **Figure 5.30** which shows the parallel-resonant LC combination removed (at resonance, the LC combination has infinite impedance), leaving only the loss resistance of 12.57 k Ω . We use an arbitrary open circuit source voltage of 2. The available power to a load is then 1 V across a resistance equaling the 2-k Ω source. If the resonator had no internal losses, this available power would be delivered to the 2-k Ω load. However, the loss R parallels the load, causing the output voltage to be 0.926 V, a bit less than the ideal 1 V. Calculation of the output power into the 2-k Ω load resistance and the available power shows that the insertion loss is 0.67 dB.

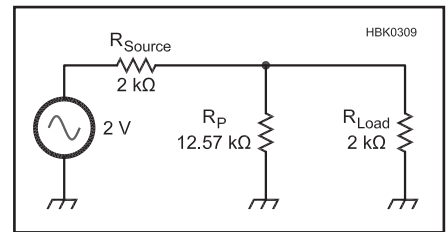


Figure 5.30 — Simplified parallel tuned circuit at resonance. The effect of loss is illustrated by removing the parallel-LC combination which at resonance has infinite impedance.

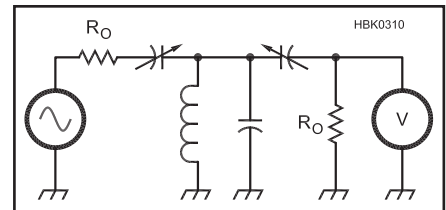


Figure 5.31 — Test setup for measuring the Q of a resonator. The source and load impedances, R_O , are assumed to be identical. The two coupling capacitors are adjusted to be equal to each other. The output signal is measured with an appropriate ac voltmeter, an oscilloscope or a spectrum analyzer.

This exercise illustrates two vital points that are general for all bandpass filters. First, the bandwidth of any filter must always be larger than the unloaded bandwidth of the resonators used to build the filter. Second, any filter built from real-world components will have an insertion loss. The closer the Q of the filter approaches the unloaded resonator Q, the greater the insertion loss becomes. A parallel tuned circuit illustrated these ideas; the series tuned filter would have produced identical results. Generally, the insertion loss of a single-tuned circuit relates to loaded and unloaded Q by

$$IL(\text{dB}) = -20 \log \left(1 - \frac{Q_L}{Q_U} \right) \quad (8)$$

The Q of a tuned LC circuit is easily measured with a signal generator of known output impedance (usually 50 Ω) and a sensitive detector, again with a known impedance level, often equal to that of the generator. The test configuration is shown in **Figure 5.31**. It uses equal loads and equal capacitors to couple from the terminations to the resonator. Equal capacitors, C1 and C2 guarantees that each termination contributes equally to the resonator parallel load resistance. The voltmeter across the load is calibrated in dB.

To begin measurement we remove the tuned circuit and replace it with a direct connection from generator to load. The available power delivered to the load is calculated after the

voltage is measured. The resonator is then inserted between the generator and load, and the generator is tuned for a peak. The measured power is less than that available from the source, with the difference being the insertion loss for the simple filter. Capacitors C1 and C2 are adjusted until the loss is 30 dB or more. With loss this high, the intrinsic loss resistance of the resonator will dominate the loss. The generator is now tuned first to one side of

the peak, and then to the other, noting the frequencies where the response is lower than the peak by 3 dB. The unloaded bandwidth, ΔF , is the difference between the two 3 dB frequencies. The unloaded Q is calculated as

$$Q_U = \frac{F}{\Delta F} \quad (9)$$

This method for Q measurement is quite

universal, being effective for audio tuned circuits, simple LC RF circuits, VHF helical resonators, or microwave resonators. The form of the variable capacitors, C1 and C2, may be different for the various parts of the spectrum, but the concepts are general. Indeed, it is not even important how the coupling occurs. The Q measurement normally determines an unloaded value, but loaded values are also of interest when testing filters.

5.4 Semiconductor Circuits at RF

The models used in the **Circuits and Components** chapter are reasonably accurate at low frequencies, and they are of some use at RF, but more sophisticated models are required for consistent results at higher frequencies. This section notes several areas in which the simple models must be enhanced. Circuit design using models accurate at RF, particularly for large signals, is performed today using design software as described in the **Electronic Design Automation (EDA)** chapter of this book. In-depth discussions of the elements of RF circuit design appear in Hayward's *Introduction to Radio Frequency Design*, an excellent text for the beginning RF designer (see the References section). See also the section of RF Amplifier Design papers and application notes in the References section of this chapter.

5.4.1 The Diode at High Frequencies

A DIODE AC MODEL

At high frequencies, the diode's behavior becomes less like a switch, especially for small signals that do not cause the diode's operating point to move by large amounts. In this case, the diode's small-signal dynamic behavior becomes important.

Figure 5.32 shows a simple resistor-diode circuit to which is applied a dc bias voltage plus an ac signal. Assuming that the voltage drop across the diode is 0.6 V and R_f is negligible, we can calculate the bias current to be $I = (5 - 0.6) / 1 \text{ k}\Omega = 4.4 \text{ mA}$. This point is marked on the diodes I-V curve in Figure 5.32. If we draw a line tangent to this point, as shown, the slope of this line represents the *dynamic resistance* of the diode, R_d , experienced by a small ac signal. At room temperature, dynamic resistance is approximately

$$R_d = \frac{25}{I} \Omega \quad (10)$$

where I is the diode current in mA. Note that this resistance changes with bias current and should not be confused with the dc forward resistance discussed in the **Circuits and Components** chapter, which has a similar value but represents a different concept. **Figure 5.33** shows a low-frequency ac model for the diode, including the dynamic resistance and junction capacitance. This model should only be used when the diode's dc operating parameters can be neglected.

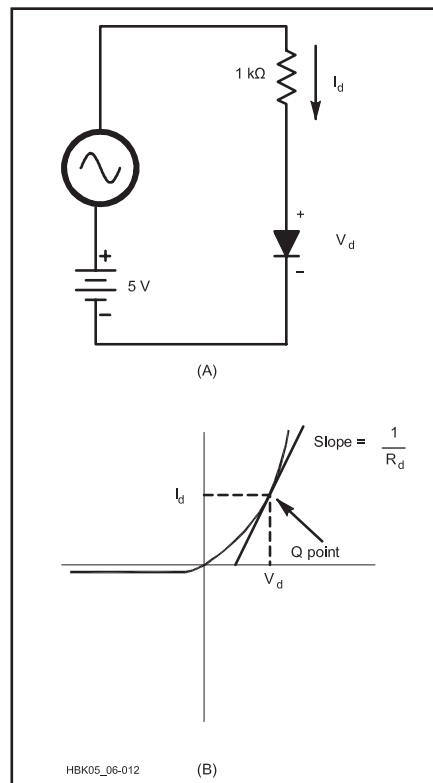


Figure 5.32 — A simple resistor-diode circuit used to illustrate dynamic resistance. The ac input voltage “sees” a diode resistance whose value is the slope of the line at the Q-point, shown in B.

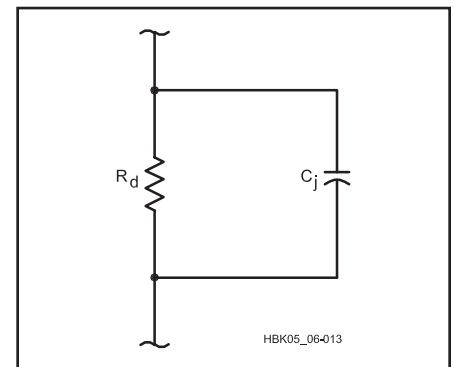


Figure 5.33 — An ac model for diodes. R_d is the dynamic resistance and C_j is the junction capacitance.

SWITCHING TIME

If you change the polarity of a signal applied to the ideal diode, current flow stops or starts instantaneously. Current in a real diode cannot do this, as a finite amount of time is required to move electrons and holes in or out of the diode as it changes states. Effectively, the diode junction capacitance, C_j , in Figure 5.33 must be charged or discharged. As a result, diodes have a maximum useful frequency when used in switching applications.

The operation of diode switching circuits can often be modeled by the circuit in **Figure 5.34**. The approximate switching time (in seconds) for this circuit is given by

$$t_s = \tau_p \frac{\left(\frac{V_1}{R_1} \right)}{\left(\frac{V_2}{R_2} \right)} = \tau_p \frac{I_1}{I_2} \quad (11)$$

where τ_p is the minority carrier lifetime of the diode, a material constant determined during manufacture, on the order of 1 ms. I_1 and I_2 are currents that flow during the switching process. The minimum time in which a diode

can switch from one state to the other and back again is therefore $2t_s$, and thus the maximum usable switching frequency is $f_{sw} \text{ (Hz)} = 1/(2t_s)$. It is usually a good idea to stay below this by a factor of two. Diode data sheets usually give typical switching times and show the circuit used to measure them.

Note that f_{sw} depends on the forward and reverse currents, determined by I_1 and I_2 (or equivalently V_1 , V_2 , R_1 , and R_2). Within a reasonable range, the switching time can be reduced by manipulating these currents. Of course, the maximum power that other circuit elements can handle places an upper limit on switching currents.

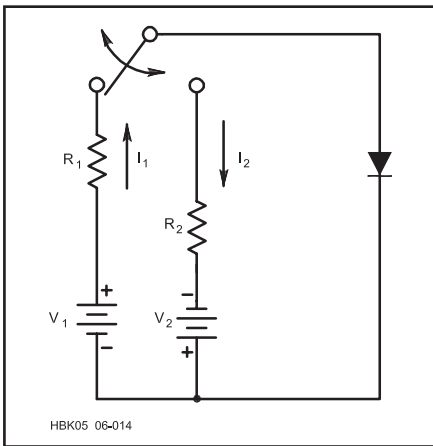


Figure 5.34 — Circuit used for computation of diode switching time.

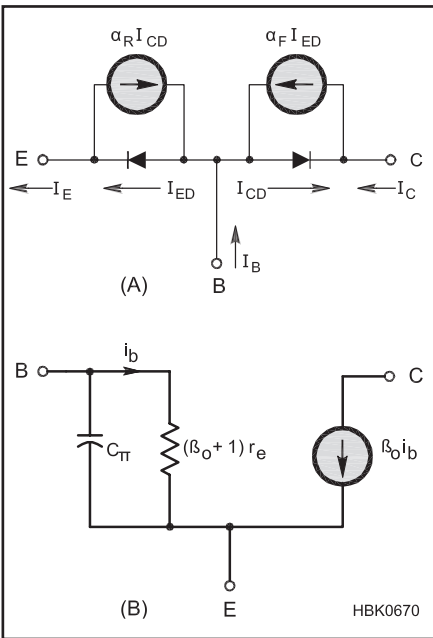


Figure 5.35 — (A) The Ebers-Moll model of the bipolar junction transistor (BJT) is used at dc and low frequencies when the transistor is in its active region. (B) The hybrid-pi model includes frequency dependence.

5.4.2 The Transistor at High Frequencies

The development and selection of suitable models for active devices at RF is an involved and nuanced process. This section presents a few of the models used for bipolar junction transistors (BJT) and field-effect transistors (FET) as examples of the issues involved. For more information on model details, start with the *SPICE* home page at bwrc.eecs.berkeley.edu/classes/icbook/spice and the user's manual for the simulation software you intend to use.

GAIN VERSUS FREQUENCY

The circuit design equations in **Circuits and Components** generally assumed that current gain in the bipolar transistor was independent of frequency. As signal frequency increases, however, current gain decreases. The low-frequency current gain, β_0 , is constant through the audio spectrum, but it eventually decreases, and at some high frequency it will drop by a factor of 2 for each doubling

of signal frequency. (The h-parameter $[h_{FE}]$ is often substituted for β at dc and h_{FE} for ac current gain. H-parameters are discussed later in this chapter.) A transistor's frequency vs current gain relationship is specified by its *gain-bandwidth product* (GBW), or F_T , the frequency at which the current gain is 1. Common transistors for lower RF applications might have $\beta_0 = 100$ and $F_T = 500$ MHz. The frequency at which current gain equals β_0 is called F_b and is related to F_T by $F_b = F_T / \beta_0$.

The *Ebers-Moll model* for the bipolar transistor, shown in **Figure 5.35A**, is a "large signal model." It is used when the transistor is in its active mode and gives good results for dc collector and emitter currents. This would be a good model to use when designing a pass-transistor voltage regulator circuit, for example.

The frequency dependence of current gain is modeled by adding a capacitor across the base resistor of **Figure 5.35B**, the *hybrid-pi* model results. The capacitor's reactance should equal the low-frequency input resistance, $(\beta + 1)r_e$, at F_b . This simulates a frequency-dependent current gain.

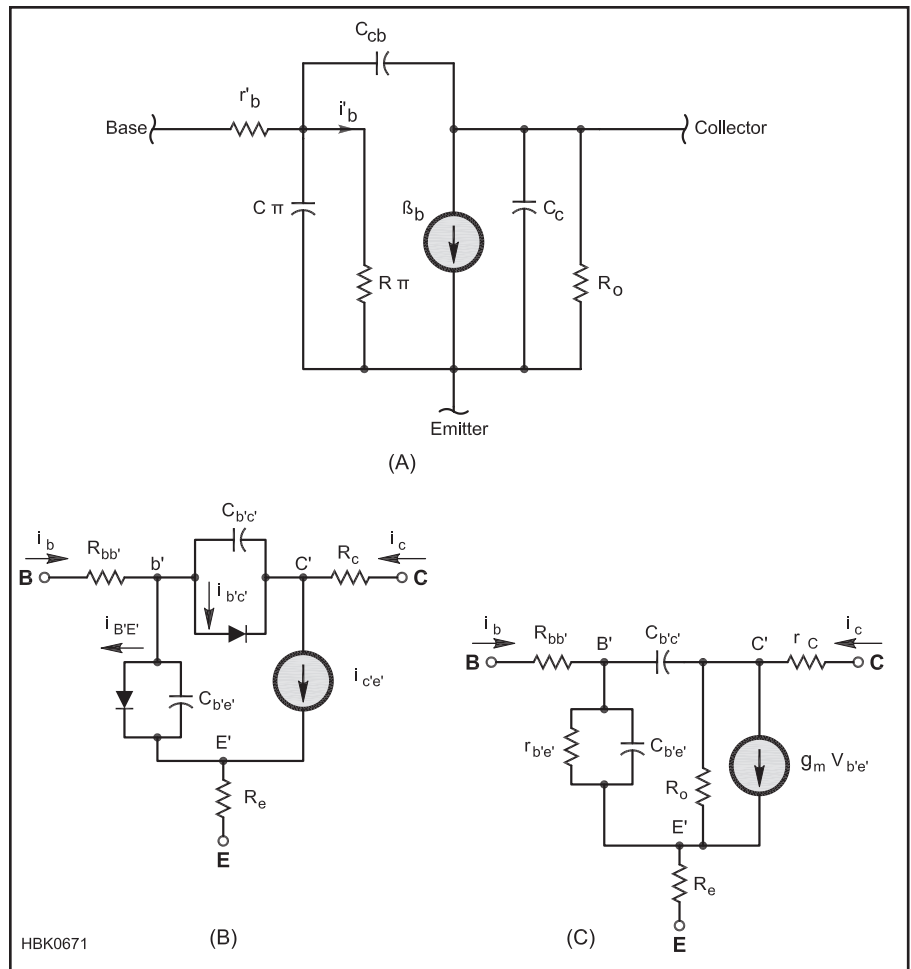


Figure 5.36 — High-frequency models for the bipolar junction transistor. (A) An improved version of the hybrid-pi model including additional device capacitances. (B) is the large-signal Gummel-Poon model used at dc and low-frequencies — the standard used for bipolar transistors by simulators based on *SPICE3* and (C) is the small-signal ac version.

Similar considerations affect the transconductance of FETs as the gate-to-source and gate-to-drain capacitances act to reduce high-frequency gain. Instead of F_T , most FETs designed for amplifier use specify input and output transconductance, susceptance, and power gain at different frequencies.

Recognizing that transistor gain varies with frequency, it is important to know the conditions under which the simpler model is useful. Calculations show that the simple model is valid, with $\beta = F_T / F$, for frequencies well above F_b . The approximation worsens, however, as the operating frequency (f_0) approaches F_T .

SMALL-SIGNAL DESIGN AT RF

The simplified hybrid- π model of Figure 5.35B is often suitable for non-critical designs, but **Figure 5.36A** shows a better small-signal model for RF design that expands on the hybrid- π . Consider the physical aspects of a real transistor: There is some capacitance across each of the PN junctions (C_{cb} and C_p) and capacitance from collector to emitter (C_c). There are also capacitances between the device leads (C_e , C_b and C_c). There is a resistance in each current path, emitter to base and collector. From emitter to base, there is r_π from the hybrid- π model and r_b , the “base spreading” resistance. From emitter to collector is R_o , the output resistance. The leads that attach the silicon die to the external circuit present three inductances.

Manual circuit analysis with this model is best tackled with the aid of a computer and specialized software. Other methods are presented in Hayward’s *Introduction to Radio Frequency Design*. Surprisingly accurate results may be obtained, even at RF, from the simple models. Simple models also give a better “feel” for device characteristics that might be obscured by the mathematics of a more rigorous treatment. Use the simplest model that describes the important features of the device and circuit at hand.

The *Gummel-Poon model* shown in Figures 5.36B and 5.36C is the standard used by simulation software based on *SPICE3*. By adding additional parasitic elements, such as lead inductance and lead-to-package capacitances, the small-signal ac model can be used accurately at high frequencies. Note how the ac model becomes progressively more sophisticated from Figure 5.35A through 5.36C.

HIGH FREQUENCY FET MODELS

At low frequencies the FET can be treated as a simple current source controlled by the gate-to-source voltage as in Figure 3.49 in the **Circuits and Components** chapter. As frequency increases, the inter-electrode capacitances become significant and must be included, such as in the model in **Figure 5.37A**. As with the BJT, separate models are used for small-

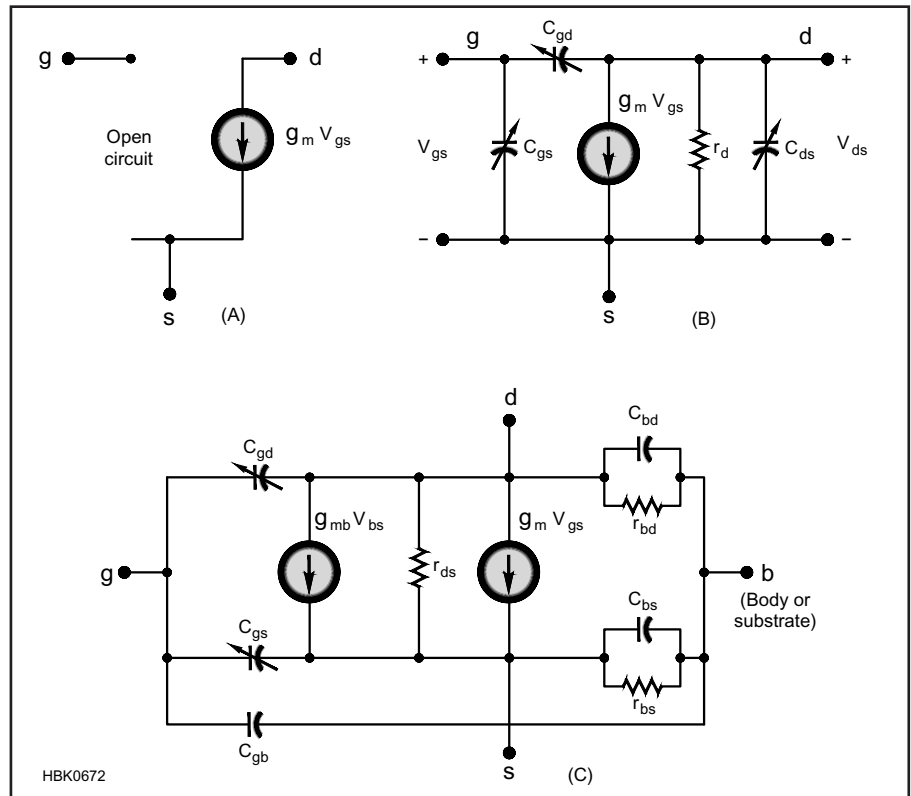


Figure 5.37 — Small-signal models for the field-effect transistor (FET). (A) is a simple low-frequency model. (B) is a common *SPICE3* large-signal model and (C) is a typical high-frequency model for the JFET.

signal and large-signal applications. Figure 5.37B shows a small-signal *SPICE3* simulation model for the JFET. All of the model’s capacitances vary with temperature and device operating characteristics. Figure 5.37C shows a typical high-frequency MOSFET model used by *SPICE3* (there are several) that includes the effect of the body or substrate elements.

The advances in CMOS integrated circuit technology have resulted in transistors (and capacitors and inductors) with sufficient performance for use in RF design work. In fact, most radio transceivers for cellular telephones, wireless LANs and similar high-volume applications are implemented almost exclusively in CMOS technology due to the high integration available. MOSFET RF design principles are similar to BJT and JFET designs, and most circuit simulators provide good models for MOSFET devices. These additional techniques are enabled by the excellent device matching available in IC technology and the ability to integrate additional circuitry at low incremental cost.

PARASITIC ELEMENTS AND NOISE

For accurate RF simulation the effects of additional parasitic elements must be included. The most significant is lead inductance — generally inserted in series with the device’s external connections. Lead-to-package and

lead-to-lead capacitances are also included in most high-frequency simulations. Depending on the simulation package used, the user may be required to install these parasitic elements as separate circuit elements or the simulator or manufacturer may provide special models for high-frequency simulation.

Simulation of device noise is not covered here, but many simulator packages include separate noise models for various active devices. Review the simulator’s documentation for information about how to include noise in your simulation.

5.4.3 Amplifier Classes

The class of operation of an amplifier is determined by the fraction of a drive cycle during which conduction occurs in the amplifying device or for switchmode devices. (Switchmode amplifiers use different criteria.) The Class A amplifier conducts for 100% of the cycle. It is characterized by constant flow of supply current, regardless of the strength of the driving signal. Most of the amplifiers we use for RF applications and many audio circuits in receivers operate in Class A.

A Class B amplifier conducts for 50% of the cycle, which is 180 degrees if we examine the circuit with regard to a driving sine wave. A Class B amplifier draws no dc current when

no input signal is applied, but current begins to flow with any input, growing with the input strength. A Class B amplifier can display good *envelope linearity*, meaning that the output amplitude at the drive frequency changes linearly with the input signal. The total absence of current flow for half of the drive cycle will create harmonics of the signal drive.

A Class C amplifier is one that conducts for less than half of a cycle. No current flows without drive. Application of a small drive produces no output and no current flow. Only after a threshold is reached does the device begin to conduct and provide output. A bipolar transistor with no source of bias for the base typically operates in Class C.

The large-signal models discussed earlier are suitable for the analysis of all amplifier classes. Small-signal models are generally reserved for Class A amplifiers. The most common power amplifier class is a cross between Class A and B — the Class AB amplifier that conducts for more than half of each cycle. A Class AB amplifier at low drive levels is indistinguishable from a Class A design. However, increasing drive produces greater collector (or drain) current and greater output.

Amplifier class letter designators for vacuum tube amplifiers were augmented with a numeric subscript. A Class AB₁ amplifier operates in AB, but with no grid current flowing. A Class AB₂ amplifier's grid is driven positive with respect to the cathode and so some grid current flows. In solid-state amplifiers, which have no grids, no numeric subscripts are used.

While wide-bandwidth Class A and Class B amplifiers are common, most circuits operating in Class C and higher are tuned at the output. The tuning accomplishes two things. First, it allows different terminations to exist for different frequencies. For example, a resistive load could be presented at the drive frequency while presenting a short circuit at some or all harmonics. The second consequence of tuning is that reactive loads can be created and presented to the amplifier collector or drain. This then provides independent control of current and voltage waveforms.

While not as common as A, B, and C, Class D and E amplifiers are of increasing interest. The Class D circuit is a balanced (two transistor) switching format where the input is driven hard enough to produce square wave collector waveforms. Class E amplifiers usually use a single switching device with output tuning that allows high current to flow in the device only when the output voltage is low. Other “switching amplifier” class designators refer to the various techniques of controlling the switched currents and voltages.

Class A and AB amplifiers are capable of good envelope linearity, so they are the most common formats used in the output of SSB amplifiers. Class B and, predominantly,

Class C amplifiers are used for CW and FM applications, but lack the envelope linearity needed for SSB.

Efficiency varies considerably between amplifier class. The Class A amplifier can reach a collector efficiency of 50%, but no higher, with much lower values being typical. Class AB amplifiers are capable of higher efficiency, although the wideband circuits popular in HF transceivers typically offer only 30% at full power. A Class C amplifier is capable of efficiencies approaching 100% as the conduction cycle becomes small, with common values of 50 to 75%. Both Class D and E are capable of 90% and higher efficiency. An engineering text treating power amplifier details is Krauss, Bostian, and Raab's *Solid State Radio Engineering*. A landmark paper by a Cal Tech group led by David Rutledge, KN6EK, targeted to the home experimenter, *High-Efficiency Class-E Power Amplifiers*, was presented in *QST* for May and June, 1997.

5.4.4 RF Amplifiers with Feedback

The feedback amplifier appears frequently in amateur RF circuits. This is a circuit with two forms of negative feedback with (usually) a single transistor to obtain wide bandwidth, well-controlled gain and well-controlled, stable input and output resistances. Several of these amplifiers can be cascaded to form a high gain circuit that is both stable and predictable.

The small-signal schematic for the feedback amplifier is shown in Figure 5.38 without bias components or power supply details. The design begins with an NPN transistor biased for a stable dc current. Gain is reduced with emitter degeneration, increasing input resistance while decreasing gain. Additional feedback is then added with a parallel feedback resistor, R_f , between the collector and base. This is much like the resistor between an op-amp output and the inverting input which reduces gain and *decreases* input resistance.

Several additional circuits are presented

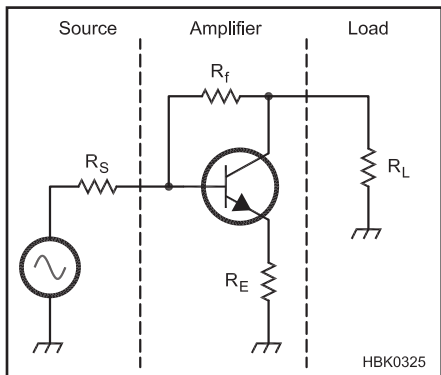


Figure 5.38 — Small-signal circuit for a feedback amplifier.

showing practical forms of the feedback amplifier. Figure 5.39 shows a complete circuit. The base is biased with a resistive divider from the collector. However, much of the resistor is bypassed, leaving only R_f active for actual signal feedback. Emitter degeneration is accoupled to the emitter. The resistor R_E dominates the degeneration since R_E is normally much smaller than the emitter bias resistor. Components that are predominantly used for biasing are marked with “B.” This amplifier would normally be terminated in 50 Ω at both the input and output. The transformer has the effect of making the 50- Ω load “look like” a larger load value, $R_L = 200 \Omega$ to the collector.

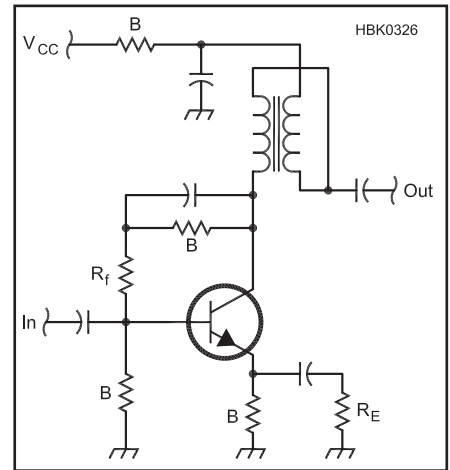


Figure 5.39 — A practical feedback amplifier. Components marked with “B” are predominantly for biasing. The 50- Ω output termination is transformed to 200 Ω at the collector. A typical RF transformer is 10 bifilar turns of #28 on a FT-37-43 ferrite toroid. The inductance of one of the two windings should have a reactance of around 250 Ω at the lowest frequency of operation.

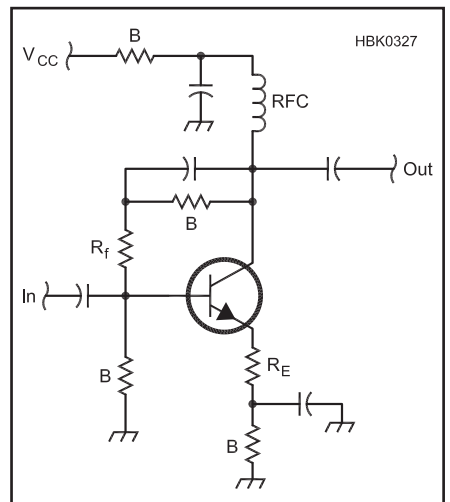


Figure 5.40 — A variation of the feedback amplifier with a 50- Ω output termination at the collector.

This is a common and useful value for many HF applications.

Figure 5.40 differs from Figure 5.39 in two places. First, the collector is biased through an RF choke instead of a transformer. The collector circuit then “sees” $50\ \Omega$ when that load is connected. Second, the emitter degeneration is in series with the bias, instead of the earlier parallel connection. Either scheme works well, although the parallel configuration affords experimental flexibility with isolation between setting degeneration and biasing. Amplifiers without an output transformer are not constrained by degraded transformer performance and often offer constant or “flat” gain to several GHz.

The variation of **Figure 5.41** may well be the most general. It uses an arbitrary transformer to match the collector. Biasing is traditional and does not interact with the feedback.

Feedback is obtained directly from the output tap in the circuit of **Figure 5.42**. While this scheme is common, it is less desirable than the others, for the transformer is part of the feedback loop. This could lead to instabilities. Normally, the parallel feedback tends to stabilize the amplifiers.

The circuit of **Figure 5.43** has several features. Two transistors are used, each with a separate emitter biasing resistor. However, ac coupling causes the pair to operate as a single device with degeneration set by R_E . The parallel feedback resistor, R_f , is both a signal feedback element and part of the bias divider. This constrains the values slightly. Finally, an arbitrary output load can be presented to the composite collector through a π -type matching network. This provides some low pass filtering, but constrains the amplifier bandwidth.

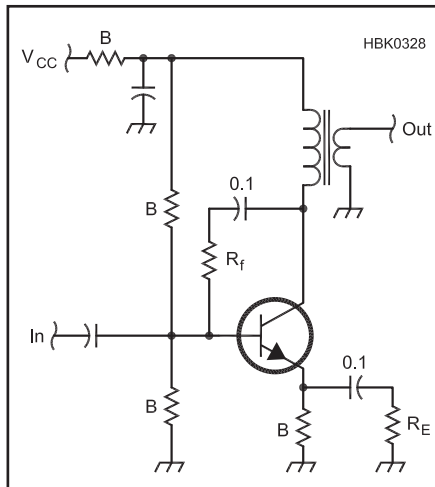


Figure 5.41 — This form of the feedback amplifier uses an arbitrary transformer. Feedback is isolated from bias components.

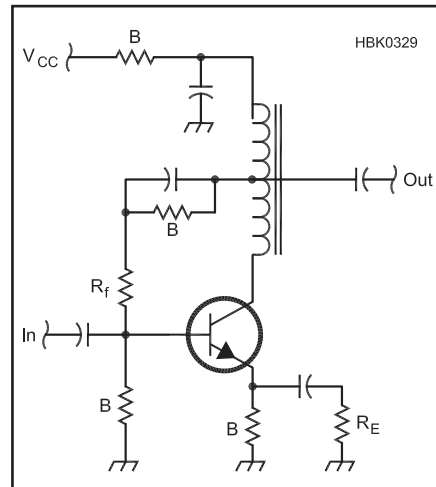


Figure 5.42 — A feedback amplifier with feedback from the output transformer tap. This is common, but can produce unstable results.

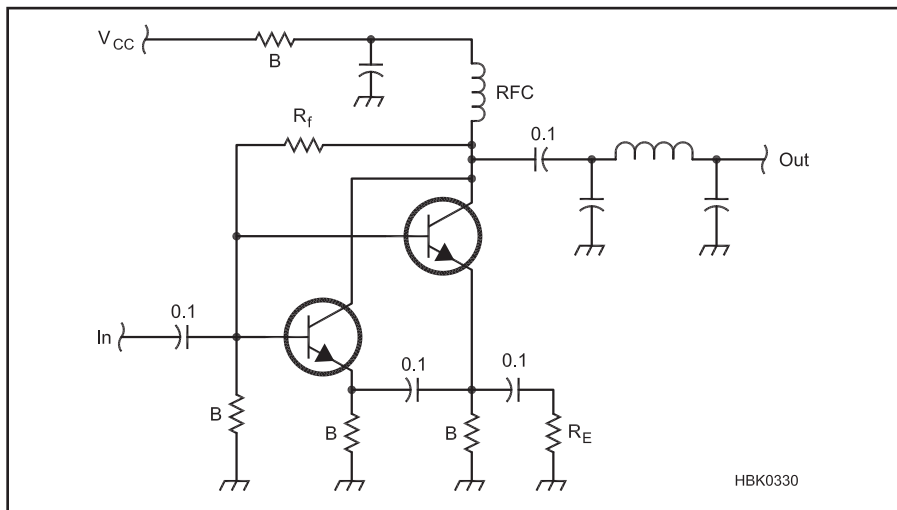


Figure 5.43 — Feedback amplifier with two parallel transistors.

5.5 Ferrite Materials

Ferrites are ceramics consisting of various metal oxides formulated to have very high permeability. Iron, manganese, manganese zinc (MnZn), and nickel zinc (NiZn) are the most commonly used oxides. Ferrite cores and beads are available in many styles, as shown in **Figure 5.44**. Wires and cables are then passed through them or wound on them.

When ferrite surrounds a conductor, the high permeability of the material provides a much easier path for magnetic flux set up by current flow in the conductor than if the wire were surrounded only by air. The short length of wire passing through the ferrite will thus see its self-inductance “magnified” by the relative permeability of the ferrite. The ferrites used for suppression are soft ferrites — that is, they are not permanent magnets.

Recalling the definition in the **Electrical Fundamentals** chapter, *permeability* (μ) is the characteristic of a material that quantifies the ease with which it supports a magnetic field. Relative permeability is the ratio of the permeability of the material to the permeability of free space. The relative permeability of nonmagnetic materials like air, copper, and aluminum is 1, while magnetic materials have a relative permeability much greater than 1. Typical values (measured at power frequencies) for stainless steel, steel and mu-metal are on the order of 500, 1000 and 20,000 respectively. Various ferrites have values from the low tens to several thousand. The permeability of these materials changes with frequency and this affects their suitability for use as an inductor’s magnetic core or as a means of providing EMI suppression.

Manufacturers vary the chemical composition (the *mix* or *material “type”*) and the dimensions of ferrites to achieve the desired electrical performance characteristics. It is important to select a mix with permeability and loss characteristics that are appropriate for the intended frequency range and application. (The **Construction Techniques** chapter includes tables showing the data for different types of

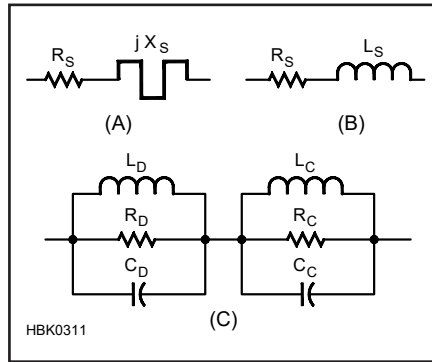


Figure 5.45 — Equivalent circuits for ferrite material. (A) shows the equivalent series circuit specified by the data sheet. (B) shows an over-simplified equivalent circuit for a ferrite choke. (C) shows a better equivalent circuit for a ferrite choke.

ferrite and powdered-iron cores and appropriate frequency ranges for each.)

Fair-Rite Products Corp. supplies most of the ferrite materials used by amateurs, and their website (www.fair-rite.com) includes extensive technical data on both the materials and the many parts made from those materials. Much can be learned from the study of this data, the most extensive of any manufacturer. The website includes two detailed application notes on the use of ferrite materials, *How to Choose Ferrite Components for EMI Suppression* and *Use of Ferrites in Broadband Transformers*.

5.5.1 Ferrite Permeability and Frequency

Product data sheets characterize ferrite materials used as chokes by graphing their series equivalent impedance, and chokes are usually analyzed as if their equivalent circuit had only a series resistance and inductance, as shown in **Figures 5.45A** and **5.45B**. (Figure 5.45 presents small-signal equivalent circuits.

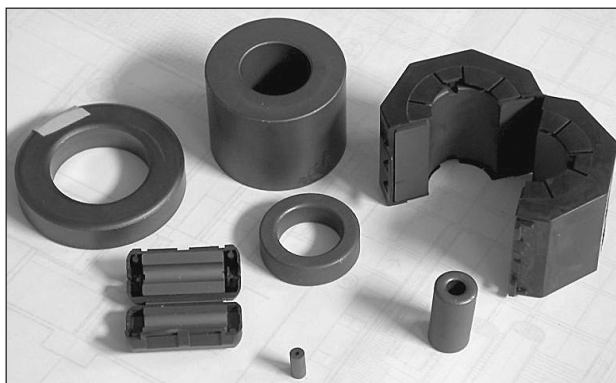


Figure 5.44 — Ferrites are made in many forms. Beads are cylinders with small center holes so that they can be slid over wires or cables. Toroidal cores are more ring-like so that the wire or cable can be passed through the center hole multiple times. Snap-on or split cores are made to be clamped over cables too large to be wound around the core or for a bead to be installed.

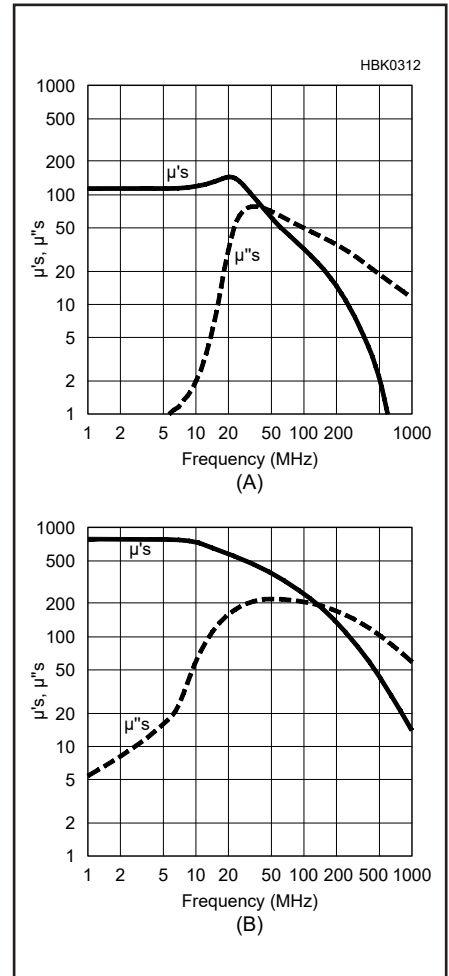


Figure 5.46 — Permeability of a typical ferrite material, Fair-Rite Type #61 (A) and of Type #43 material (B). (Based on product data published by Fair-Rite Products Corp.)

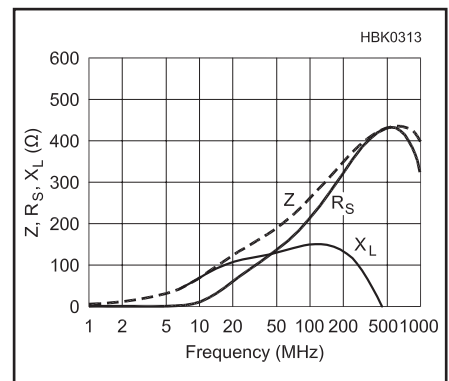


Figure 5.47 — Impedance of a bead for EMI suppression at UHF, Fair-Rite Type #61. (Based on product data published by Fair-Rite Products Corp.)

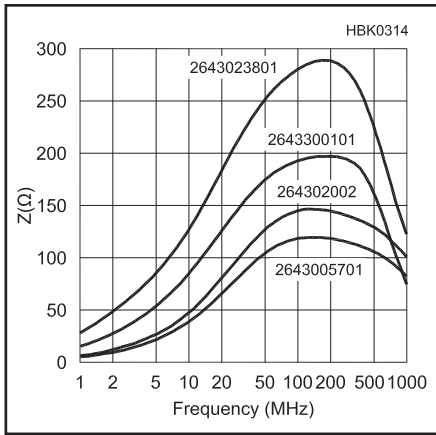


Figure 5.48 — Impedance of different length beads of Fair-Rite Type #43 material. The longer the bead, the higher the impedance. (Based on product data published by Fair-Rite Products Corp.)

Issues of temperature and saturation at high power levels are not addressed in this section.) The actual equivalent circuit is closer to Figure 5.45C. The presence of both inductance and capacitance creates resonances visible in the graphs of impedance versus frequency as discussed below. One resonance is created by the pair $L_D C_D$ and the other by $L_C C_C$.

Figure 5.46A graphs the permeabilities μ'_S and μ''_S for Fair-Rite Type #61 ferrite material (Fair-Rite products are identified by a material “Type” and a number), one of the many mix choices available. This material is recommended for use in inductive applications below 25 MHz and for EMI suppression at frequencies above 200 MHz.

For the simple series equivalent circuit of Figure 5.45A and B, the permeability constant for ferrite is actually complex; $\mu = \mu'_S + j \mu''_S$. In this equation, μ'_S represents the component of permeability defining ordinary inductance, and μ''_S describes the component that affects losses in the material. You can see that up to approximately 20 MHz, μ'_S is nearly constant, meaning that an inductor wound on a core of this material will have a stable inductance. Below about 15 MHz, the chart shows that μ''_S is much smaller than μ'_S , so that losses are small, making this material good for high power inductors and transformers in this frequency range.

Above 15 MHz, μ''_S increases rapidly and so do the material’s associated losses, peaking between 300 and 400 MHz. That makes the inductor very lossy at those frequencies and good for suppressing EMI by absorbing energy in the unwanted signal. **Figure 5.47** shows the manufacturer’s impedance data for one “turn” of wire through a cylindrical ferrite bead (a straight wire passing through the bead) made of mix #61 with the expected peak in impedance above 200 MHz. Interestingly,

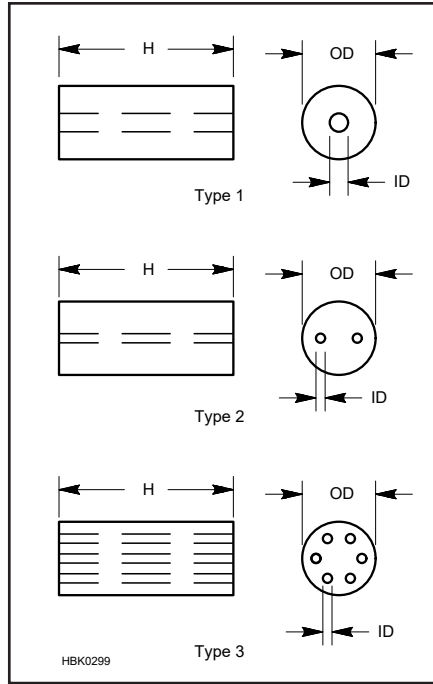


Figure 5.49 — Typical one-piece ferrite bead configurations. Component leads or cables can be inserted through beads one or more times to create inductance and loss as described in the text.

X_L goes below the graph above resonance, but it isn’t zero. The negative reactance is created by the capacitors in Figure 5.45C.

The Type #43 mix (see Figure 5.46B) used for the beads of **Figure 5.48** is optimized



Figure 5.50 — A ferrite choke consisting of multiple turns of cable wound on a 2.4-in. OD × 1.4-in. ID × 0.5-in. toroid core.

for suppression at VHF (30-300 MHz). Type #43 material’s μ'_S is much higher than type #61, meaning that fewer turns are required to achieve the needed inductance. But μ''_S for #43 remains significant even at low frequencies, limiting its usefulness for inductor and transformer cores that must handle high power. The figure shows the impedance data for several beads of different lengths. The longer the bead, the higher the impedance. The same effect can be obtained by stringing multiple beads together on the same wire or cable.

5.5.2 Resonances of Ferrite Cores

Below resonance, the impedance of a wire passing through a ferrite cylinder is propor-

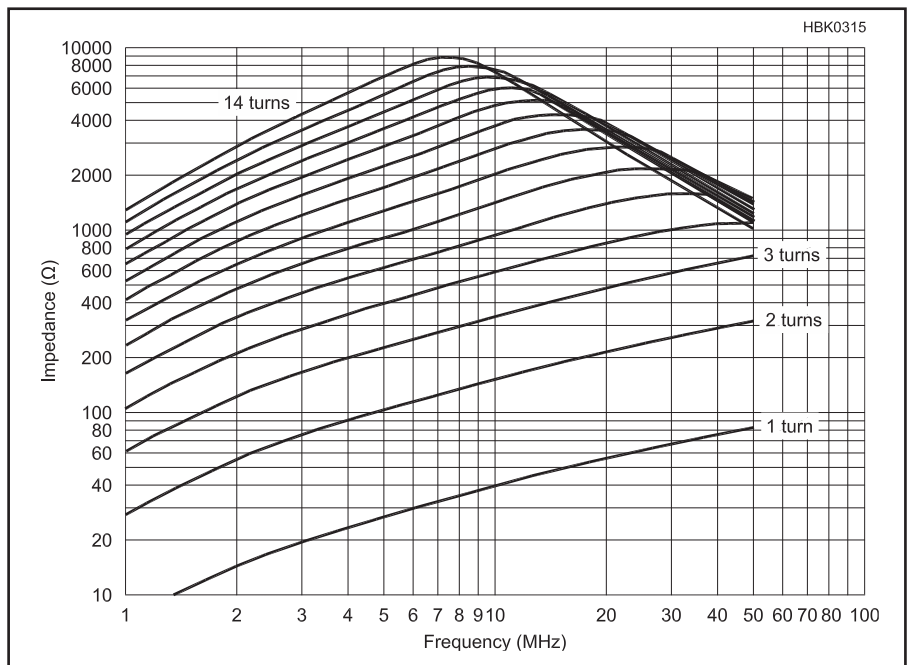


Figure 5.51 — Impedance of multi-turn choke wound on a Fair-Rite Type #43 core as shown in Figure 5.50. Type #43 material is optimized for use as a choke for the VHF range. (Measured data)

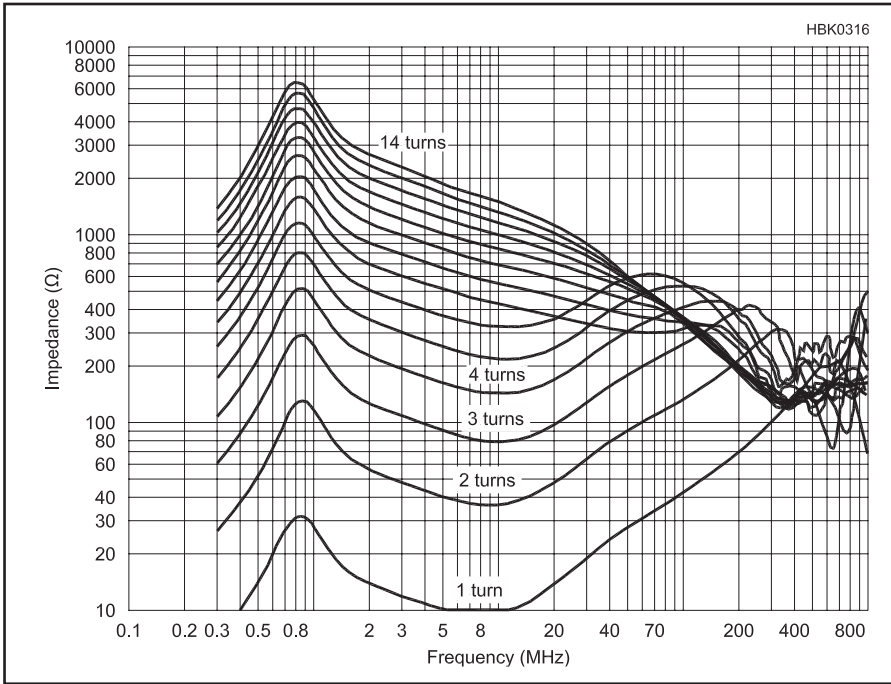


Figure 5.52 — Impedance of multi-turn choke wound on a Fair-Rite Type #78 core as shown in Figure 5.50. Type #78 material is optimized for use as a choke below 2 MHz. (Measured data)

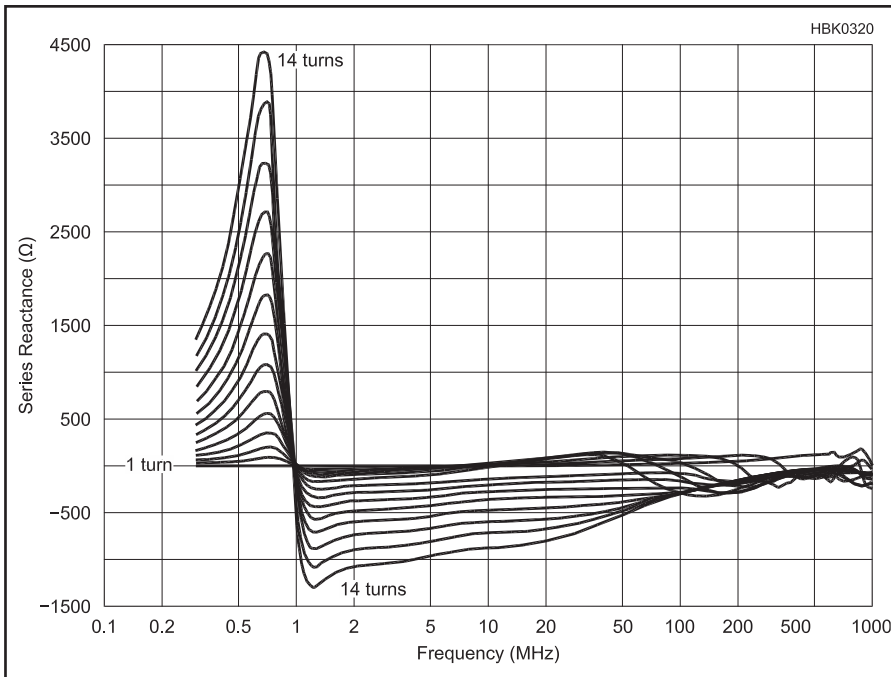


Figure 5.53 — Series reactive component of the chokes of Figure 5.52. (Measured data)

tional to the length of the cylinder. Figure 5.48 shows the impedance of a family of beads that differ primarily in their length. There are also small differences in their cross section, which is why the resonant frequency shifts slightly as discussed below. **Figure 5.49** shows some typical ferrite bead configurations.

Like all inductors, the impedance of a ferrite choke below resonance is approximately proportional to the square of the number of turns passing through the core. **Figure 5.50** shows a multi-turn choke wound on a 2.4-inch OD × 1.4-inch ID × 0.5-inch ferrite toroid core. **Figure 5.51** is measured data for the

choke in Figure 5.50 made of ferrite optimized for the VHF range (30-300 MHz). The data of **Figure 5.52** are for toroids of the same size, but wound on a material optimized for use below 2 MHz.

The measured data for Figures 5.51, 5.52, and 5.53 are for chokes wound with small diameter wire. The choke of Figure 5.50 will exhibit a somewhat lower resonant frequency for the same number of turns because the larger diameter cable has more capacitance between turns. The cable in the photo is a high quality braid-shielded twisted pair with an outside diameter comparable to RG-59.

We'll study the $L_D C_D$ resonance first. A classic text (*Soft Ferrites, Properties and Applications*, by E. C. Snelling, published in 1969), shows that there is a dimensional resonance within the ferrite related to the velocity of propagation (V_p) within the ferrite and standing waves that are set up in the cross-sectional dimensions of the core. In general, for any given material, the smaller the core, the higher will be the frequency of this resonance, and to a first approximation, the resonant frequency will double if the core dimension is halved. In Figure 5.45C, L_D and C_D account for this dimensional resonance, and R_D for losses within the ferrite. R_D is mostly due to eddy currents (and some hysteresis) in the core.

Now it's time to account for R_C , L_C and C_C . Note that there are two sets of resonances for the chokes wound around the Type #78 material (Figure 5.52), but only one set for the choke of Figure 5.51. For both materials, the upper resonance starts just below 1 GHz for a single turn and moves down in frequency as the number of turns is increased. **Figure 5.53**, the reactance for the chokes of Figure 5.52, also shows both sets of resonances. That's why the equivalent circuit must include two parallel resonances!

The difference between these materials that accounts for this behavior is their chemical composition (the mix). Type #78 is a MnZn ferrite, while Type #43 is a NiZn ferrite. The velocity of propagation (V_p) in NiZn ferrites is roughly two orders of magnitude higher than for MnZn, and, at those higher frequencies, there is too much loss to allow the standing waves that establish dimensional resonance to exist.

To understand what's happening, we'll return to our first order equivalent circuit of a ferrite choke (Figure 5.45C). L_C , and R_C , and C_C are the inductance, resistance, (including the effect of the μ of the ferrite), and stray capacitance associated with the wire that passes through the ferrite. This resonance moves down in frequency with more turns because both L and C increase with more turns. The dimensional resonance does not move, since it depends only on the dimensions V_p of the ferrite.

What is the source of C_C if there's no "coil," only a single wire passing through a cylinder?

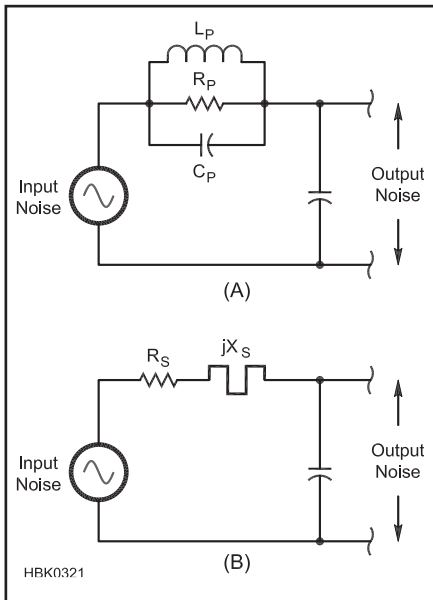


Figure 5.54 — At A, the series element of the divider is a parallel-resonant circuit. At B, the series element of the divider is the series-equivalent circuit used by ferrite data sheets.

It's the parasitic capacitance from the wire at one end of the cylinder to the wire at the other end, with the ferrite acting as the dielectric. Yes, it's a very small capacitance, but you can see the resonance it causes in the measured data and on the data sheet.

5.5.3 Ferrite Series and Parallel Equivalent Circuits

Let's talk briefly about series and parallel equivalent circuits. Many impedance analyzers express the impedance between their terminals as Z with a phase angle, and the series equivalent R_S and X_S . They could just have easily expressed that same impedance using the parallel equivalent R_P and X_P but R_P and X_P will have values that are numerically different from R_S and X_S . (See the section on series-parallel impedance transformation in the **Electrical Fundamentals** chapter.)

It is important to remember that in a series circuit, the larger value of R_S and X_S has the greatest influence, while in a parallel circuit, the smaller value of R_P and X_P is dominant. In other words, for R_P to dominate, R_P must be small.

Both expressions of the impedance (series or parallel) are correct at any given frequency, but whether the series or parallel representation is most useful will depend on the physics of the device being measured and how that device is used in a circuit. We've just seen, for example, that the parallel equivalent circuit is a more realistic representation of a ferrite

choke — the values of R_P , L_P , and C_P will come much closer to remaining constant as frequency changes than if we use the series equivalent. (R_P , L_P and C_P won't be precisely constant though, because the physical properties of all ferrites — permeability, resistivity and permittivity — all vary with frequency.)

But virtually all product data for ferrite chokes is presented as the series equivalent R_S and X_S . Why? First, because it's easy to measure and understand, second, because we tend to forget there is stray capacitance, and third because ferrite beads are most often used as chokes to reduce current in a series circuit! **Figure 5.54A** and **Figure 5.54B** are both

useful representations of the voltage divider formed by a ferrite choke and a small bypass capacitor across the device input. Which we use will depend on what we know about our ferrite.

If we know R_P , L_P and C_P and they are constant over the frequency range of interest, **Figure 5.54A** may be more useful, because we can insert values in a circuit model and perhaps tweak the circuit. But if we have a graph of R_S and X_S vs frequency, **Figure 5.54B** will give us a good answer faster. Because we will most often be dealing with R_S and X_S data, the series circuit equivalents are used most often. Another reason for using R_S and X_S

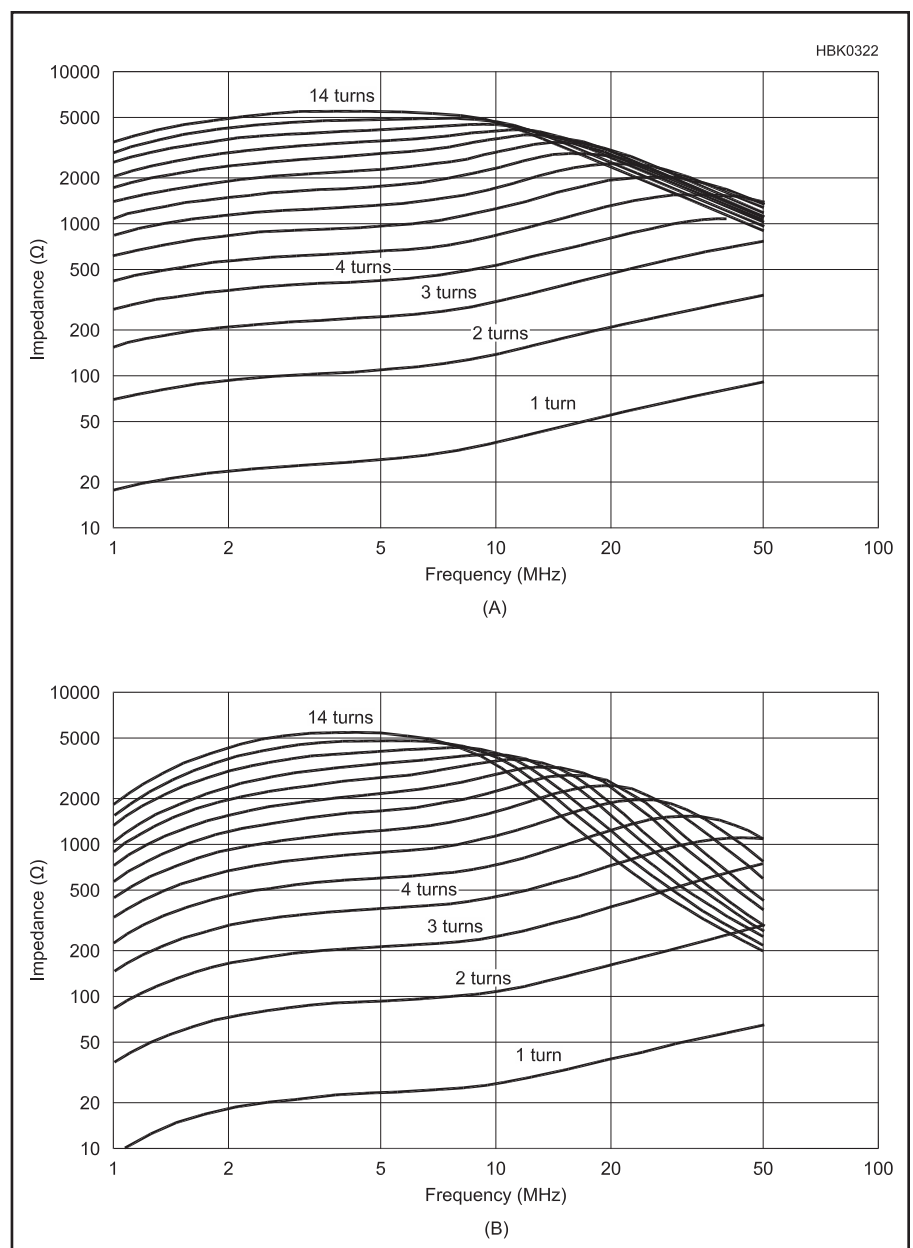


Figure 5.55 — At A, the impedance of multi-turn chokes on a Type #31 2.4-in. OD toroidal core. At B, the equivalent series resistance of the chokes of (A). (Measured data)

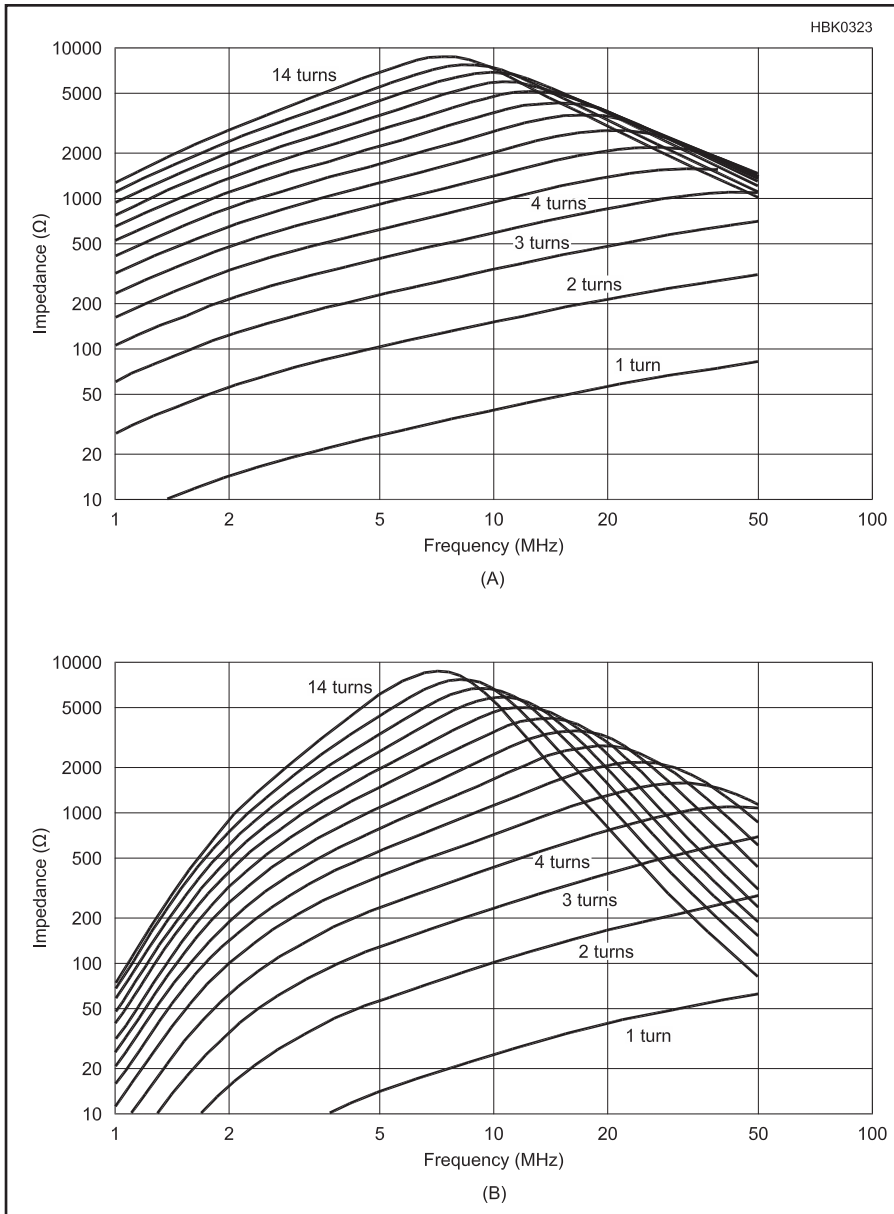


Figure 5.56 — At A, the impedance of multi-turn chokes wound with small-diameter wire on a Type #43 2.4-in. OD toroidal core. At B, the equivalent series resistance of the chokes of A. (Measured data).

is that the impedance of two or more ferrite chokes in series can be computed simply by adding their R_S and X_S components, just as with any other series impedances! When you look at the data sheet plots of R_S , X_L and Z for a standard ferrite part, you are looking at the series equivalent parameters of their dominant resonance. For most MnZn materials, it is dimensional resonance, while, for most NiZn materials, it is the circuit resonance.

Values for R_p , L_p and C_p for nearly any NiZn ferrite choke can be obtained by curve-fitting the data for its parallel-resonance curve. This is much more difficult for MnZn ferrite chokes, especially type #31. (Self-resonance is discussed earlier in this chapter.) Because

the C_p of many practical chokes is quite small and their impedance at resonance is often rather high, they are quite difficult to measure accurately, especially with reflection-based measurement systems. See the **Test Equipment and Measurements** chapter for a simple measurement method that can provide good results. More information on the use of ferrite cores and beads for EMI suppression is available in the chapter on **RF Interference** and in *The ARRL RFI Book*. A thorough treatment of the use of these ferrite materials for EMI suppression is continued in the online publication *A Ham's Guide to RFI, Ferrites, Baluns, and Audio Interfacing* at k9yc.com/publish.htm. The use of ferrite beads and

cores for transmitting chokes is presented in the **Transmission Lines** chapter.

5.5.4 Type 31 Material

Type #31 material made by Fair-Rite Products is extremely useful as a choke core, especially if some component of your problem occurs below 5 MHz. Measured data for the new material is displayed in **Figures 5.55A** and **5.55B**. Compare it with **Figures 5.56A** and **5.56B**, which are corresponding plots for the older Type #43 material. By comparison, Type #31 provides nearly 7 dB greater choking impedance at 2 MHz, and at least 3 dB more on 80 meters. At 10 MHz and above, the two materials are nearly equivalent, with Type #43 being about 1 dB better. If your goal is EMI suppression or a feed line choke (a so-called “current balun”), the Type #31 material is the best all round performer to cover all HF bands, and is clearly the material of choice at 5 MHz and below. Between 5 MHz and 20 MHz, Type #43 has a slight edge (about 1 dB), and above 20 MHz they're equivalent. (Baluns are discussed more in the section below on Transmission Line Transformers and in the chapters on **Transmission Lines** and **Antennas**.)

Type #31 material is useful because it exhibits both of the resonances in our equivalent circuit — that is, the dimensional resonance of the core and the resonance of the choke with the lossy permeability of the core material. Below 10 MHz, these two resonances combine (in much the manner of a stagger-tuned IF) to provide significantly greater suppression bandwidth (roughly one octave, or one additional harmonically related ham band). The result is that a single choke on a Type #31 core can be made to provide very good suppression over about 8:1 frequency span, as compared to 4:1 for Type #43. Type #31 also has somewhat better temperature characteristics at HF.

5.5.5 Determining Ferrite Type

The type of mix for ferrite cores and beads without identification is not easily determined, unfortunately. This makes ferrite components of unknown type hard to use properly. Unlike powdered-iron cores, most ferrite components are not manufactured with a colored coating that identifies the type of material. It is a good idea to label these components as soon as they are purchased. Colored tape using standard color codes or labels work well. (As of early 2022, DX Engineering adds a paint stripe to the ferrite cores they distribute.) A light-color paint or silver Sharpie-type marker will write indelibly on the charcoal-color cores.

Three electrical tests described below can identify an unknown mix with reasonable confidence:

1. Begin with an ohmmeter to determine the general ceramic compound: MnZn or NiZn.

2. Measure the material's relative permeability, μ_r , using an inductance meter or impedance analyzer and compare it to published values for different mixes.

3. Finally make swept-frequency measurements using a vector impedance analyzer (VIA) or vector network analyzer (VNA) to confirm the most likely mix based on the behavior of the material's reactance and impedance magnitude with frequency.

OBTAINING CORE DATA

The vast majority of ferrite cores encountered by hams are manufactured by Fair-Rite. Data for their cores can be accessed from the PRODUCTS tab at fair-rite.com, then selecting SUPPRESSION COMPONENTS or POWER & INDUCTIVE COMPONENTS. For POWER AND INDUCTIVE COMPONENTS, select CLOSED MAGNETIC CIRCUIT, then TOROIDS (assuming that is the type of component being tested).

For SUPPRESSION COMPONENTS, select CABLE COMPONENTS, then either ROUND CABLE EMI SUPPRESSION CORES (toroids and beads) or ROUND CABLE SNAP-ITS (also known as "snap-on cores"). Selecting the type of core will display a table listing components of the type selected.

For both types of materials, the dropdown showing ALL MATERIALS / FREQS can limit the listing to only one suppression mix. From that table, clicking on the part number of a core will display its data sheet.

IDENTIFYING FERRITE WITH AN OHMMETER

Ferrites are semiconductors with resistivity varying by seven orders of magnitude from 100 Ω -cm to 10⁹ Ω -cm. In general, MnZn ferrite materials have lower values of resistivity; in the range of 100 – 300 Ω -cm for Fair-Rite type #73, #75, #77, and #78, and 3,000 Ω -cm for type #31. NiZn ferrites have much higher bulk resistivities: 10⁵ Ω -cm for type #43, 10⁷ Ω -cm for type #67, 10⁸ Ω -cm for type #61, and 10⁹ Ω -cm for types #44 and #52.

First suggested by W1HIS, these bulk resistivity differences allow us to partially identify the mix of MnZn cores with an ohmmeter. Of the MnZn cores tested by K9YC, types #75, #77, and #78 measure in the range of 1 – 10 k Ω while type #31 measured in the range of 100 k Ω – 700 k Ω .

Ferrite parts are likely to have a protective coating, so test probes must scratch aggressively through that coating to make contact with the core. K9YC used three multimeters; a Simpson 260 analog volt/ohm meter (VOM), a Fluke 8060A digital VOM, and an inexpensive digital VOM. All three meters made the same identifications with good contact between the probe and the ferrite material.

Note that these are not quantitative mea-

surements: They don't show how good or bad the part is, they simply allow us to differentiate between MnZn and NiZn mixes, and for the MnZn materials to tentatively identify the difference between type #31 and types #75, #77, and #78. To get a better idea of the exact mix, we must make additional measurements.

IDENTIFYING FERRITE BY INDUCTANCE

In this method a coil is wound on a ferrite core and the resulting inductance is measured at low frequencies, well below any dimensional resonance. An LCR meter can be used with a test frequency at 50 kHz or lower. Some analyzers and/or their software can compute and display inductance vs. frequency from a swept measurement. A sweep starting at 50 kHz or an impedance bridge or meter that can measure in this range is recommended. This method may not yield definitive results for cores of very low permeability like Fair-Rite type #61. For very low permeability cores, the swept impedance method described below should be used.

The resonance of a multi-turn winding and the dimensional resonance in MnZn materials reduce the measured inductance as frequency increases approaching either resonance. Use a value for inductance measured at lower frequencies where it is approximately constant. An instrument that can plot inductance vs. frequency from a swept measurement should display a straight line in the frequency range where an inductance measurement is valid for this method. (See the multi-turn plots below for examples.)

From the inductance and number of turns, relative permeability μ_r , is calculated from the equation $\mu_r = (79.55 N^2 L l_c) / A_c$, where N is the number of turns, L is in μ H, l_c is in cm, and A_c is in cm². A_c is the cross-sectional area of the core and l_c is the length of the path for magnetic flux around the core. (These mechanical dimensions can usually be found in catalog data for cores with the same dimensions, regardless of the type of material.) Remember that the number of turns is the number of times the winding passes through the core. The calculated value of μ_r is then compared to values for cores of the same dimension from manufacturer data sheets. (See the **Circuits and Components** chapter for tables of relative permeability for some ferrite materials.)

From the Fair-Rite data listing the type of component (see above), clicking on the selector at the top of the page showing ALL MATERIALS / FREQS will list those materials and their μ_r values. A_c and l_c values are published in the component data sheet. POWER & INDUCTIVE COMPONENTS and EMI SUPPRESSION parts having the same dimensions will have the same l_c and A_c values.

If no catalog data is available, A_c and l_c can

often be computed from dimensions of the core. A_c is the cross-sectional area of the core and l_c is the length of the path for magnetic flux around the core. For a cylindrical core (including toroids), A_c and l_c are easy to calculate from their dimensions: $A_c = (OD - ID) \times (\text{core length}) / 2$, and to a first approximation, $l_c = \pi (OD + ID) / 2$, the average of the inner and outer diameters of the core.

For cores of other shapes it's not so simple. For cores with a circular internal diameter and a square, rectangular, hexagonal, or octagonal outer shape (typical of snap-on cores), A_c is the area of that outer shape minus the area of the internal circular cross section. But a lot more math is needed to determine l_c for these cores with sufficient precision to be meaningful.

IDENTIFYING FERRITE WITH SWEEPED IMPEDANCE

In this test, one or more turns of wire are close-wound on the core or bead and a vector analyzer measures the resulting impedance over a wide frequency range. The component's impedance and reactance are then plotted against frequency. The shape of the plots is characteristic of the mix type. It is important that the turns be close-wound. Wide turn spacing will move measured resonances higher in frequency, particularly for the NiZn and type #31 mixes.

The analyzer measures S parameter S11, the reflection coefficient of a single-port network or device, from which its complex impedance can be computed at each frequency. (See the Two-Port Networks section later in this chapter for information on S parameters.) The type of ferrite can then be determined from the shape of the reactance and impedance plots. The technique of using a vector analyzer to make swept-frequency impedance measurements is explained in more detail in

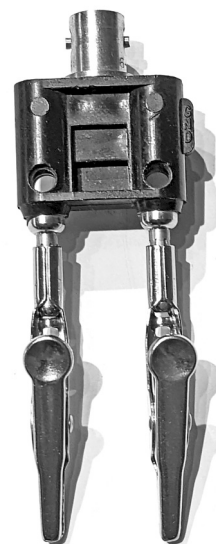


Figure 5.57 — A simple test fixture for measuring component impedance with a vector analyzer. The adaptor is a BNC-to-Banana Plug adapter. Large alligator clips will usually slide on to the banana plugs. The cable used to connect the adaptor to the analyzer must be included in the fixture calibration. (Photo by Jim Brown, K9YC)

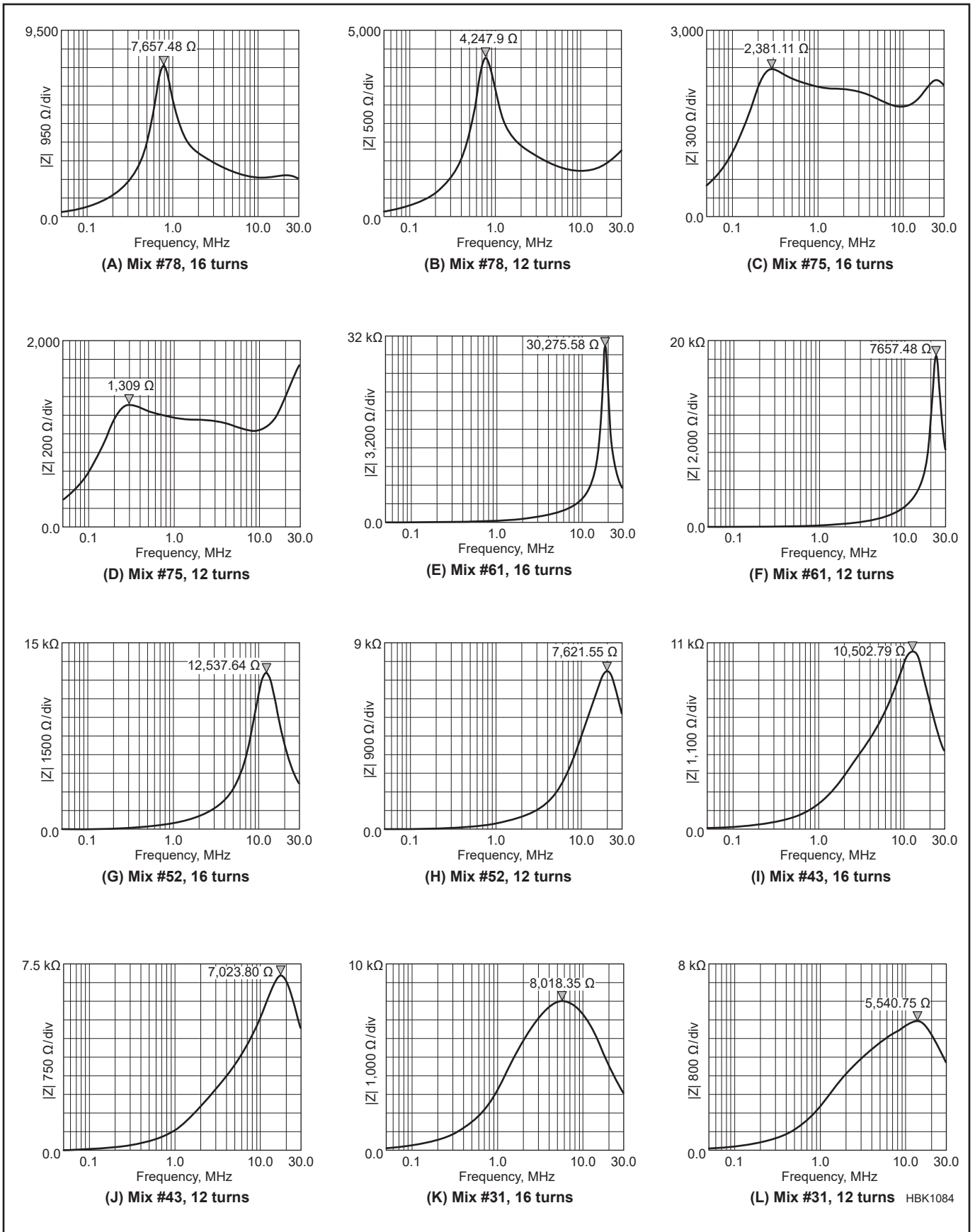


Figure 5.58 — Measured impedance magnitude (Zmag) for Fair-Rite Type #78, #75, #61, #52, #43, and #31 toroidal cores with 16 and 12 turns of #18 AWG insulated wire.

the **Test Equipment and Measurements** chapter.

For the purpose of measuring windings on a ferrite core, it is most convenient to make a simple test fixture as in **Figure 5.57** from a BNC-to-Banana Plug adapter with alligator clips mounted on the banana plugs. This test fixture is then attached to the analyzer with a convenient length of high-quality cable such as RG-400. The measurement plane for this fixture is at the tips of the alligator clip jaws. This fixture can be used to measure any component that can be attached to the clips, provided the leads are short enough to not add enough inductance or stray capacitance to create a resonance in or near the measured frequency range.

Particularly for the higher-frequency data, be sure the core and test fixture are not near conducting objects or surfaces. Letting the fixture hang over the edge of a work surface or chair with the clips facing down and the core suspended in the air from the clips is a good arrangement.

When evaluating measurements, remember that ferrite parts have wide manufacturing tolerances, so don't expect to duplicate these plots, but do expect parts of the same type of material to show similar shapes. Fair-Rite's inductive parts are specified with +/- 25% tolerances for inductance; their suppression parts are specified only for minimum impedance values at selected frequencies.

Materials from other manufacturers are

likely to behave very differently from Fair-Rite materials having similar values for μ_r , but will likely have similar manufacturing tolerances. Both identification methods should be used to make sure it is or is not a Fair-Rite part, and if not, to learn more about its characteristics.

In general, manufacturers do not provide impedance versus frequency data, only permeability, for parts sold as Power and Inductive components under the assumption they will be used at low enough frequencies that their loss component is insignificant. Fair-Rite types #43, #61, and #75 are sold both as Power & Inductive Components at low frequencies and as EMI Suppression Components at higher frequencies but carry different part numbers for the two applications. The difference is testing for production tolerances — EMI Suppression Components are controlled only for minimum impedance at specific high frequencies, Power and Inductive Components are specified by their initial relative permeability, μ_r , which is measured at very low frequencies.

DATA FOR COMMON FERRITE MIXES

Figures 5.58A – L show data from testing randomly selected 2.4-inch O.D. cores of different ferrite types from Fair-Rite. To compare a core to this data, close-wind 16 turns of #18 AWG insulated wire on the core, trim leads to minimum length, make a measurement,

and save the data. Remove four turns, trimming leads to minimum length, and repeat the measurement. Smaller cores may need to be swept over a higher frequency range to see comparable plot shapes.

In these data plots the curve is the magnitude of the impedance (Z_{MAG}) with zero at bottom of the vertical scale. The frequency scale is logarithmic and the same for all cores. (Note that the plot shapes will be very different on a linear frequency scale.) The amplitude scale is varied to set the resonant peak value near the top of the plot so that curve shapes can be best compared. Scales are shown at the left edge of each plot.

The general shape of the Z_{MAG} curves and the frequency range in which the impedance peak occurs are what distinguishes the different mixes. MnZn cores of types #75, #77, and #78 clearly show dimensional resonance, even for only a single turn. These occur at frequencies that are *not* dependent on the number of turns but *do* depend on the size and/or shape of the core. For these materials, the resonances don't move (much) in frequency with the number of turns. The peak simply gets stronger with more turns. Type #31 will show a broad resonance that moves and changes shape with the number of turns as the dimensional resonance combines with the resonance of the winding. NiZn mixes will show a single resonance, usually in the upper HF range, that moves higher in frequency with fewer turns. It's formed by the inductance of

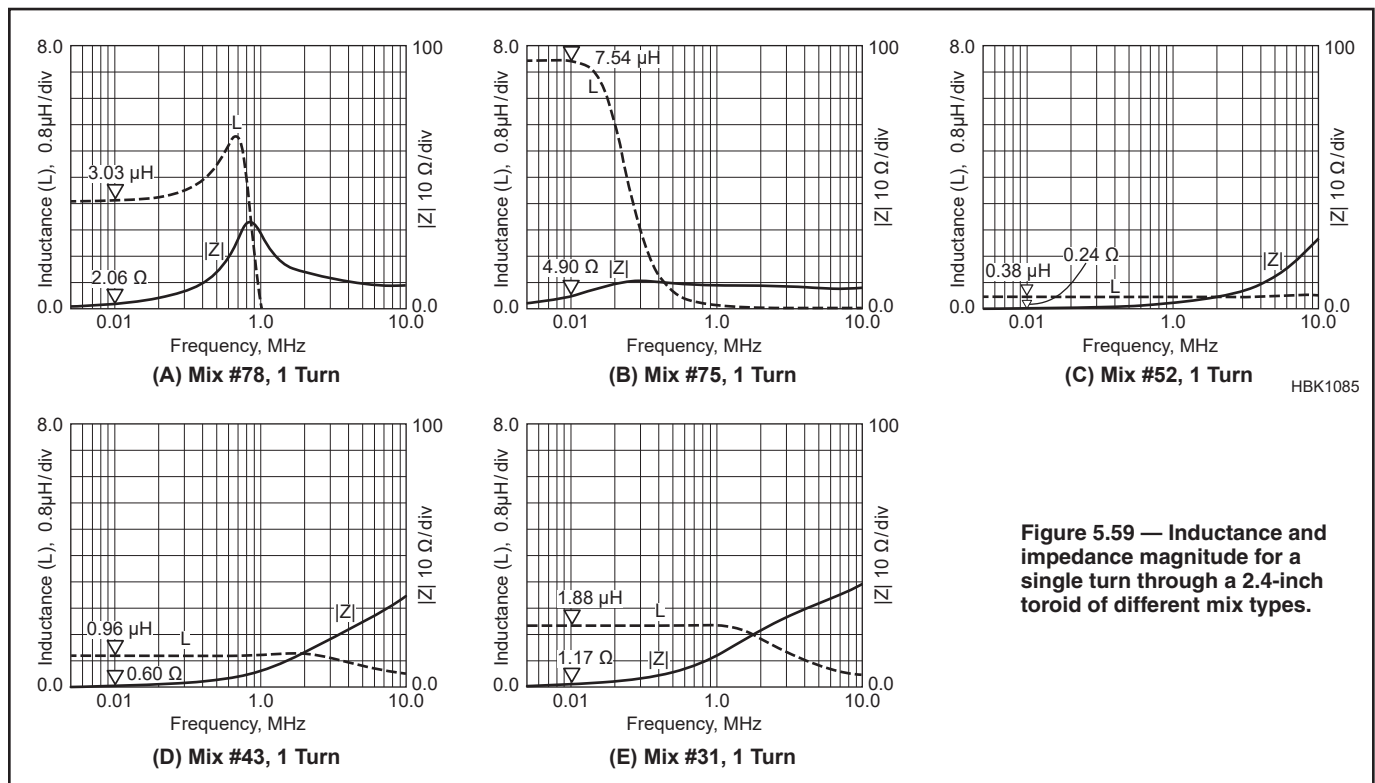


Figure 5.59 — Inductance and impedance magnitude for a single turn through a 2.4-inch toroid of different mix types.

the winding and the stray (parasitic) capacitance between turns, as shown in the plots for types #43, #52, and #61 material.

Note that these data for #18 insulated wire differ from comparable measurements for transmitting chokes because the transmission lines used for the chokes have larger conductors, different insulation, and greater inter-winding capacitance. (See the chapter **Transmission Lines** section Transmitting Ferrite Chokes and Baluns.)

Figures 5.59 A – E are for a single turn through a 2.4-inch O.D. toroid core. The dashed curve is inductance and the solid curve is the magnitude of the impedance, Z_{MAG} , both with zero at the bottom of the vertical scale.

- Type #78: resonances should appear in the range of 700 – 1000 kHz, they should not

move much in frequency, and the peak's amplitude should get lower as turns are removed.

- Type #77: should measure about the same as type #78, except that the resonance will be in the range of 1300 – 1500 kHz.

- Type #75: resonances will be below 700 kHz.

- Type #61: Swept-frequency measurements of Type #61 were unreliable due to the material's very low resistive component and are not shown here as a graph. If the permeability falls below 200 and the multi-turn measurements show a strong, high-Q resonance, the material is probably Type #61 or a similar material from another manufacturer.

- Type #43 and #52: multi-turn tests can be ambiguous, but measuring A_L will be clear for distinguishing between these types. Both of these types are not recommended for chokes at HF in favor of Type #31.

- Type #31: the resonance will be much broader, will move up in frequency as turns are removed, and the impedance at resonance will be lower with fewer turns.

For use in RF chokes, only Type #31 is recommended for chokes at HF and 160 meters, Type #75 is useful only on 630 meters, and mixes like Type #43, #52, and #61 should only be used for chokes at VHF and above.

For use in RF transformers and inductors, Type #43, #52, and #61 are useful at HF.

Surplus round cores are most likely to be either 1) intended for EMC compliance above 30 MHz, which are likely to be Type #43 or something similar; or 2) those used for power magnetics at low frequencies, which are likely to be MnZn mixes; or 3) those used for transformers, which are most likely to be MnZn at low frequencies or NiZn at high frequencies.

5.6 Impedance Matching Networks

An impedance transforming or matching network is one that accepts power from a generator with one characteristic impedance, the source, and delivers virtually all of that power to a load at a different impedance. The simple designs in this section provide matching at only one frequency. More refined methods discussed in the reference texts can encompass a wide band of frequencies.

Both source and load impedances are likely to be complex with both real and imaginary (reactive) parts. The procedures given in this section allow the reader to design the common impedance-matching networks based on the simplification that both the source and load impedance are resistive (with no reactive component). To use these procedures with a complex load or source impedance, the usual method is to place a reactance in series with the impedance that has an equal and opposite reactance to cancel the reactive component of the impedance to be matched. Then treat the resulting purely-resistive impedance as the resistance to be transformed. For example, if a load impedance to be matched is $120 + j40 \Omega$, add capacitive reactance of $-j40 \Omega$ in series with the load, resulting in a load impedance of $120 + j0 \Omega$ so that the following procedures can be used. The series reactance-canceling component may then be combined with the matching network's output component in some configurations.

A set of 14 simple resonant networks, and their equations, is presented in **Figure 5.61**. Note that in these diagrams R_S is the low impedance side and R_L is the high impedance side and that the X values are calculated in the top-down order given.

The formulas for the various networks use and produce values of reactance. To convert the reactances to L and C values, use the formulas

$$C = \frac{1}{2\pi f X_C} \text{ and } L = \frac{X_L}{2\pi f}$$

The program *MATCH.EXE* in the online content can perform the calculations.

You may wish to review the section on series-parallel impedance transformations in the **Electrical Fundamentals** chapter as those techniques form the basis of impedance-matching network design. There is additional discussion of L networks in the chapters on **Transmission Lines** and of Pi networks in the **RF Power Amplifiers** chapter. These discussions apply to more specific applications of the networks.

5.6.1 L Networks

Perhaps the most common LC impedance transforming network is the L network, so named because it uses two elements — one series element and one parallel — resembling the capital L on its side. There are eight different types of L networks as shown in **Figure 5.60**. (Types G and H are not as widely used and not covered here.) The simplified Smith Chart sketches show what range of impedance values can be transformed to the required impedance Z_0 and the path on the chart by which the transformation is achieved by the two reactances. (An introductory discussion of the Smith Chart is provided with the online content, and a detailed treatment is available in *The ARRL Antenna Book*.) Z_{DEV} represents the output impedance of a device, such as a transistor amplifier or any piece of equipment.

The process of transformation works the same in both “directions.” That is, a network designed to transform Z_{DEV} to Z_0 will also transform Z_0 to Z_{DEV} if reversed. The L network (and the Pi and T networks discussed below) is *bilateral*, as are all lossless networks.

Purely from the standpoint of impedance matching, the L network can be constructed with inductive or capacitive reactance in the series arm and the performance will be exactly the same in either case. However, the usual case in amateur circuits is to place the inductive reactance in the series arm to act as a low pass filter. Your particular circumstances may dictate otherwise, however. For example, you may find it useful that the series-C/parallel-L network places a dc short circuit across one side of the network while blocking dc current through it.

The design procedure for L network configurations A through F in **Figure 5.60** is as follows:

Given the two resistance values to be matched, connect the series arm of the circuit to the smaller of the two (R_S) and the parallel arm to the larger (R_P).

Find the ratio R_P/R_S and the L network's Q:

$$Q = \sqrt{\frac{R_P}{R_S} - 1}$$

Calculate the series reactance $X_S = QR_S$

Calculate the parallel reactance $X_P = R_P/Q$.

5.6.2 Pi Networks

Another popular impedance matching network is the Pi network shown in circuits 1 and 2 of **Figure 5.61**. The Pi network

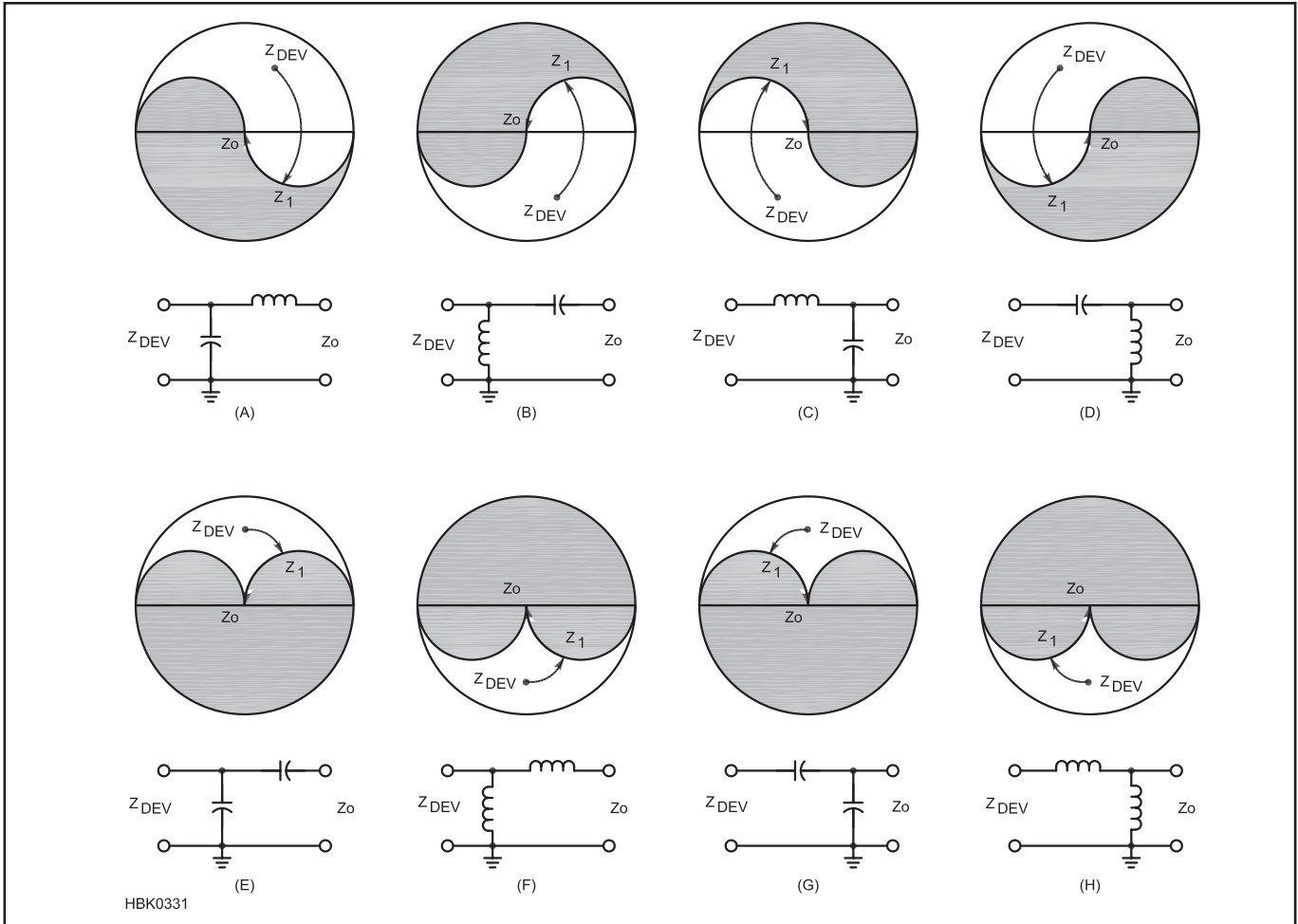


Figure 5.60 — L networks which will match a complex impedance (shown here as Z_{DEV} , the output impedance of a device) to Z_0 , a resistive source or load. Impedances within the shaded portion of the simplified Smith Chart cannot be matched by the network. Z_1 represents the impedance that is transformed from Z_{DEV} by the series element.

can be thought of as two L networks “back to back.” For example, the Pi network in circuit 1 can be split into the L network of circuit 13 on the right and its mirror image on the left. The two inductors in series are combined into the single inductance of the Pi network. There are other forms of the Pi network with different configurations of inductance and capacitance, but the version shown is by far the most common in amateur circuits.

The use of two transformations allows the designer to choose Q for the Pi network, unlike the L network for which Q is determined by the ratio of the impedances to be matched. This is particularly useful for matching amplifier outputs as discussed in the **RF Power Amplifier** chapter because it allows more control of the network’s frequency response and of component values. Q must be high enough that $(Q^2 + 1) > (R_1 / R_2)$. If these two quantities are equal, X_{C2} becomes infinite, meaning zero capacitance, and the Pi network reduces to the L network in Figure 5.60A. The design procedure for the Pi network in Figure 5.61 is as follows:

Determine the two resistance values to be matched, $R_1 > R_2$, and select a value for Q . Follow the calculation sequence for circuit 1 or 2 in Figure 5.61.

Calculate the value of the parallel reactance $X_{C1} = R_1 / Q$.

Calculate the value of the parallel reactance X_{C2}

$$X_{C2} = R_2 \sqrt{Q^2 + 1 - R_1 / R_2}$$

Calculate the value of the series reactance X_L

$$X_L = \frac{QR_1 + R_1R_2 / X_{C2}}{Q^2 + 1}$$

5.6.3 T Networks

Many amateur transmission line impedance matching units (“antenna tuners”) use the version of the T network in circuit 6 of Figure 5.61. The circuits are constructed using variable capacitors and a tapped inductor. This

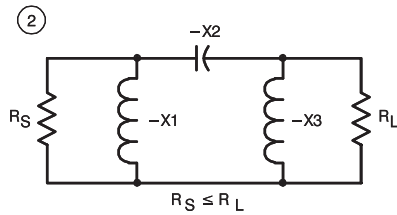
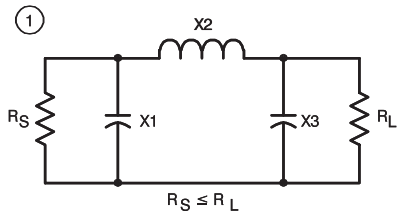
is easier and less expensive to construct than a fully-adjustable version of circuit 5 in which two variable inductors are required. Circuit 5 is especially useful in matching relatively low input impedances from solid-state amplifier outputs to 50-Ω loads with low Q and good harmonic suppression due to the series inductances. Circuit 7 is also useful in solid-state amplifier design as described in the reference texts listed at the end of this chapter.

The T network shown in circuit 5 of Figure 5.61 is especially useful for matching to relatively low impedance from 50-Ω sources with practical components and low Q . Like the Pi network, Q must be high enough that $(Q^2 + 1) > (R_1 / R_2)$. Designing the component values for this network requires the calculation of a pair of intermediate values, A and B, to make the equations more manageable.

Determine the two resistance values to be matched, $R_1 > R_2$, and select a value for Q .

Calculate the intermediate variables A and B

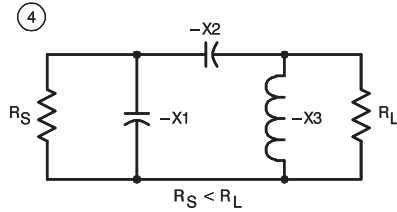
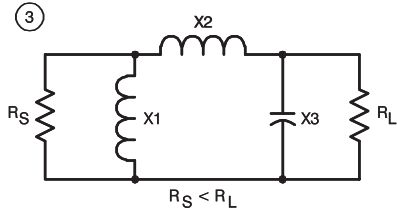
$$A = R_1(Q^2 + 1) \text{ and } B = \sqrt{\left(\frac{A}{R_2} - 1\right)}$$



$$X1 = -R_S \sqrt{\frac{R_L / R_S}{Q^2 + 1 - (R_L / R_S)}}$$

$$X2 = \frac{Q \times R_L - (R_S \times R_L / X1)}{Q^2 + 1}$$

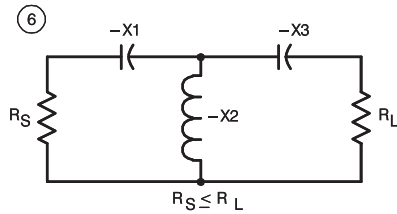
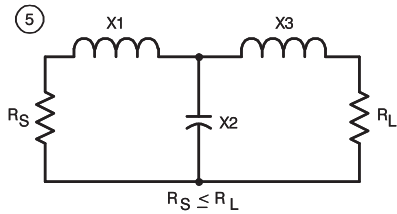
$$X3 = -\frac{R_L}{Q}$$



$$X1 = \frac{R_S}{\sqrt{\frac{R_S (Q^2 + 1)}{R_L} - 1}}$$

$$X2 = \frac{R_L \times Q}{Q^2 + 1} \left(1 - \frac{R_S}{Q \times X1}\right)$$

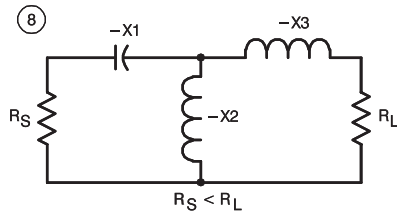
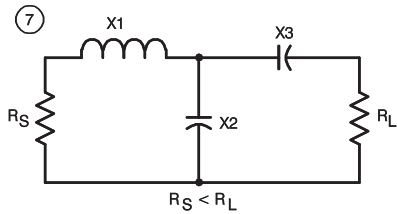
$$X3 = -\frac{R_L}{Q}$$



$$X1 = R_S \times Q$$

$$X2 = \frac{-R_S(1 + Q^2)}{Q + \sqrt{\frac{R_S(1 + Q^2)}{R_L} - 1}}$$

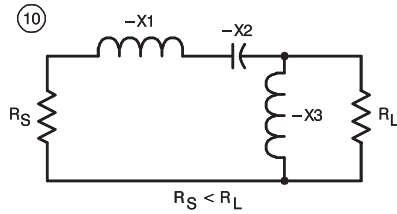
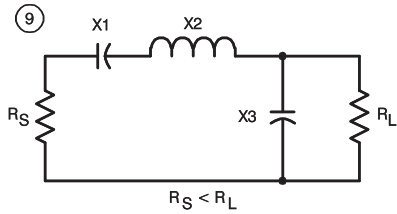
$$X3 = R_L \sqrt{\frac{R_S(1 + Q^2)}{R_L} - 1}$$



$$X1 = Q \times R_S$$

$$X2 = \frac{-R_S(1 + Q^2)}{Q - \sqrt{\frac{R_S(1 + Q^2)}{R_L} - 1}}$$

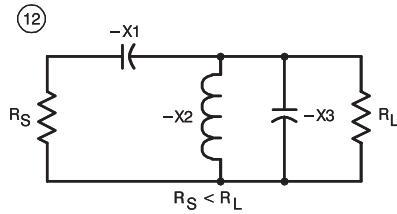
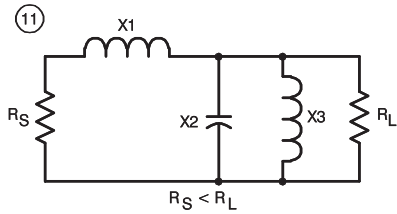
$$X3 = -R_L \sqrt{\frac{R_S(1 + Q^2)}{R_L} - 1}$$



$$X1 = -Q \times R_S$$

$$X2 = \sqrt{R_S \times R_L - R_S^2 - X1}$$

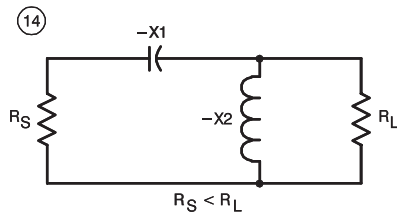
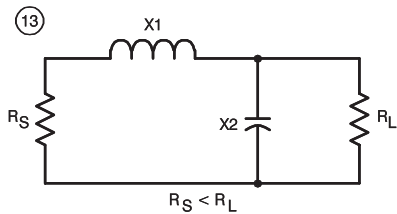
$$X3 = \frac{-R_S \times R_L}{X1 + X2}$$



$$X1 = R_S \sqrt{\frac{R_L}{R_S} - 1}$$

$$X3 = \frac{R_L}{Q}$$

$$X2 = \frac{-X3}{\frac{X1}{Q \times R_S} + 1}$$



$$X1 = \sqrt{R_S \times R_L - R_S^2}$$

$$X2 = -\frac{R_S \times R_L}{X1}$$

HBK0674

Figure 5.61 — Fourteen impedance transforming networks with their design equations (for lossless components).

Calculate the value of the input series reactance $X_{L1} = R_1 Q$.

Calculate the value of the output series reactance $X_{L2} = R_2 B$.

Calculate the value of the parallel reactance $X_C = A / (Q + B)$.

Convert the reactances to component values:

$$C = \frac{1}{2\pi f X_C} \text{ and } L = \frac{X_L}{2\pi f}$$

5.6.4 Impedance Inversion

Symmetrical Pi and T networks have the useful property of *impedance inversion* when the reactances of all elements are the same at the design frequency: $X_C = X_L = |X|$, resulting in a Q of 1. For either type of network, the impedance looking into the network, Z_{IN} , will be the load impedance, Z_{OUT} , inverted about X:

$$Z_{IN} = \frac{X^2}{Z_{OUT}}$$

This is the same effect as if the network were replaced with a $\frac{1}{4}$ -wavelength transmission line with $Z_0 = |X|$. Since the network is symmetrical, the inversion occurs in either direction through the network. The result is true only at the frequency for which all reactances are equal.

For example, to invert all impedances about 50Ω , set $X = 50 \Omega$ at the design frequency. The input impedance will then be $50^2/Z_{OUT}$. If $Z = 10 + j10 \Omega$ is connected to one end of the network, the impedance looking into the other end of the network will be $2500 / (10 + j10) = 125 - j125 \Omega$.

5.7 RF Transformers

5.7.1 Air-Core Nonresonant RF Transformers

Air-core transformers often function as mutually coupled inductors for RF applications. They consist of a primary winding and a secondary winding in close proximity. Leakage reactances are ordinarily high, however, and the coefficient of coupling between the primary and secondary windings is low. Consequently, unlike transformers having a magnetic core, the turns ratio does not have as much significance. Instead, the voltage induced in the secondary depends on the mutual inductance.

In a very basic transformer circuit operating at radio frequencies, such as in **Figure 5.62**, the source voltage is applied to L1. R_S is the series resistance inherent in the source. By virtue of the mutual inductance, M, a voltage is induced in L2. A current flows in the secondary circuit through the reactance of L2 and the load resistance of R_L . Let X_{L2} be the reactance of L2 independent of L1, that is, independent of the effects of mutual inductance. The impedance of the secondary circuit is then:

$$Z_S = \sqrt{R_L^2 + X_{L2}^2} \quad (12)$$

where

Z_S = the impedance of the secondary circuit in ohms,

R_L = the load resistance in ohms, and

X_{L2} = the reactance of the secondary inductance in ohms.

The effect of Z_S upon the primary circuit is the same as a coupled impedance in series with L1. **Figure 5.63** displays the coupled impedance (Z_p) in a dashed enclosure to indicate that it is not a new physical component. It has the same absolute value of phase angle as in the secondary impedance, but the sign of the

reactance is reversed; it appears as a capacitive reactance. The value of Z_p is:

$$Z_p = \frac{(2\pi f M)^2}{Z_S} \quad (13)$$

where

Z_p = the impedance introduced into the primary,

Z_S = the impedance of the secondary circuit in ohms, and

$2\pi f M$ = the mutual reactance between the reactances of the primary and secondary coils (also designated as X_M).

5.7.2 Air-Core Resonant RF Transformers

The use of at least one resonant circuit in place of a pair of simple reactances eliminates the reactance from the transformed impedance in the primary. For loaded or operating Q of at least 10, the resistances of individual components is negligible. **Figure 5.63** represents just one of many configurations in which at least one of the inductors is in a resonant circuit. The reactance coupled into the primary circuit is cancelled if the circuit is tuned to resonance while the load is connected. If the reactance of

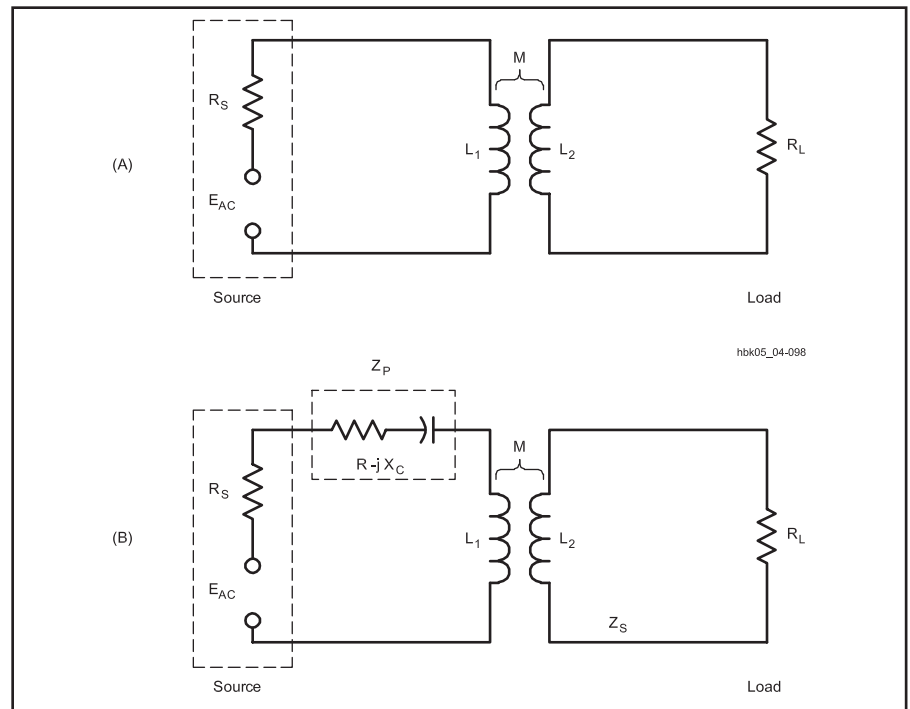


Figure 5.62 — The coupling of a complex impedance back into the primary circuit of a transformer composed of nonresonant air-core inductors.

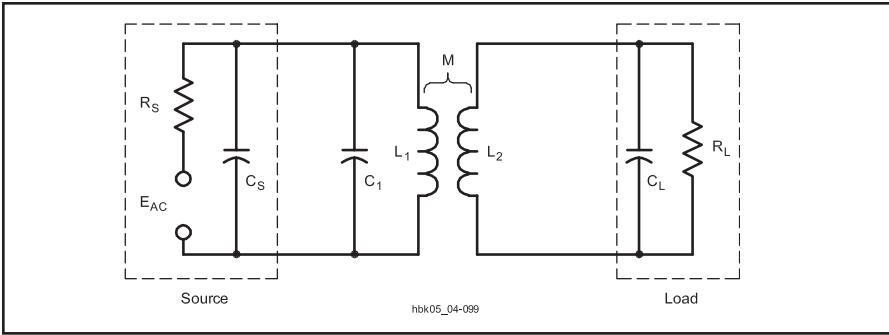


Figure 5.63 — An air-core transformer circuit consisting of a resonant primary circuit and an untuned secondary. R_S and C_S are functions of the source, while R_L and C_L are functions of the load circuit.

the load capacitance, C_L is at least 10 times any stray capacitance in the circuit, as is the case for low impedance loads, the value of resistance coupled to the primary is

$$R1 = \frac{X_M^2 R_L}{X_2^2 + R_L^2}$$

where:

$R1$ = series resistance coupled into the primary circuit,

X_M = mutual reactance,

R_L = load resistance, and

X_2 = reactance of the secondary inductance.

The parallel impedance of the resonant circuit is just $R1$ transformed from a series to a parallel value by the usual formula, $R_p = X_2 / R1$.

The higher the loaded or operating Q of the circuit, the smaller the mutual inductance required for the same power transfer. If both the primary and secondary circuits consist of resonant circuits, they can be more loosely coupled than with a single tuned circuit for the same power transfer. At the usual loaded Q of 10 or greater, these circuits are quite selective, and consequently narrowband.

Although coupling networks have to a large measure replaced RF transformer coupling that uses air-core transformers, these circuits are still useful in antenna tuning units and other circuits. For RF work, powdered-iron toroidal cores have generally replaced air-core inductors for almost all applications except where the circuit handles very high power or the coil must be very temperature stable. Slug-tuned solenoid coils for low-power circuits offer the ability to tune the circuit precisely to resonance. For either type of core, reasonably accurate calculation of impedance transformation is possible. It is often easier to experiment to find the correct values for maximum power transfer, however.

5.7.3 Broadband Ferrite RF Transformers

The design concepts and general theory of ideal transformers presented in the **Electrical Fundamentals** chapter apply also to transformers wound on ferromagnetic-core materials (ferrite and powdered iron). As is the case with stacked cores made of laminations in the classic I and E shapes, the core material has a specific permeability factor that determines the inductance of the windings versus the number of wire turns used. (See the earlier discussion on Ferrite Materials in this chapter.)

One of the most common ferromagnetic transformers used in amateur circuits is the conventional broadband transformer. Broadband transformers with losses of less than 1 dB are employed in circuits that must have a uniform response over a substantial frequency range, such as a 2- to 30-MHz broadband amplifier. In applications of this sort, the reactance of the windings should be at least four times the impedance that the winding is designed to look into at the lowest design frequency.

Example: What should be the winding reactances of a transformer that has a 300- Ω primary and a 50- Ω secondary load? Relative to the 50- Ω secondary load:

$$X_S = 4 Z_S = 4 \times 50 \Omega = 200 \Omega$$

and the primary winding reactance (X_p) is:

$$X_p = 4 Z_p = 4 \times 300 \Omega = 1200 \Omega$$

The core-material permeability plays a vital role in designing a good broadband transformer. The effective permeability of the core must be high enough to provide ample winding reactance at the low end of the operating range. As the operating frequency is increased, the effects of the core tend to disappear until there are scarcely any core effects at the upper limit of the operating range. The limiting factors for high frequency response are distributed

capacity and leakage inductance due to uncoupled flux. A high-permeability core minimizes the number of turns needed for a given reactance and therefore also minimizes the distributed capacitance at high frequencies.

Ferrite cores with a permeability of 850 are common choices for transformers used between 2 and 30 MHz. Lower frequency ranges, for example, 1 kHz to 1 MHz, may require cores with permeabilities up to 2000. Permeabilities from 40 to 125 are useful for VHF transformers. Conventional broadband transformers require resistive loads. Loads with reactive components should use appropriate networks to cancel the reactance. See www.w8ji.com/core_selection.htm for more guidelines on core material selection. Also see the article by Trask, which is included in the online content and listed in the References section.

The equivalent circuit in Figure 5.45 applies to any coil wound on a ferrite core, including transformer windings. (See the section on Ferrite Materials.) However, in the series-equivalent circuit, $\mu'S$ is not constant with frequency as shown in Figure 5.46A and 5.46B. Using the low-frequency value of $\mu'S$ is a useful approximation, but the effects of the parallel R and C should be included. In high-power transmitting and amplifier applications, the resistance R may dissipate some heat, leading to temperature rise in the core. The parasitic capacitances of each winding are shown as C_{PP} and C_{SP} in parallel with the primary and secondary circuits, respectively. These capacitances act to reduce high-frequency response.

Regarding C, there are at least two forms of stray capacitance between windings of a transformer as shown in **Figure 5.64A**; from wire-to-wire through air and from wire-to-wire through the ferrite, which acts as a dielectric material. These capacitances are combined as C_W from the primary to secondary circuits. (Ferrites with low iron content have a relative dielectric constant of approximately 10 to 12.)

For further information on conventional transformer matching using ferromagnetic materials, see the **RF Power Amplifiers** chapter. Refer to the **Circuits and Components** chapter for more detailed information on available ferrite cores. A standard reference on conventional broadband transformers using ferromagnetic materials is *Ferromagnetic Core Design and Applications Handbook* by Doug DeMaw, W1FB, published by MFJ Enterprises.

TOROIDAL CORE TRANSFORMERS

Toroidal cores are useful from a few hundred hertz well into the UHF spectrum. The principal advantage of this type of core is the self-shielding characteristic. Another

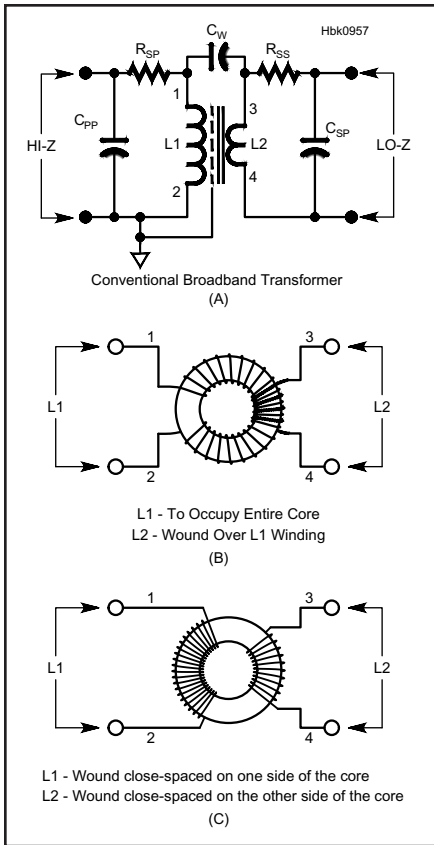


Figure 5.64 — (A) Schematic representation of a conventional broadband transformer wound on a toroid core. A Faraday shield (see text) can also be used to reduce capacitive coupling between the primary and secondary circuits. At (B) a pictorial showing the secondary winding (L2) is wound over the primary winding (L1) which provides very good coupling but low isolation. For designs emphasizing isolation over coupling, wind the transformer as in C with the primary and secondary windings separated on the core.

feature is the compactness of a transformer or inductor. Therefore, toroidal-core transformers are excellent for use not only in dc-to-dc converters, where tape-wound steel cores are employed, but at frequencies up to at least 1000 MHz with the selection of the proper core material for the range of operating frequencies. Toroidal cores are available from micro-miniature sizes up to several inches in diameter that can handle multi-kW military and commercial powers.

Figure 5.64B illustrates one method of transformer construction using a single toroid as the core. The primary of a step-down impedance transformer is wound to occupy the entire core, with the secondary wound over the primary. Conventional broadband transformers provide dc isolation between the primary and secondary circuits.

Winding-to-winding capacitance C_W re-

duces isolation between primary and secondary circuits. If isolation is an important characteristic of the transformer, then the windings should *not* be layered but separated on the core as in Figure 5.64C. The effect of C_W will increase with increasing frequency. This is a likely path for coupling of HF noise onto Ethernet cables if the network interface uses transformers.

A Faraday shield can be used to minimize C_W . It is made of conductive material, such as aluminum foil, that is connected to the circuit reference as in Figure 5.64A. (Faraday shields can also be connected to the secondary circuit reference.) Faraday shields are also used between windings in transformers for use in power, data, and audio circuits to prevent capacitive coupling of noise between windings.

The high voltages encountered in high-impedance-ratio step-up transformers may require that the core be wrapped with glass electrical tape before adding the windings (as an additional protection from arcing and voltage breakdown), especially with ferrite cores that tend to have rougher edges. In addition, high voltage applications should also use wire with high-voltage insulation and a high temperature rating.

The first step in designing the transformer is to select a core of the desired permeability. Convert the required reactances determined earlier into inductance values for the lowest frequency of use. To find the number of turns for each winding, use the A_L value for the selected core and the equation for determining the number of turns:

$$L = \frac{A_L \times N^2}{1,000,000} \quad (15)$$

where

- L = the inductance in mH,
- A_L = the inductance index in mH per 1000 turns, and
- N = the number of turns.

Be certain the core can handle the power by calculating the maximum flux and comparing the result with the manufacturer's guidelines.

$$B_{\max} = \frac{E_{\text{RMS}} \times 10^8}{4.44 \times A_c \times N \times f} \quad (16)$$

where

- B_{\max} = the maximum flux density in gauss,
- E_{RMS} = the voltage across the inductor,
- A_c = the cross-sectional area of the core in square centimeters,
- N = the number of turns in the inductor, and
- f = the operating frequency in Hz.

(Both equations are from the section on ferrite toroidal inductors in the **Electrical Fundamentals** chapter and are repeated here for convenience.)

Example: Design a small broadband transformer having an impedance ratio of 16:1

for a frequency range of 2.0 to 20.0 MHz to match the output of a small-signal stage (impedance $\approx 500 \Omega$) to the input (impedance $\approx 32 \Omega$) of an amplifier.

Since the impedance of the smaller winding should be at least 4 times the lower impedance to be matched at the lowest frequency,

$$X_S = 4 \times 32 \Omega = 128 \Omega$$

The inductance of the secondary winding should be

$$L_S = \frac{X_S}{2 \pi f} = \frac{128}{6.2832 \times 2.0 \times 10^6 \text{ Hz}} = 0.0101 \text{ mH}$$

Select a core with a suitable size for the power level and ferrite mix for the frequency range. For this low-power application, a $\frac{3}{8}$ inch ferrite core with permeability of 850 is suitable. The core has an A_L value of 420. Calculate the number of turns for the secondary.

$$N_S = 1000 \sqrt{\frac{L}{A_L}} = 1000 \sqrt{\frac{0.010}{420}} = 4.88 \text{ turns}$$

A 5-turn secondary winding should suffice. The primary winding derives from the impedance ratio:

$$N_P = N_S \sqrt{\frac{Z_P}{Z_S}} = 5 \sqrt{\frac{16}{1}} = 5 \times 4 = 20 \text{ turns}$$

This low-power application will not approach the maximum flux density limits for the core, and #28 AWG enamel wire should both fit the core and handle the currents involved.

NOTES ON TOROID WINDINGS

For a toroidal (cylindrical) core, the number of turns is the number of times the conductor passes through the core. A wire passing once through a cylindrical core constitutes one turn. Likewise, a split or "clamp-on" core that is simply clamped onto a conductor forms a single-turn choke. A wire passing twice through the core is a two-turn choke, even though there is only one pass external to the core.

The inductance of a toroid can be adjusted. If the turns can be pressed closer together or separated a little, inductance variations of a few percent are possible.

In general, all of the flux associated with ferrite inductors (and chokes) is confined to the core material—for all practical purposes, there is no inductive coupling between inductors (or chokes) that are physically adjacent but

wound on different cores. Coupling between adjacent coils can be eliminated by placing a Faraday shield between them as discussed earlier in this section.

Toroidal windings do exhibit a small amount of leakage flux. Toroid coils are wound in the form of a helix (screw thread) around the circular length of the core. This means that there is a small component of the flux from each turn that is perpendicular to the circle of the toroid (parallel to the axis through the hole) and is therefore not adequately linked to all the other turns. This effect is responsible for a small leakage flux and the effect is called the “one-turn” effect.

BINOCULAR CORE TRANSFORMERS

Broadband transformer can also be made using a binocular core — a large bead-style core with two parallel holes as shown in **Figure 5.65B**. The windings on a binocular core have tighter coupling between the primary and secondary than separate windings on a toroid core. (Both the binocular and toroid

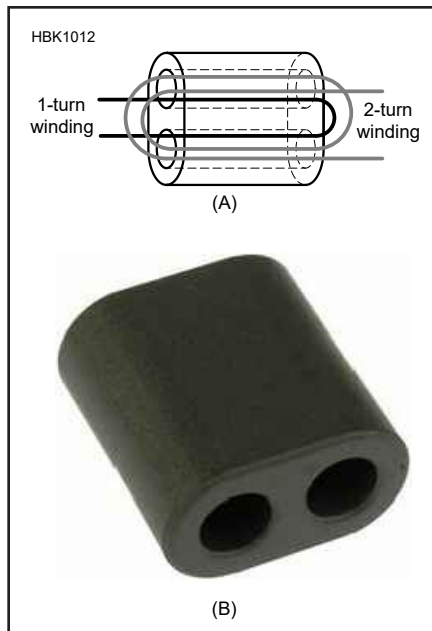


Figure 5.65 — Binocular ferrite cores. When used as a transformer (A) each full turn of a winding must pass through both holes. Cores (B) are available as small beads or large cores for high-power applications.

5.8 Noise

The following material was contributed by Paul Wade, W1GHZ. The section on background noise by Joe Taylor, K1JT, is reproduced from his discussion of Earth-Moon-Earth (EME) communications in this book's online content. Additional discussion of noise measurement is available in the **Test Instruments and Measurements** chapter and in the *Noise Instrumentation* document provided with the online content.

As anyone who has listened to a receiver suspects, everything in the universe generates noise. In communications, the goal is to maximize the desired signal in relation to the undesired noise we hear. In order to accomplish this goal, it would be helpful to understand where noise originates, how much our own receiver adds to the noise we hear, and how to minimize it.

It is difficult to improve something unless we are able to measure it. Measurement of noise in receivers does not seem to be clearly understood by many amateurs, so this section attempts to explain the concepts and clarify the techniques, and to describe the standard “measure of merit” for receiver noise performance: “noise figure.” In addition, the *Noise Instrumentation* document with the online content describes how to build your own noise generator for noise figure measurements.

A number of equations are included, but only a few need be used to perform noise figure measurements. The rest are included

to as an aid to understanding supported by explanatory text.

5.8.1. Noise Power

The most pervasive source of noise is *thermal noise* (also called *Johnson* or *Johnson-Nyquist noise*), due to the motion of thermally agitated free electrons in a conductor. Since everything in the universe is at some temperature above absolute zero, every conductor must generate noise.

Every resistor (and all conductors have resistance) generates an RMS noise voltage:

$$e = \sqrt{4kTRB} \quad (17)$$

where R is the resistance, T is the absolute temperature in kelvins (K), B is the bandwidth in hertz, and k is Boltzmann's constant, 1.38×10^{-23} joules /K (or $J K^{-1}$).

Converting to power, e^2/R , and adjusting for the Gaussian distribution of noise voltage, the noise power generated by the resistor is:

$$P_n = kTB \text{ (watts)} \quad (18)$$

which is independent of the resistance. Thus, all resistors at the same temperature generate the same noise power.

Thermal noise is *white noise*, meaning that the power density does not vary with frequency, but always has a *power density* or *spectral density* of kT watts/Hz. (The corresponding

transformers can use multifilar windings for even tighter coupling.) Binocular cores are used in broadband impedance transformers with ratios of 9:1 or 16:1 for receiving antennas, such as Beverages and small loops.

To make one complete turn in a binocular core, the wire must go through one of the holes and back through the other hole. This is different than a toroid where the wire passing through the core just once counts as a complete turn. Like toroids, binocular transformers must be wound with insulated or enameled wire so there is no direct contact between the metal and the core material.

A high-power version of a binocular core transformer can be made from two stacks of ferrite cores or a single large core. A single-turn winding can be made with copper or brass tubing through the stack that is soldered to strips of PC-board at each end. See the **RF Power Amplifiers** chapter and the previously referenced article by Trask for examples of this type of transformer.

noise voltage distribution is a *spectral voltage density*, measured in volts / $\sqrt{\text{Hz}}$, spoken as “volts per root hertz.”) More important is that the noise power is directly proportional to absolute temperature T, since k is a constant. At the nominal ambient temperature of 290 K, we can calculate this power; converted to dBm, we get the familiar -174 dBm/Hz. Multiply by the bandwidth in hertz to get the available noise power at ambient temperature. The choice of 290 K for ambient might seem a bit cool, since the equivalent 17°C or 62°F would be a rather cool room temperature, but the value 290 makes for an easier-to-remember numeric calculation of $P_n = (1.38 \times 10^{-23} \times 290) B = 400 \times 10^{-23} B$.

The *instantaneous* noise voltage has a *Gaussian distribution* around the RMS value. The Gaussian distribution has no limit on the peak amplitude so at any instant the noise voltage may have any value from $-\infty$ to $+\infty$. For design purposes we can use a value that will not be exceeded more than 0.01% of the time. This voltage is 4 times the RMS value, or 12 dB higher, so our system must be able to handle peak powers 12 dB higher than the average noise power if we are to measure noise without errors. (See Pettai in the Reference section.)

5.8.2. Signal to Noise Ratio

Now that we know the noise power in a given bandwidth, we can easily calculate how

much signal is required to achieve a desired *signal to noise ratio*, *S/N* or *SNR*. For SSB, perhaps 10 dB SNR is required for good communications; since ambient thermal noise in a 2.5 kHz bandwidth is -140 dBm, calculated as follows:

$$P_n = kTB = 400 \times 10^{-23} \times 2500 \\ = 1.0 \times 10^{-17} \text{ W}$$

$$\text{dBm} = 10 \log (P_n \times 1000) \text{ [multiplying} \\ \text{watts by 1000 converts to milliwatts]}$$

The signal power must be 10 dB larger, so minimum signal level of -130 dBm is required for a 10 dB S/N. This represents the noise and signal power levels at the antenna. We are then faced with the task of amplifying the signal without degrading SNR.

5.8.3. Noise Temperature

There are many types of noise, but most have similar characteristics to thermal noise and are often added together, creating a single equivalent noise source whose output power per unit of bandwidth is P_N . The *noise temperature* of the source is defined as the temperature $T = P_N / k$ at which a resistor would generate the same noise power per unit of bandwidth as the source. This is a useful way to characterize the various sources of noise in a communications system.

All amplifiers add additional noise to the noise present at their input. The input noise per unit of bandwidth is $N_i = kT_g$, where T_g is the noise temperature at the amplifier's input. Amplified by power gain G , the output noise is $kT_g G$. The additional noise contributed by the amplifier can also be represented as a noise temperature, T_n . The noise power added by the amplifier, kT_n , is then added to the amplified input noise to produce a total output noise:

$$N_o = kT_g G + kT_n$$

We can treat the amplifier as ideal and noise-free but with an additional noise-generating resistor of temperature $T_e = T_n / G$ at the input so that all sources of noise can be treated as inputs to the amplifier as illustrated by **Figure 5.66**. The output noise is then:

$$N_o = kG (T_g + T_e)$$

The noise added by an amplifier can then be represented as kGT_e , which is amplifier's noise temperature amplified by the amplifier gain. T_e is sometimes referred to as *excess temperature*.

Note that while the noise temperature of a resistor is the same as its physical temperature, the noise temperature of a device such as a diode or transistor can be many times the physical temperature.

SINAD

Signal-to-noise and distortion ratio (SINAD) is often used to measure of the quality of a demodulated signal.

$$\text{SINAD} = \frac{P_{\text{signal}} + P_{\text{noise}} + P_{\text{distortion}}}{P_{\text{noise}} + P_{\text{distortion}}} \quad (19)$$

where P is an average power. SINAD is usually expressed in dB and is often used as a condition at which a receiver's RF sensitivity is measured. For example: a sensitivity of $0.1 \mu\text{V}$ for 12 dB SINAD. (A thorough explanation of SINAD and several related terms such as THD is provided by the Analog Devices tutorial MT-003 by Kester listed in the References section of this chapter.)

5.8.4. Noise Factor and Noise Figure

The *noise factor*, F , of an amplifier is the ratio of the total noise output of an amplifier with an input T_g of 290 K to the noise output of an equivalent noise-free amplifier. A more useful definition is to calculate it from the excess temperature T_e :

$$F = 1 + T_e / T_g, \text{ where } T_g = 290 \text{ K} \quad (20)$$

It is often more convenient to work with *noise figure*, NF , the logarithm of noise factor expressed in dB:

$$NF = 10 \log (1 + T_e / T_g) = 10 \log F \quad (21)$$

$$F = \log^{-1} (NF/10)$$

Expressed in terms of signal, S , and noise power, N , at the input and output of a device:

$$F = (S_{\text{in}}/N_{\text{in}})/(S_{\text{out}}/N_{\text{out}}) \text{ and}$$

$$F = G_{\text{noise}}/G_{\text{signal}}$$

where G_{signal} is the device's power gain and G_{noise} is the device's *noise gain*. If SNR in dB is known at the input and output:

$$NF = \text{SNR}_{\text{in}} - \text{SNR}_{\text{out}}$$

If NF or F is known, then T_e may be calculated as:

$$T_e = (F - 1) T_g$$

Typically, T_e is specified for very low noise amplifiers where the NF would be fraction of a dB. NF is used when it seems a more manageable number than thousands of K.

Noise figure is sometimes stated as *input noise figure* to emphasize that all noise sources and noise contributions are converted to an equivalent set of noise sources at the input of a noiseless device. In this way, noise performance can be compared on equal terms across a wide variety of devices.

Noise figure is particularly important at VHF and UHF where atmospheric and other artificial noise is quite low. Typical noise figures of amateur amplifiers range from 1 to 10 dB. Mixers are generally toward the high end of that range. Modern GaAsFET and HEMT preamplifiers are capable of attaining an NF of 0.1 to 0.2 dB at UHF with NF under 1 dB even at 10 GHz.

5.8.5. Losses

We know that any loss or attenuation in a system reduces the signal level. If attenuation also reduced the noise level then we could suppress thermal noise by adding attenuation. We know intuitively that this can't be true — the attenuator or any lossy element has a noise temperature, T_x , which contributes noise to the system while the input noise is being attenuated.

The output noise after a loss L (expressed as ratio) expressed as an equivalent input noise temperature is:

$$T_g' = T_g / L + [(L - 1)/L] T_x$$

If the original source temperature, T_g , is higher than the attenuator temperature, T_x , then the noise contribution is found by adding the loss in dB to the NF . However, for low source temperatures the degradation can be much more dramatic. If we do a calculation for the effect of 1 dB of loss ($L = 1.26$) on a T_g of 25 K:

$$T_g' = 25/1.26 + (0.26/1.26) \times 290 = 80 \text{ K}$$

The resulting T_g' is 80 K, a 5 dB increase in noise power (or 5 dB degradation of signal to noise ratio). Since noise power = kT and k is a constant, the increase is the ratio of the two temperatures, $80/25$, or in dB, $10 \log (80/25) = 5$ dB.

It is also useful to note that for linear, pas-

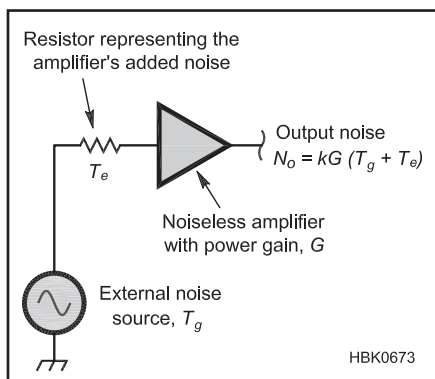


Figure 5.66 — The noise generated by an amplifier can be represented as an external resistor with a noise temperature of T_e connected at the input of a noiseless amplifier.

sive devices, such as resistors or resistive attenuators, noise figure is the same as loss in dB. A resistive attenuator with 6 dB loss has a noise figure of 6 dB which is equal to a noise factor of 4.

5.8.6. Cascaded Amplifiers

If several amplifiers are cascaded, the output noise N_o of each becomes the input noise T_g to the next stage. We can create a single equation for the total system of amplifiers. After removing the original input noise term, we are left with the added noise:

$$N_{\text{added}} = (k T_{e1} G_1 G_2 \dots G_N) + (k T_{e2} G_2 \dots G_N) + \dots + (k T_{eN} G_N)$$

where N is the number of stages cascaded. Substituting in the total gain $G_T = (G_1 G_2 \dots G_N)$ results in the total excess noise:

$$T_{eT} = T_{e1} + \frac{T_{e2}}{G_1} + \frac{T_{e2}}{G_1 G_2} + \dots + \frac{T_{eN}}{G_1 G_2 \dots G_{N-1}}$$

with the relative noise contribution of each succeeding stage reduced by the gain of all preceding stages.

The Friis formula for noise (a.k.a. the Friis equation) expresses this in terms of noise factor:

$$F = F_1 + \frac{F_2 - 1}{G_1} + \frac{F_3 - 1}{G_1 G_2} + \dots + \frac{F_N - 1}{G_1 G_2 \dots G_{N-1}} \quad (22)$$

Clearly, if the gain of the first stage, G_1 , is large, then the noise contributions of the succeeding stages become too small to be significant. In addition, the noise temperature of the first stage is the largest contributor to the overall system noise because it is amplified by all remaining stages. The effect on overall noise figure of adding a low-noise preamplifier ahead of a noisy receiver are illustrated in **Figure 5.67**, in which the system's noise figure changes from 20 dB for the receiver alone to 7.1 dB with the preamplifier added.

Any lossy component of an antenna system, such as the feed line, increases the noise figure at its input by an amount equal to the loss. As a result, it is important to concentrate noise-reduction efforts on the first amplifier or preamplifier in a system. Because noise performance is so important in early stages of cascaded systems such as receivers, low-noise VHF+ preamplifiers are usually mounted at the antenna so that their gain occurs ahead of the feed line loss. **Figure 5.68** compares the results of adding a preamplifier before and after 1.5 dB of feed line loss. Moving the preamplifier to the antenna improves the system's noise figure from 2.57 to 1.13 dB.

5.8.7. Antenna Temperature

Antenna temperature, T_A , is a way of describing how much noise an antenna produc-

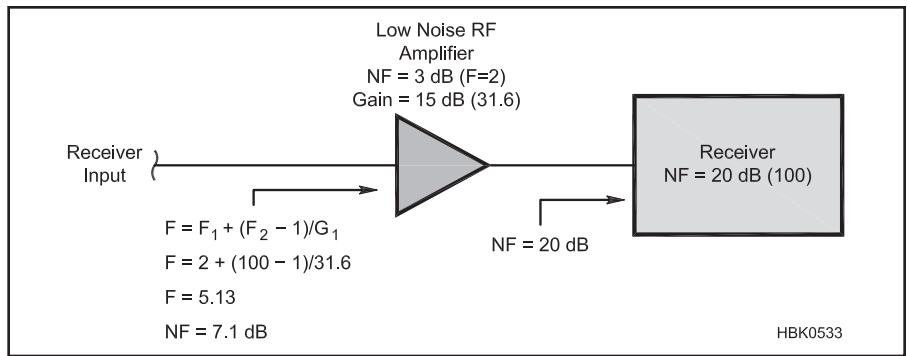


Figure 5.67 — The effect of adding a low-noise preamplifier in front of a noisy receiver system.

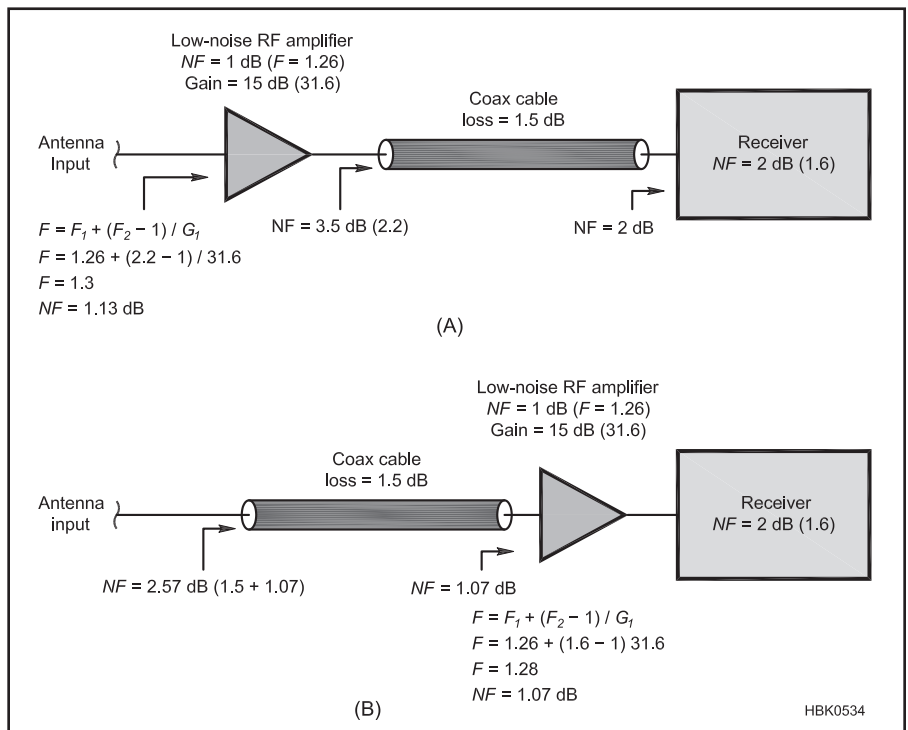


Figure 5.68 — The effect of adding a low-noise preamplifier at the antenna (A) compared to adding it at the receiver input (B).

es. It is not the physical temperature of the antenna because the antenna gathers noise from the environment according to its radiation pattern. If the antenna is directional and looks at a warm environment, T_A will be higher than if the antenna is looking at something cooler.

For example, if a lossless dish antenna is receiving signals from space rather than the warm Earth then the background noise is much lower than the warmer ambient temperature of 290 K or so. The background temperature of the universe has been measured as about 3.2 K. An empirical temperature for a 10 GHz antenna pointing into clear sky is about 6 K, since the antenna must always look through attenuation and temperature of the atmosphere. (See Graves in the Reference section.)

If the antenna's radiation pattern has any

sidelobes that must be accounted for in the total noise received by the antenna. This raises the noise temperature. If a warm body, such as the Sun, moves into the antenna's view, the additional *sun noise* will raise T_A as well. If the antenna is looking directly at the Earth, T_A will be close to ambient temperature. As an example, T_A will vary with frequency, but a good EME antenna might have a T_A of around 20 K at UHF and higher frequencies.

5.8.8. Image Response

Most receiving systems use at least one frequency converting mixer which has two responses: the desired frequency and an image frequency above and below the frequency of the local oscillator. If the image response is

not filtered out, it will add additional noise to the mixer output. Since most preamps are sufficiently broadband to have significant gain (and thus, noise output) at both the desired frequency, G_{desired} , and at the image frequency, G_{image} , an image filter must be placed between the preamplifier and the mixer. The total NF including image response is:

$$\text{NF} = 10 \log \left[\left(\frac{1 + T_c}{T_0} \right) \left(1 + \frac{G_{\text{image}}}{G_{\text{desired}}} \right) \right] \quad (23)$$

assuming equal noise bandwidth for the desired and image responses.

Without any filtering, $G_{\text{image}} = G_{\text{desired}}$ so $G_{\text{image}}/G_{\text{desired}} = 1$, doubling the noise figure, which is the same as adding 3 dB. Thus, without any image rejection, the overall noise figure is at least 3 dB regardless of the NF of the preamplifier. For the image to add less than 0.1 dB to the overall NF, gain at the image frequency must be at least 16 dB lower than at the operating frequency.

As the state of the art improves beyond the typical numbers in this and previous sections, system performance also improves. The very best low-noise preamplifiers today have noise figures as low as 0.2 dB, or a T_r of about 14 K, at UHF and 1296 MHz. The best EME dishes can have a T_a in the neighborhood of 20 K at 1296 MHz when pointed at clear sky. Thus the potential T_{sys} is perhaps 40 K. At these low noise temperatures any small loss or stray noise is significant — a loss of just 0.2 dB will reduce the signal to noise ratio by 1 dB, and low SNR communications such as EME rarely have many dB to spare. The preamp must be right at the antenna for optimum performance, and have sufficient gain so that subsequent stages have little effect.

5.8.9. Background Noise

A received signal at VHF and higher frequencies necessarily competes with noise generated in the receiver as well as that picked up by the antenna, including contributions from the warm Earth, the atmosphere, the lunar surface, the diffuse galactic and cosmic background and possibly the Sun and other sources, filling the whole sky. If P_n is the total noise power collected from all such noise sources expressed in dBW, we can write the expected signal-to-noise ratio of a communications link as

$$\text{SNR} = P_r - P_n = P_t + G_t + L + G_r - P_n \quad (24)$$

where P_r is received power, P_n is noise power, P_t is transmitted power, G_t of the transmitting antennas, L is isotropic path loss, and G_r is the gain of the receiving antennas. All powers are expressed in dBW and all gains in dBi. (Isotropic path loss is explored further in the material on Earth-Moon-Earth (EME)

communications in this book's online content on **Space Communications**.)

Since isotropic path loss L is essentially fixed by choice of a frequency band, optimizing the signal-to-noise ratio generally involves trade-offs designed to maximize P_r and minimize P_n — subject, of course, to such practical considerations as cost, size, maintainability, and licensing constraints.

It is convenient to express P_n (in dBW) in

terms of an equivalent system noise temperature T_s in kelvin (K), the receiver bandwidth B in Hz, and Boltzmann's constant $k = 1.38 \times 10^{-23} \text{ J K}^{-1}$:

$$P_n = 10 \log (kT_s B)$$

The system noise temperature may in turn be written as

$$T_s = T_r + T_a$$

Table 5.2

Typical Contributions to System Noise Temperature

Freq (MHz)	CMB (K)	Atm (K)	Moon (K)	Gal (K)	Side (K)	T_a (K)	T_r (K)	T_s (K)
50	3	0	0	2400	1100	3500	50	3500
144	3	0	0	160	100	260	50	310
222	3	0	0	50	50	100	50	150
432	3	0	0	9	33	45	40	85
902	3	0	1	1	30	35	35	70
1296	3	0	2	0	30	35	35	70
2304	3	0	4	0	30	37	40	77
3456	3	1	5	0	30	40	50	90
5760	3	3	13	0	30	50	60	110
10368	3	10	42	0	30	85	75	160
24048	3	70	170	0	36	260	100	360

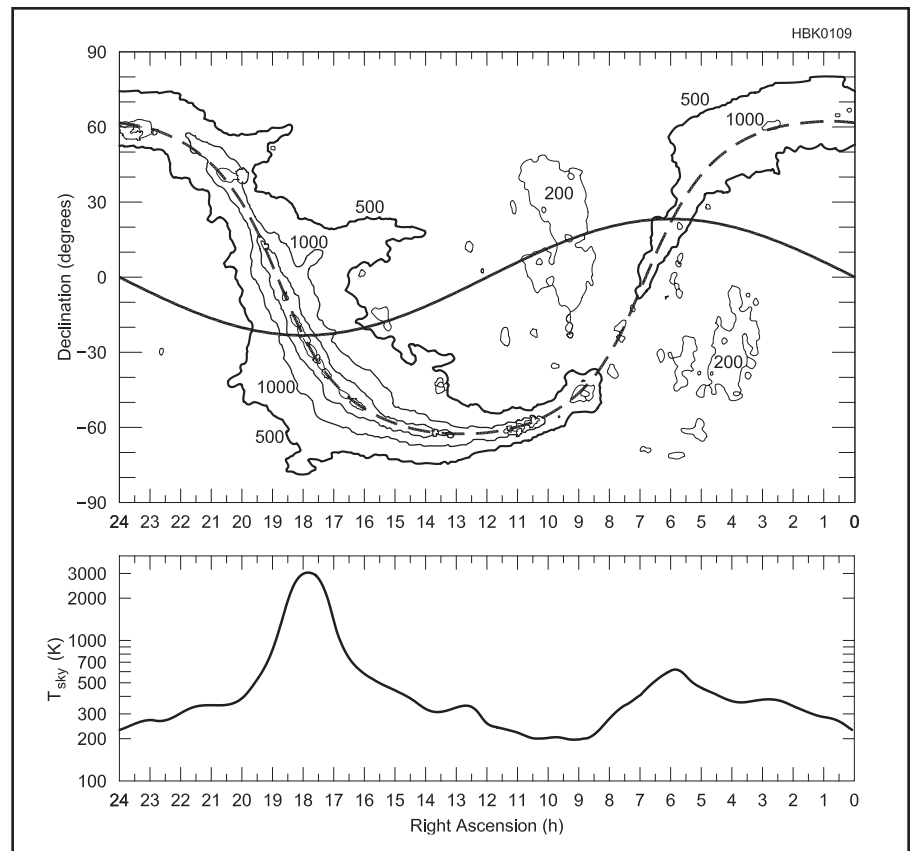


Figure 5.69 — Top: All-sky contour map of sky background temperature at 144 MHz. The dashed curve indicates the plane of our galaxy, the Milky Way; the solid sinusoidal curve is the plane of the ecliptic. The sun follows a path along the ecliptic in one year; the Moon moves approximately along the ecliptic ($\pm 5^\circ$) each month. Map contours are at noise temperatures 200, 500, 1000, 2000 and 5000 K. Bottom: One-dimensional plot of sky background temperature at 144 MHz along the ecliptic, smoothed to an effective beamwidth of 15° .

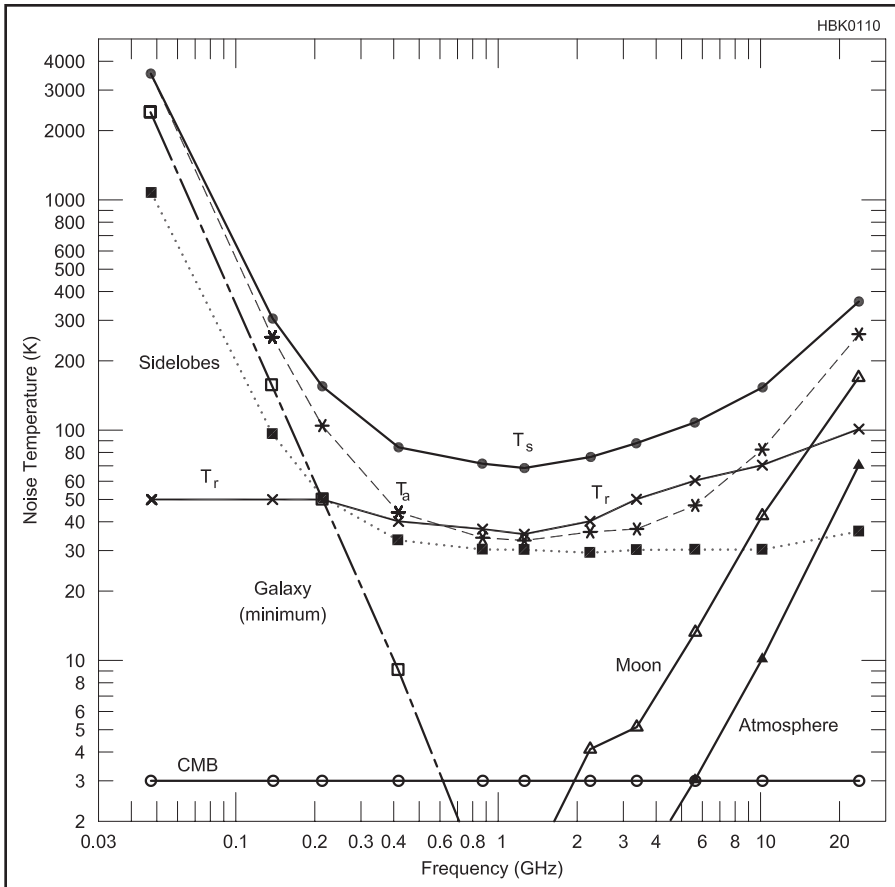


Figure 5.70 — Typical contributions to system noise temperature T_s as function of frequency. See text for definitions and descriptions of the various sources of noise.

Here T_r is receiver noise temperature, related to the commonly quoted noise figure (NF) in dB by

$$T_r = 290 (10^{0.1NF} - 1)$$

Antenna temperature T_a includes contributions from all noise sources in the field of view, weighted by the antenna pattern. Sidelobes are important, even if many dB down from the main beam, because their total solid angle is large and therefore they are capable of collecting significant unwanted noise power.

At VHF the most important noise source is diffuse background radiation from our galaxy, the Milky Way. An all-sky map of noise temperature at 144 MHz is presented in the top panel of **Figure 5.69**. This noise is strongest along the plane of the galaxy and toward the galactic center. Galactic noise scales as frequency to the -2.6 power, so at 50 MHz the temperatures in Figure 5.69 should be multiplied by about 15, and at 432 divided by 17. At 1296 MHz and above galactic noise is negligible in most directions. (See the previously mentioned online content on EME for the effects of lunar noise.)

The galactic background (GB) is a factor for HF reception as well. For daytime communications, it is less obvious due to the contributions of daytime band noise. Somewhere above 10 MHz, however, what today's quiet HF receivers hear at night becomes dominated by the GB. The frequency at which GB noise overtakes band noise depends on sunspot activity, the strength of atmospheric noise sources such as storms, geomagnetic conditions, the position of the galaxy in the sky, and the antenna's radiation pattern.

The GB has a negative spectral index, meaning it gets weaker with increasing frequency, but is still strong in the 15, 17, and 20 meter bands. Below 10 MHz the GB continues to increase, peaking around 3 MHz, but ionospheric attenuation increases with decreasing frequency, making it less of a factor than atmospheric

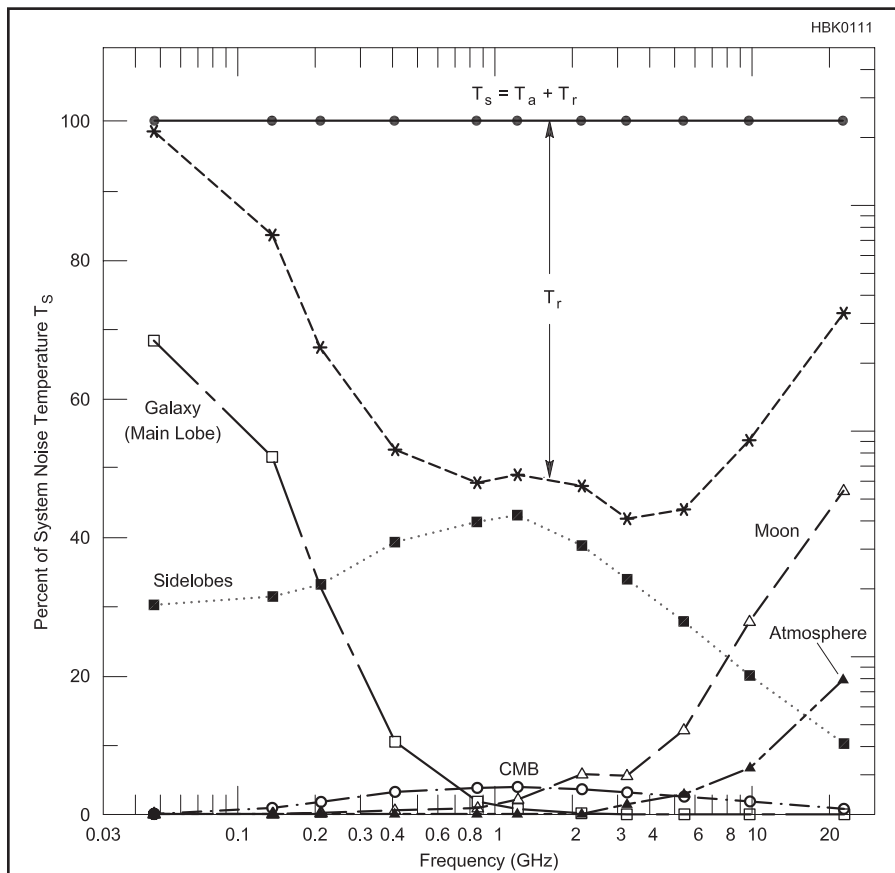


Figure 5.71 — Percentage contributions to system noise temperature as a function of frequency.

noise. (The article “The Galactic Background in the Upper HF Band” by Dave Typinksi, AJ4CO discusses the GB at HF and is available with this book’s online content.)

By definition the Sun also appears to an observer on Earth to move along the ecliptic,

and during the day solar noise can add significantly to P_n if the antenna has pronounced sidelobes. At frequencies greater than about 5 GHz the Earth’s atmosphere also contributes significantly. An ultimate noise floor of 3 K, independent of frequency, is set by

cosmic background radiation that fills all space. A practical summary of significant contributions to system noise temperature for the amateur bands 50 MHz through 24 GHz is presented in Table 5.2, and Figures 5.70 and 5.71.

5.9 Two-Port Networks

A *two-port network* is one with four terminals. The terminals are arranged into pairs, each being called a *port*. The general network schematic is shown in **Figure 5.72**. The input port is characterized by input voltage and current, V_1 and I_1 , and the output is described by V_2 and I_2 . By convention, currents into the network are usually considered positive.

Many devices of interest have three terminals rather than four. Two-port methods are used with these by choosing one terminal to be common to both input and output ports. The two-port representations of the common emitter, common base and common collector connections of the bipolar transistor are shown in **Figure 5.73**. Similar configurations may be used with FETs, vacuum tubes, ICs or passive networks.

The general concepts of two-port theory are applicable to devices with a larger number of terminals. The theory is expandable to any number of ports. Alternatively, the bias on some terminals can be established with attention fixed only upon two ports of a multi-element device. An example would be a dual-gate MOSFET in a common-source configuration as shown in **Figure 5.74**. The input port contain the source and gate 1 while the output port contains the source and drain leads. The fourth device terminal, gate 2, has a fixed bias potential and is treated as an ac ground. Signal currents at this terminal are ignored in the analysis.

5.9.1 Two-Port Parameters

There are four variables associated with any two-port network; two voltages and two currents. These are signal components. Any two variables may be picked as independent. The remaining variables are then dependent variables. These are expressed as an algebraic

linear combination of the two independent quantities. The following overview are intended for definition purposes. A complete discussion of the use of two-port parameters can be found in the reference texts at the end of this chapter and examples of their use in RF circuit design in Hayward’s *Introduction to Radio Frequency Design*.

Y AND Z PARAMETERS

Assume that the two voltages are chosen as independent variables. The two currents are then expressed as linear combinations of the voltages, $I_1 = K_a V_1 + K_b V_2$ and $I_2 = K_c V_1 + K_d V_2$. The constants of proportionality, K_a through K_d , have the dimensions of admittance. The usual representation is

$$\begin{aligned} I_1 &= y_{11}V_1 + y_{12}V_2 \\ I_2 &= y_{21}V_1 + y_{22}V_2 \end{aligned}$$

The independent and dependent variable sets are column vectors, leading to the equivalent matrix representation

$$\begin{pmatrix} I_1 \\ I_2 \end{pmatrix} = \begin{pmatrix} y_{11} & y_{12} \\ y_{21} & y_{22} \end{pmatrix} \begin{pmatrix} V_1 \\ V_2 \end{pmatrix} \quad (25)$$

The y matrix for a two-port network uniquely describes that network. The set of y_{11} through y_{22} are called the two-port network’s *Y parameters* or *admittance parameters*. Consider the y parameters from an experimental viewpoint. The first y parameter, y_{11} , is the input admittance of the network with V_2 set to zero. Hence, it is termed the *short-circuit input admittance*. y_{21} is the *short-circuit forward transadmittance*, the reciprocal of

transconductance. Similarly, if V_1 is set to zero, realized by short circuiting the input, y_{22} is the *short-circuit output admittance* and y_{12} is the *short-circuit reverse transadmittance*.

The matrix subscripts are sometimes replaced by letters. The set of y parameters can be replaced by y_i , y_r , y_f , and y_o where the subscripts indicate respectively input, reverse, forward, and output. The subscripts are sometimes modified further to indicate the connection of the device. For example, the short circuit forward transfer admittance of a common emitter amplifier would be y_{21e} or y_{fe} .

The y parameters are only one set of two-port parameters. The open-circuited *Z parameters* or *impedance parameters* result if the two currents are treated as independent variables

$$\begin{pmatrix} V_1 \\ V_2 \end{pmatrix} = \begin{pmatrix} z_{11} & z_{12} \\ z_{21} & z_{22} \end{pmatrix} \begin{pmatrix} I_1 \\ I_2 \end{pmatrix} \quad (26)$$

The parameter sets describe the same device; hence, they are related to each other. If

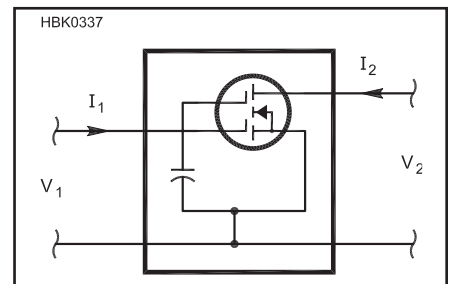


Figure 5.74 — A dual-gate MOSFET treated as a three-terminal device in a two-port network.

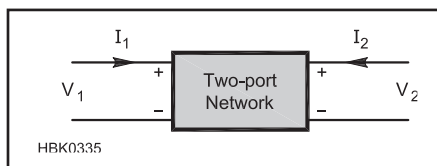


Figure 5.72 — General configuration of a two-port network. Note the voltage polarities and direction of currents.

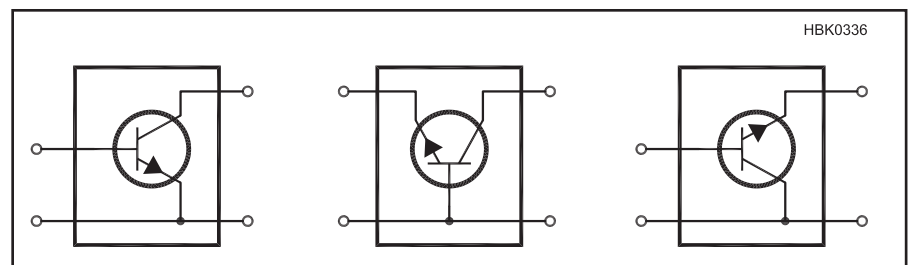


Figure 5.73 — Two-port representations of the common emitter, common base and common collector amplifiers.

the KVL equations are multiplied by y_{12} and the resulting equations subtracted, the result is the input voltage as a function of the currents

$$V_1 = \frac{I_1 y_{22} - y_{12} I_2}{y_{11} y_{22} - y_{12} y_{21}}$$

A similar procedure is used to find the output voltage as a function of the currents, leading to the general relationships

$$z_{11} = \frac{y_{22}}{\Delta y} \quad z_{12} = \frac{-y_{12}}{\Delta y}$$

$$z_{21} = \frac{-y_{21}}{\Delta y} \quad z_{22} = \frac{y_{11}}{\Delta y}$$

where Δy is the determinant of the y matrix, $y_{11}y_{22} - y_{12}y_{21}$. The inverse transformations, yielding the y parameters when z parameters are known, are exactly the same except that the y_{jk} and z_{jk} values are interchanged. The similarity is useful when writing transformation programs for a programmable calculator or computer.

H PARAMETERS

The H parameters or *hybrid parameters* are defined if the input current and output voltage are selected as independent variables

$$\begin{pmatrix} V_1 \\ I_2 \end{pmatrix} = \begin{pmatrix} h_{11} & h_{12} \\ h_{21} & h_{22} \end{pmatrix} \begin{pmatrix} I_1 \\ V_2 \end{pmatrix} \quad (27)$$

The input term, h_{11} , is an impedance, while h_{22} represents an output admittance. The forward term, h_{21} , is the ratio of the output to the input current, beta for a bipolar transistor. The reverse parameter, h_{12} , is a voltage ratio. The mixture of dimensions accounts for the “hybrid” name of the set.

SCATTERING (S) PARAMETERS

The two-port parameters presented above deal with four simple variables; input and output voltage and current at the ports. The variables are interrelated by appropriate matrices. The choice of which matrix is used depends upon which of the four variables are chosen to be independent.

There is no reason to limit the variables to simple ones. Linear combinations of the simple variables are just as valid. The more complicated variables chosen should be linearly independent and, ideally, should have some physical significance.

A transformation to other variables is certainly not new. For example, logarithmic transformations such as the dB or dBm are so common that we used them interchangeably with the fundamental quantities without even mentioning that a transformation has occurred. Such a new viewpoint can be of great utility in working with transmission line when an impedance is replaced

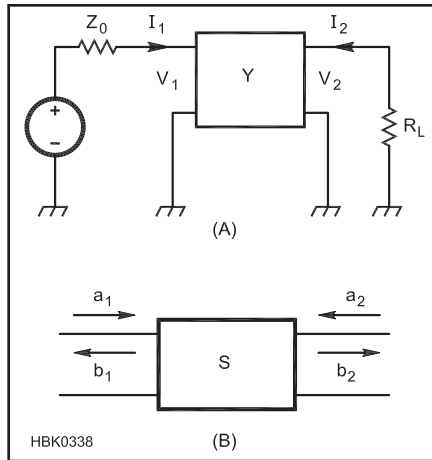


Figure 5.75 — A two-port network viewed as being driven by voltages and currents (A) or voltage waves (B). The voltages and currents are related by Y parameters while the voltage waves are related by scattering or S parameters.

by a reflection coefficient, $\Gamma = (Z - Z_0) / (Z + Z_0)$.

Scattering parameters or S parameters are nothing more than a repeat of this viewpoint. Instead of considering voltages and currents to be the fundamental variables, we use four “voltage waves.” They are interrelated through an appropriate matrix of s parameters.

Figure 5.75 shows the traditional two-port network and an alternate one with voltage waves incident on and reflected from the ports. The voltage waves are defined with the letters $a_1, b_1, a_2,$ and b_2 . The a waves are considered to be incident waves on the parts and are the independent variables. The b waves are the result of reflection or “scattering” and are the dependent variables. The waves are related to voltages and currents and defined with respect to a characteristic impedance, Z_0 .

The scattered waves are related to the incident ones with a set of linear equations just as the port currents were related to the port voltages with y parameters. The relating equations are

$$b_1 = S_{11}a_1 + S_{12}a_2$$

$$b_2 = S_{21}a_1 + S_{22}a_2$$

or, in matrix form

$$\begin{pmatrix} b_1 \\ b_2 \end{pmatrix} = \begin{pmatrix} S_{11} & S_{12} \\ S_{21} & S_{22} \end{pmatrix} \begin{pmatrix} a_1 \\ a_2 \end{pmatrix} \quad (28)$$

Consider the meaning of S_{11} . If the incident wave at the output, a_2 , is set to zero, the set of equations 27 reduce to $b_1 = S_{11}a_1$ and $b_2 = S_{21}a_1$. S_{11} is the ratio of the input port reflected

wave to the incident one. This reduces, using the defining equations for a_1 and b_1 to

$$S_{11} = \frac{Z - Z_0}{Z + Z_0} \quad (29)$$

This is the *input port reflection coefficient*. Similarly, S_{21} is the voltage wave emanating from the output as the result of an incident wave at the network input. In other words, S_{21} represents a forward gain. The other two S parameters have similar significance. S_{22} is the *output reflection coefficient* when looking back into the output port of the network with the input terminated in Z_0 . S_{12} is the reverse gain if the output is driven and the signal at the input port detected.

The reflection coefficient nature of S parameters makes them especially convenient for use in design and specification and even more so when displayed on a Smith Chart.

5.9.2 Return Loss

Although SWR as described in the **Transmission Lines** chapter is usually used by amateurs to describe the relationship between a transmission line’s characteristic impedance and a terminating impedance, the engineering community generally finds it more convenient to use *return loss, RL*, instead.

Return loss and SWR measure the same thing — how much of the incident power, P_{INC} , in the transmission line is transferred to the load and how much is reflected by it, P_{REFL} — but state the result differently.

$$\text{Return Loss (dB)} = -10 \log \left(\frac{P_{REFL}}{P_{INC}} \right) \quad (30)$$

Because P_{REFL} is never greater than P_{FWD} , RL is always positive. The more positive RL , the less the amount of power reflected from the load compared to forward power. If all the power is transferred to the load because $Z_L = Z_0$, $RL = \infty$ dB. If none of the power is transferred to the load, such as at an open- or short-circuit, $RL = 0$ dB. (You may encounter negative values for RL in literature or data sheets. Use the absolute magnitude of these values — the negative value does not indicate power gain.)

RL can also be calculated directly from power ratios, such as dBm (decibels with respect to 1 mW) or dBW (decibels with respect to 1 watt). In this case, $RL = P_{INC} - P_{REFL}$ because the logarithm has already been taken in the conversion to dBm or dBW. (Ratios in dB are computed by subtraction, not division.) For example, if $P_{INC} = 10$ dBm and $P_{REFL} = 0.5$ dBm, $RL = 10 - 0.5 = 9.5$ dB. Both power measurements must have the same units (dBm, dBW, and so on) for the subtraction to yield the correct results — for example, dBW can’t be subtracted from dBm directly.

Since SWR and RL measure the same thing — reflected power as a fraction of forward power — they can be converted from one to the other. Start by converting RL back to a power ratio:

$$\frac{P_{\text{REFL}}}{P_{\text{INC}}} = \log^{-1}(-0.1 \times \text{RL}) \quad (31)$$

Now use the equation for computing SWR from forward and reflected power (see the **Transmission Lines** chapter):

$$\text{SWR} = \frac{1 + \sqrt{\frac{P_{\text{REFL}}}{P_{\text{INC}}}}}{1 - \sqrt{\frac{P_{\text{REFL}}}{P_{\text{INC}}}}} \quad (32)$$

SWR can also be converted to RL by using the equation for power ratio in terms of SWR:

$$\frac{P_{\text{REFL}}}{P_{\text{INC}}} = \left[\frac{\text{SWR} - 1}{\text{SWR} + 1} \right]^2 \quad (33)$$

Then convert to RL using equation 30.

5.10 References and Bibliography

- Alley, C., and Atwood, K., *Electronic Engineering* (John Wiley & Sons, 1973)
- Brown, J., K9YC, “Measured Data For HF Ferrite Chokes,” audiosystemsgroup.com/publish.htm.
- Brown, J., K9YC, “A Ham’s Guide to RFI, Ferrites, Baluns, and Audio Interfacing,” audiosystemsgroup.com/publish.htm.
- Bruene, W., W5OLY, “Introducing the Series-Parallel Network,” *QST*, June 1986, pp. 21 – 23.
- Counselman, C., W1HIS, “Common-Mode Chokes,” www.yccc.org/Articles/W1HIS/mmonModeChokesW1HIS2006Apr06.pdf.
- DeMaw, D., W1FB, “Under Construction: Understanding and Constructing RF Chokes,” *QST*, Feb. 1987, pp. 19 – 21, 22.
- Dorf, R., Ed., *The Electrical Engineering Handbook* (CRC Press, 2006).
- Grammer, G., W1DF, “Simplified Design of Impedance-Matching Networks,” *QST*, Part 1, Mar. 1957, pp. 38 – 42; Part 2, Apr. 1957, pp. 32 – 35; and Part 3, May 1957, pp. 32 – 35.
- Hall, C. “RF chokes — Their Performance Above and Below Resonance,” *ham radio*, June 1978, pp. 40 – 42.
- Kaiser, C., *The Resistor Handbook* (CJ Publishing, 1994).
- Kaiser, C., *The Capacitor Handbook* (CJ Publishing, 1995).
- Kaiser, C., *The Inductor Handbook* (CJ Publishing, 1996).
- Kester, W., “Understand SINAD, ENOB, SNR, THD, THD + N, and SFDR so You Don’t Get Lost in the Noise Floor,” Analog Devices, MT-003 Tutorial, www.analog.com/media/en/training-seminars/tutorials/MT-003.pdf.
- Maxwell, W., W2DU, “Reflections III,” *CQ Communications*, 2010.
- Pettai, R., *Noise in Receiving Systems* (Wiley, 1984).
- Silver, W., NØAX “About Impedance Matching Circuits,” *QST*, Oct. 2019, pp. 43 – 46.
- Trask, C., “Designing Wide-band Transformers for HF and VHF Power Amplifiers,” *QEX*, Mar./Apr. 2005, pp. 3 – 15.
- Van Valkenburg, M., *Reference Data for Engineers* (Newnes, 2001).
- Zavrel, R., W7SX, *Antenna Physics: An Introduction* (ARRL, 2016).
- RF AMPLIFIER DESIGN
- Carr, J., *Secrets of RF Circuit Design* (McGraw-Hill/TAB Electronics, 2000).
- DeMaw, D., W1FB, *Practical RF Design Manual* (MFJ Enterprises, 1997).
- “FET RF Amplifier Design Techniques,” Motorola Application Note AN423.
- “RF Small Signal Design Using Two-Port Parameters,” Freescale Application Note AN215A.
- Hayward, W., W7ZOI, and DeMaw, D., W1FB, *Solid-State Design for the Radio Amateur* (ARRL, 1994).
- Hayward, W., Campbell, R., and Larkin, B., *Experimental Methods in Radio Frequency Design* (ARRL, 2009).
- Hayward, W., W7ZOI, *Introduction to RF Design* (ARRL, 1994, out of print)
- Hayward, W., W7ZOI, “A SMT Dual Gate MOSFET Preamp for 50 MHz,” w7zoi.net/lna50.pdf.
- Pozar, D., *Microwave Engineering*, 4th Edition (John Wiley & Sons, 2012).
- Raab, F., et al., “RF and Microwave Power Amplifier and Transmitter Technologies — Parts 1–5,” *High Frequency Electronics*, May, July, Sep., Nov., 2003, and Jan. 2004 issues.
- “Small-Signal RF Design with Dual-Gate MOSFETS,” Motorola Application Note AN478A, archive.org/details/AN478A.
- Terman, F., *Electronic and Radio Engineering* (McGraw-Hill, 1955).

